Identification and Functional Role of *Myo*-Inositol Polyphosphate 5-Phosphatase Protein Complexes

Elitsa A. Ananieva-Stoyanova

Dissertation submitted to the faculty of the Virginia Polytechnic Institute and State University
in partial fulfillment of the requirements for the degree of

Doctor of Philosophy
In
Biochemistry

Dr. Glenda E. Gillaspy, Chair
Dr. Dorothea B. C. Tholl,
Dr. Zhijian Tu,
Dr. Thomas O. Sitz

June 8, 2009
Blacksburg, VA

Keywords: *myo*-inositol polyphosphate 5-phosphatase, sucrose nonfermenting-1-related kinase, arabidopsis homolog of p80, inositol trisphosphate [Ins(1,4,5)P_3], *Arabidopsis thaliana*

Identification and Functional Role of *Myo*-Inositol Polyphosphate 5-Phosphatase Protein Complexes

Elitsa A. Ananieva-Stoyanova

ABSTRACT

To survive, an organism must constantly adjust its internal state to changes in the environment from which it receives signals. The signals set off a chain of events referred to signal transduction. Signal transduction systems are especially important in multicellular organisms, such as plants and animals, because of the need to coordinate the activities of hundreds to trillions of cells. Plants, in particular, have a special need for perceiving signals from their environment because of their static nature. As in the animal cell, the first steps in perception of a signal include signal interaction with a receptor, signal amplification through second messenger production, and signal termination through second messenger hydrolysis. *Myo*-inositol polyphosphate 5-phosphatases (5PTases) (EC 3.1.3.56) have unique signal terminating abilities toward the second messenger inositol trisphosphate (Ins (1,4,5)P_3, InsP_3). In *Arabidopsis thaliana* there are 15 members of the 5PTase family, the majority of which contain a single 5PTase catalytic domain. Four members of the Arabidopsis 5PTase family, however, have a unique protein domain structure, with additional N-terminal WD40 repeats that are implicated in protein-protein interactions. The research presented here focused on the identification of 5PTase interacting proteins and the characterization of their functional role in Arabidopsis. To accomplish this goal, I examined a 5PTase13-interacting protein, the

sucrose (Suc) nonfermenting-1-related kinase, SnRK1.1, an important energy sensor that is highly conserved among eukaryotes. My identification of a 5PTase13:SnRK1.1 complex points to the novel interaction of this metabolic modulator and inositol signaling/metabolism. 5PTase13, however, plays a regulatory role in other plant specific processes as well, since I also identified the Arabidopsis homolog (Atp80) of the human WDR48 (HsWDR48, Hsp80) as a novel protein interactor of 5PTase13. My results indicate that Atp80 is important for leaf emergence, leaf development and senescence likely via a regulatory interaction with 5PTase13 and PINOID –binding protein (PBP1).

ACKNOWLEDGEMENTS

I would like to acknowledge my advisor Glenda Gillaspy for giving me the opportunity to work with this exciting project, for letting me have the freedom to develop my own ideas and to grow as an independent researcher, for being with me when I needed her help and wise advice and last but not least for supporting me greatly in the most challenging time of my life.

I would like also to acknowledge Dr. Les Erickson of Salisbury University for being a great collaborator and an excellent mentor, Janet Donahue, our technician, for teaching me so many techniques in molecular cloning and for answering patiently all my questions, my labmates, Shannon Alford, Natasha Safaee and William Slade, for providing a friendly working environment, my committee members, Dr. Dorothea Tholl, Dr. Zhijian Tu and Dr. Thomas Sitz, for helpful advice and assistance during my journey as a PhD student.

ATTRIBUTION

Several colleagues and coworkers aided in the writing and research of Chapter II and Chapter III of this dissertation. A brief description of their background and their contributions are included here.

Prof. Glenda E. Gillaspy- Ph.D. (Department of Biochemistry, Virginia Tech) is the primary Advisor and Committee Chair. Prof. Gillaspy performed the subcellular localization studies of the 5PTase13:GFP fusion protein in Chapter II as well as the phylogenetic analysis in Chapters II and III.

Prof. Les F. Erickson- Ph.D. (Department of Biological Sciences, Salisbury University, MD) is a collaborator of Prof. Gillaspy. Prof. Erickson performed the yeast two hybrid assay in Chapters II and III and provided seed stocks of the *atp80* mutants and Atp80 transgenic plants.

Ryan N. Burnette- Ph.D. (Department of Biochemistry, Virginia Tech) was a student in Prof. Gillaspy's group and contributed during his graduate studies to Chapter II in terms of cloning the WD40 region of 5PTase13 gene as well as the SnRK1.1 and Atp80 genes by using pCRT7/CT-TOPO and pCRT7/NT-TOPO vectors.

Amanda Ely (Department of Biological Sciences, Salisbury University, MD) was a student in Prof. Erickson's group and contributed during her undergraduate studies to Chapter II in terms of assisting with the yeast two hybrid assay.

Janet Donahue- M.S. (Department of Biochemistry, Virginia Tech) is a technician in Prof. Gillaspy's group. Janet helped with the measurement of the mass Ins (1,4,5)P_3 levels and she performed the qPCR analysis in Chapter III.

TABLE OF CONTENTS

LIST OF FIGURES

LIST OF TABLES

LIST OF ABBREVIATIONS

5PTase	*myo*-inositol polyphosphate 5-phosphatase
ABA	abscisic acid
AMPK	AMP-dependent protein kinase
Atp80	arabidopsis homolog of the human p80
CAB1	chlorophyll A/B binding protein
CaMV	cauliflower mosaic virus
DAG	diacylglycerol
DGlcA	D-glucuronic acid
Gal	galactose
GFP	green fluorescent protein
Glu	glucose
GUS	β-glucuronidase
Ins	*myo*-inositol
Ins(1,4,5)P3	*myo*-inositol-(1,4,5)-trisphosphate
InsP6	inositol hexakisphosphate
InsPs	inositol phosphates
KIN1	antifreeze protein
Man	mannitol
MIOX	*myo*-inositol oxygenase
MS	Murashige & Skoog (plant culture salts)

PAS	protein A sepharose
PBP1	PINOID binding protein
PIs	phosphoinositides
PLC	phospholipase C
PtdIns	phosphatidylinositol
PtdInsPs	phosphatidylinositol phosphates
qPCR	quantitative PCR
RD29A	responsive to desiccation 29A
Snf1	sucrose nonfermenting-1
SnRK1	sucrose nonfermenting-1-related kinase
Suc	sucrose
WT	wild type

CHAPTER I

OBJECTIVES

The presence of WD40 regions in the Arabidopsis 5PTases provides compelling evidence for protein: protein interactions in the $InsP_3$ signal termination in plants. To date, WD40 repeats are found to be only a part of the plant and certain filamentous fungal 5PTases, a unique combination that may confer a new functional specificity for these enzymes. Additionally, the WD40 repeats of 5PTases have not been functionally characterized, and no potential protein partners have been identified. Therefore the goal of my research was to identify 5PTase interacting proteins and to understand the functional role of these protein complexes. To accomplish this goal, I focused on one member of the Arabidopsis 5PTase family, called 5PTase13 and identified two interacting proteins, a sucrose nonfermenting-1-related kinase (SnRK1.1, AKIN10; At3g01090) and an arabidopsis homolog (Atp80; At3g05090) of the human WDR48 (HsWDR48; Hsp80), with the following two specific objectives:

Objective I. Role of 5PTase13 in Sugar and Stress Signaling via Formation of a Protein Complex with SnRK1.1. "Interaction of the WD40 Domain of a *Myo*-inositol Polyphosphate 5-Phosphatase with SnRK1 Links Inositol, Sugar, and Stress Signaling"

Objective II. Identification and Functional Role of Atp80, a novel interactor of 5PTase13

LITERATURE REVIEW

I. Overview of Inositol Signaling

Inositol phosphates (InsPs) are among the most widespread second messengers in eukaryotic cell signaling (Berridge, 2008; Munnik and Testerink, 2008). They are composed of a six-member carbon ring polyol named *myo*-inositol that can be phophorylated in different positions to generate an array of signaling molecules. All eukaryotes make *myo*-inositol (poly) phosphates, in which some or all of the Ins hydroxyls can be phosphorylated. *Myo*-inositol (with D-*myo*-inositol abbreviated as Ins) is one of the nine isomeric forms of cyclohex-anehexol, a group of small and chemically very stable polar molecules that have versatile properties (Michell, 2008). When phosphorylated on hydroxyl positions D1, D4 and D5 it forms the second messenger Ins(1,4,5)P_3. Other important higher phophorylated inositols are Ins(1,3,4,6)P_4 and Ins(1,2,3,4,5,6)P_6 (Figure 1) (Balla, 2001):

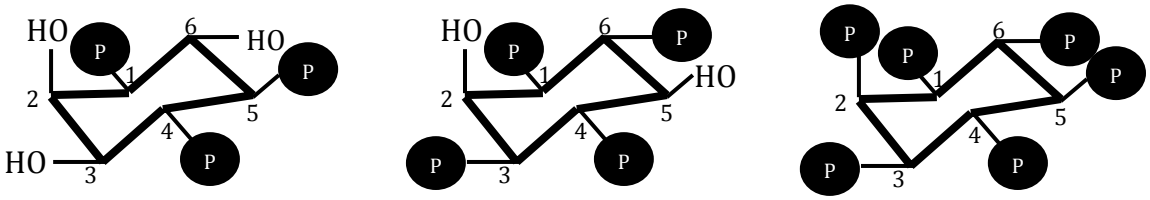

Ins(1,4,5)P_3 Ins(1,3,4,6)P_4 Ins(1,2,3,4,5,6)P_6

Figure 1. Structure of water soluble inositol phosphates. The core structure is a ring of six carbons with six hydroxyl groups that can be phosphorylated to form different inositol (poly) phosphates.

Functional Role of Water Soluble Inositol Phosphates

In animals, $Ins(1,4,5)P_3$ is the second messenger that links receptor-mediated phospholipase C (PLC) activation to Ca^{2+} signaling (Figure 2) (Berridge, 2008). $Ins(1,4,5)P_3$ acts on specific receptors that are located mainly in the endoplasmic reticulum but also in other intracellular membranes including the nuclear envelope (Berridge, 2008). The $InsP_3$ receptor is a large protein of 260-300 kDa in size that forms a tetramer and functions as a Ca^{2+} channel. After $Ins(1,4,5)P_3$ binding, Ca^{2+} moves through the $Ins(1,4,5)P_3$ receptor-channel along a concentration gradient from the intracellular stores to the cytosol (Balla, 2001) (Figure 2). A remarkable feature of the $Ins(1,4,5)P_3$ /Ca^{2+} pathway is that it participates in the control of a large number of cellular processes such as exocytosis, cell contraction, proliferation, differentiation, aggregation, liver cell metabolism and others. In some cases, it plays a direct role in generating Ca^{2+} signals whereas in other cases it functions to modulate the Ca^{2+} signals produced by other signalling pathways (Berridge, 2008).

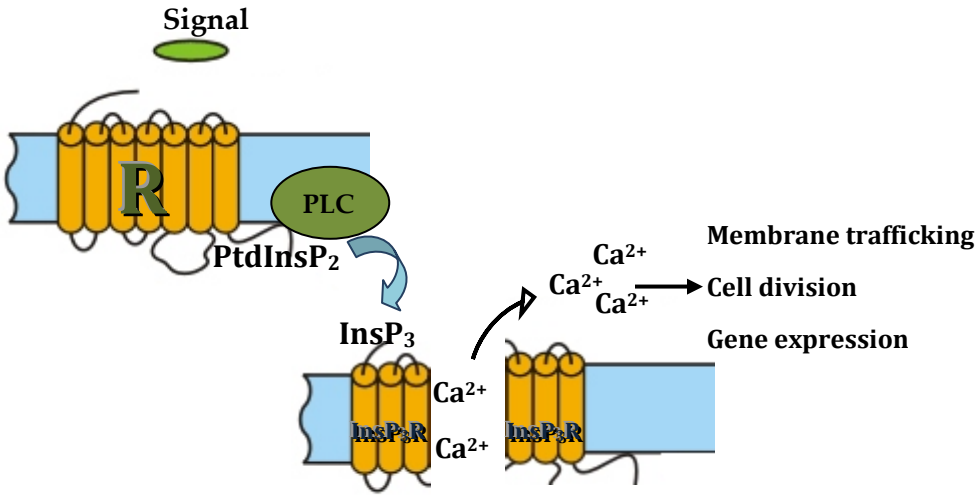

Figure 2. Role of Ins(1,4,5)P_3 in Inositol Signaling Pathway. Signals are perceived by a membrane bound receptor (R) that upon activation stimulates PLC to convert the substrate phosphatidylinositol 4,5-bisphosphate (Ptd$InsP_2$) into the second messenger Ins(1,4,5)P_3. Ins(1,4,5)P_3 acts on a specific $InsP_3$ binding receptor ($InsP_3$R) to stimulate Ca^{2+} release which triggers downstream biological responses.

In plants, Ins(1,4,5)P_3 plays a role in reversible turgor-driven processes, such as the regulation of stomatal aperture and cellular osmotic homeostasis (Lee et al., 1996; Burnette et al., 2003). Additionally, long-term increases in both Ins(1,4,5)P_3 and Ptd$InsP_2$ synthesis are involved in the regulation of cell elongation as shown in studies with pollen tubes (Franklin-Tong et al., 1996), and graviresponsive pulvinal cells of cereal grasses (Perera et al., 1999; Perera et al., 2001) and hypocotyls elongation in seedlings (Gunesekera et al., 2007). Other studies with plant species have indicated changes in Ins(1,4,5)P_3 in response to variety of stresses such as abscisic acid, (ABA; Sanchez and Chua, 2001; Burnette et al., 2003;

Gunesekera et al., 2007; Lee et al., 2007), salt stress (DeWald et al., 2001) and pathogens (Ortega and Perez, 2001).

The precise mechanism of $Ins(1,4,5)P_3$ action in plants is not known partially because a plant $Ins(1,4,5)P_3$ receptor has not been identified in higher plants (Krinke et al., 2007; Munnik and Testerink, 2008). This raises the question whether other inositol polyphosphates serve as second messengers in plants. One potential candidate is $InsP_6$ [$Ins(1,2,3,4,5,6)P_6$] also known as phytate. Plants accumulate phytate in seeds, which mainly reflects the mechanism to store huge amounts of phosphate and inositol required for germination. Nonetheless, $InsP_6$ may play a completely different role during plant development (Michell, 2008). An exciting example is the unexpected discovery of $InsP_6$ in the crystal structure of the auxin receptor, TIR1 where it is structurally required for auxin binding and receptor function (Tan et al., 2007). In addition, $InsP_6$ is shown to release Ca^{2+} at a 10-fold lower concentration than $Ins(1,4,5)P_3$ and when $Ins(1,4,5)P_3$ is microinjected, it is rapidly converted into $InsP_6$ (Lemtiri-Chlieh et al., 2003).

General Structure of Phosphoinositides

Lipid-derived inositol phosphates also know as phosphoinositides (PIs) are glycerophospholipids with a phosphoinositol (PtdIns)-containing head group. Hydroxyl groups at positions D3, D4 and D5 of the head group are accessible for lipid kinases giving rise to Ptdlns-monophosphates (Ptdlns3P, Ptdlns4P), Ptdlns-bisphosphates [$Ptdlns(3,5)P_2$, $Ptdlns(4,5)P_2$] and Ptdlns-trisphosphate [$Ptdlns(3,4,5)P_3$] (Figure 3). With the exception of

Ptdlns(3,4,5)P_3, all known PIs from other eukaryotic systems have been detected in plants (Heilmann, 2009).

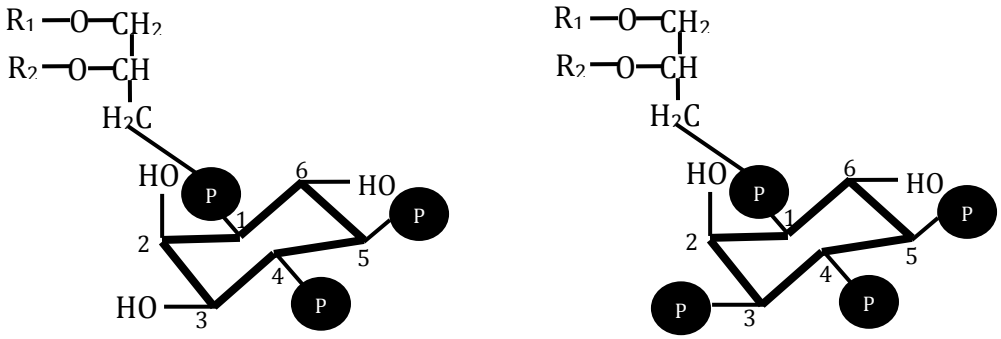

Figure 3. Structure of PIs. PIs are glycerophospholipids characterized by a phosphoinositol-containing head group. The D3, D4 and D5 hydroxyl positions of PIs (indicated by numbers in the inositol ring) are accessible for phosphorylation by specific lipid kinases such as PI 3-Kinase, PI 4-Kinase and PIP Kinase. The diacylglycerol backbone can hold different fatty acids, indicated by R1 and R2.

Functional Role of PIs

PIs are membrane bound signaling molecules that are involved in the regulation of key physiological processes. For example, PtdIns(4,5)P_2 that can be generated by phosphatidylinositol phosphate kinases type I an II (PIPKI and PIPKII) serves as a substrate of phospholipase C to produce the second messenger Ins(1,4,5)P_3. PtdIns(4,5)P_2 acts as a second messenger itself as it is able to bind hundreds of effectors present in most membrane compartments and in the nucleus (Bunce et al., 2006; Ling et al., 2006; Schill and Anderson, 2009). A well-characterized example of this is the regulation of focal adhesion dynamics via

the site-specific generation of PtdIns(4,5)P_2 by PIPKIγ (Ling et al., 2002). Focal adhesions, which are sites of integrin-mediated cellular contact with the extracellular matrix, are dependent upon assembly with the actin cytoskeleton mediated by the scaffolding molecule talin (Critchley, 2004). Talin is a PtdIns(4,5)P_2 effector, and PtdIns(4,5)P_2 regulates the interaction of talin with integrins (Calderwood, 2004). The ability of cells to form cell contacts is essential for development, wound healing, metastasis, cell survival and the immune response (Ling et al., 2002).

The functional role of PtdIns(4,5)P_2 is much less known for plants, but some evidence suggests that PtdIns(4,5)P_2 plays a role in vesicular trafficking (Zhong et al., 2004). Profilin, a G-actin binding protein thought to be regulated by PtdIns(4,5)P_2, is a potent controller of actin dynamics and is found to be localized in the bulges of outgrowing root hairs (Braun et al., 1999) and pollen tubes (Kost et al., 1999).

Another PI that has an important functional role in animals but is not present in plants is PtdIns(3,4,5)P_3. Its formation is catalyzed by a PI3- kinases (PI3-K) (Heilmann, 2009). PtdIns(3,4,5)P_3 binds PH-domain-containing proteins and recruits to the plasma membrane a variety of effectors including Rho-GEFs, non-receptor tyrosine kinases such as Btk, PLCγ and Akt, leading to their allosteric activation and initiation of downstream signalling cascades that promote a variety of cellular effects (Ooms et al., 2009). Control of PI 3-K pathway and PtdIns(3,4,5)P_3 levels have emerged as an important target in cardiovascular disease, cancer, allergy, autoimmune disease and diabetes (Wymann et al., 2003; Prestwich, 2004; Ciraolo et al., 2008; Wymann and Schneiter, 2008).

II. *Myo*-Inositol Polyphosphate 5-Phosphatases

To control signaling events driven by inositol (poly) phosphates, cells must metabolize them. The first step in inositol second messenger breakdown utilizes the *myo*-inositol polyphosphate 5-phosphatases (5PTases; EC 3.1.3.56)(Erneux et al., 1998; Astle et al., 2007). All eukaryotes contain multiple 5PTase genes that encode 5PTase protein family members with a conserved 5PTase catalytic domain. They are a family of Mg^{2+}-dependant phosphoesterases that hydrolyze the 5-position phosphate from the inositol ring of various second messengers, including the water-soluble inositol phosphates Ins(1,4,5)P_3 and Ins(1,3,4,5)P_4, and the lipid-bound PtdIns-derived molecules PtdIns(4,5)P_2, PtdIns(3,4,5)P_3, and PtdIns (3,5) P_2 (Figure 4).

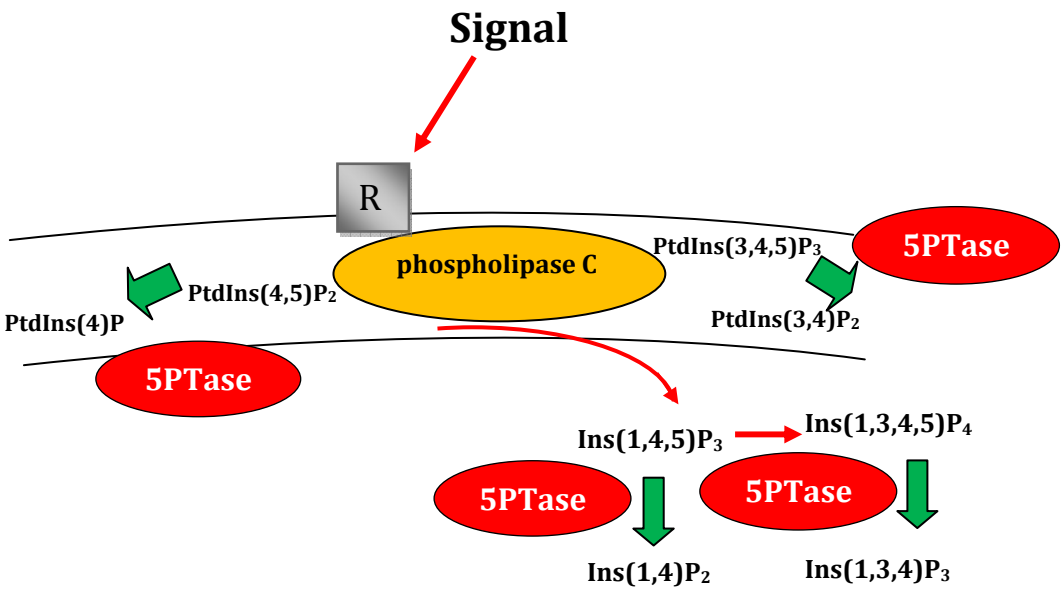

Figure 4. General role of 5PTases in terminating Inositol Signaling. 5PTases hydrolyze the second messenger Ins(1,4,5)P_3, along with other inositol-containing second messengers.

II.1. Mammalian 5PTases

The *myo*-inositol polyphosphate 5-phosphatases (5PTases) are a large family of signal modifying enzymes comprising 10 charachterized mammalian members (Figure 5). The mammalian 5PTases regulate diverse cellular processes such as protein trafficking, phagocytosis and synaptic vesicle recycling by degrading various 5-position phosphorylated inositol (poly) phosphates. They are classified in four groups based on their substrate preferences. *Group I* 5PTases are the enzymes that dephosphorylate only water-soluble Ins(1,4,5)P_3 and Ins(1,3,4,5)P_4 and hence, regulate Ca^{2+} signaling. *Group II* 5PTases, can dephosphorylate the lipids, PtdIns(4,5)P_2 and PtdIns(3,4,5)P_3, in addition to the soluble inositol phosphates. *Group III* 5PTases only hydrolyze substrates that contain a phosphate group at position 3 of the inositol ring, i.e. Ins(1,3,4,5)P_4 or PtdIns(3,4,5)P_3. *Group IV* 5PTases are enzymes that hydrolyze PtdIns(3,4,5)P_3, and to a lesser degree PtdIns(4,5)P_2 (Balla, 2001; Ercetin and Gillaspy, 2004).

Mammalian 5PTases Domain Structure

5PTases contain a conserved 300-amino-acid catalytic domain (5PTase domain) with two highly conserved motifs I and II (**GDL/FNF/YR** and **PA/SW/YC/TDRI/VL/I,** respectively). These motifs are part of the active site as demonstrated by the use of chemical modification of arginyl residues in the active site of type I 5PTase and/or site-directed mutagenesis of type II 5PTase (Communi et al., 1996; Jefferson and Majerus, 1996). Resolution of the crystal structure of SPsynaptojanin has revealed that the 5PTase domain folds in a manner similar to that of the apurinic/apyrimidinic endonuclease family of DNA-

modifying enzymes with a His/Asp active site pair (Tsujishita et al., 2001). Numerous other domains including SH2, Sac-1, proline-rich, CAAX, RhoGAP (RhoGTPase-activating protein) and SKICH [SKIP (skeletal muscle- and kidney-enriched inositol phosphatase) carboxyl homology domains] have been identified in the mammalian 5PTases which are important for mediating their subcellular localization and/or protein–protein interactions (Ooms et al., 2009) (Figure 5).

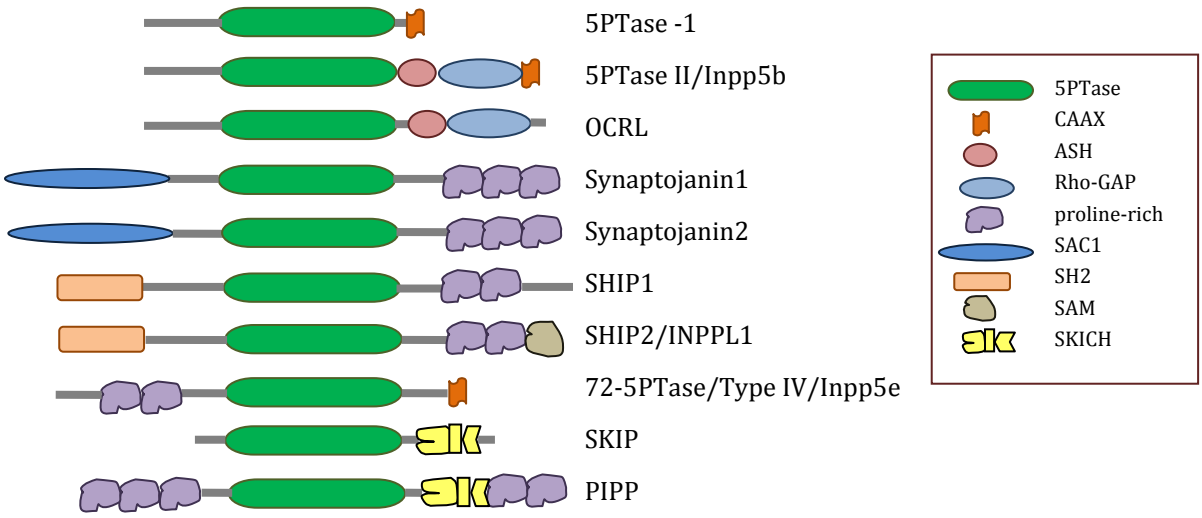

Figure 5. Domain organization of the mammalian 5PTases. Each of the 5PTase family members contains a central conserved 5PTase catalytic domain. The 5PTase1, 5PTase II and Type IV 5PTases each contain a C-terminal CAAX (C = cysteine, A = alanine and X = any amino acid) motif, which can mediate plasma membrane targeting, while membrane localization of PIPP and SKIP is mediated by their respective SKICH (SKIP carboxyl homology) domains. The Src-homology-2 (SH2) domains of SHIP1 and SHIP2 mediate protein interactions with tyrosine phosphorylated receptors. The proline-rich domains of synaptojanin-1 and synaptojanin-2, SHIP1 and SHIP2, Type IV and PIPP are likely to mediate protein-protein interactions. The Sac-1-like (suppressor of actin) domains of synaptojanin-1 and -2 mediate hydrolysis of PtdIns(4)P. The figure is modified from (Ooms et al., 2009).

Role of Mammalian 5PTases in Human Diseases

PI3K-dependent Insulin Signalling: Role of SHIP2 and SKIP

Type 2 diabetes is a complex disorder, caused by insulin resistance in skeletal muscle, liver and adipose tissues and impaired pancreatic islet insulin secretion. Insulin binding to the IR (insulin receptor) induces several distinct signaling pathways including the PI3K-Akt pathway. As mentioned above the lipid kinase PI3K produces PtdIns(3,4,5)P_3 that serves as a membrane binding site for the Akt family of serine-threonine kinases (Sleeman et al., 2005). Akt activity is essential for the translocation and fusion of GLUT4 (glucose transporter 4) with the plasma membrane in skeletal muscle and fat tissue and thereby glucose uptake (Shisheva, 2003).

SHIP2 (SH2-domain-containing inositol phosphatase) plays a negative role in insulin signaling. This has been demonstrated in *in vitro* cellular models such as 3T3-L1 adipocytes. In such models, SHIP2 overexpression decreases insulin stimulated PI3K signalling and Akt activation, leading to reduced GLUT4 translocation to the plasma membrane and subsequent glucose uptake and glycogen synthesis (Wada et al., 2001). In patients, polymorphisms in the *SHIP2* gene (*INPPL1*) may contribute to the pathogenesis of Type 2 diabetes and hypertension. For example, a 16 bp deletion located in the proximal region of the *SHIP2* gene 3-UTR (untranslated region) is significantly associated with individuals with Type 2 diabetes, compared with healthy individuals, as shown by a cohort study of ethnically Caucasian residents from the U.K. and Belgium (Marion et al., 2002).

SKIP (skeletal muscle and kidney-enriched inositol phosphatase) is proposed to play a major role in regulating insulin signalling in skeletal muscle. It localizes to the perinuclear

region, overlapping with the ER (endoplasmic reticulum) and translocates to the plasma membrane upon EGF (epidermal growth factor) or insulin stimulation (Gurung et al., 2003; Ijuin and Takenawa, 2003). SKIP overexpression attenuates insulin-stimulated GLUT4 translocation to the plasma membrane. Conversely, SKIP knockdown using antisense oligonucleotides or siRNA (short interfering RNA) results in increased Akt phosphorylation following insulin stimulation (Ijuin and Takenawa, 2003). The increased Akt phosphorylation could be suppressed by re-expression of SKIP, but not by expression of SHIP2 or PTEN, suggesting that SKIP plays a role in insulin signalling distinct from these other lipid phosphatases(Ijuin et al., 2008).

LOWE's Syndrome–Role of OCRL

Lowe's oculocerebrorenal syndrome, first described in 1952, is a rare X-linked disorder affecting approx. 1 in 200000 births. The disease is characterized by growth and mental retardation, bilateral congenital cataracts and renal failure, with impaired solute and protein reabsorption in the kidney proximal tubule and renal tubular acidosis (Lowe, 2005). The Lowe syndrome is linked to a gene encoding a ubiquitously expressed 105 kDa 5PTase called OCRL (oculocerebrorenal syndrome of Lowe) (Attree et al., 1992). The OCRL gene is deficient in OCRL patients due to mutations. Among the mutations reported in OCRL patients are many missense mutations within the 5PTase catalytic domain (Tsujishita et al., 2001). Although OCRL can hydrolyze Ins(1,4,5)P_3, Ins(1,3,4,5)P_4, PtdIns(3,5)P_2 and PtdIns(3,4,5)P_3 it preferentially acts on PtdIns(4,5)P_2 (Zhang et al., 1995; Schmid et al., 2004). PtdIns(4,5)P_2 levels are increased in cells from Lowe's syndrome (Zhang et al., 1998) and MRI (magnetic

resonance imaging) brain scans of affected individuals exhibit cystic abnormalities in the white matter, suggestive of PtdIns(4,5)P_2 accumulation (Schneider et al., 2001).

Neuronal Function and Neurological Diseases- Role of Synaptojanin 1

Several 5PTases play important roles in neuronal differentiation and function. One of them, Synaptojanin 1 plays a significant role in regulating synaptic vesicle recycling and thus neuronal function. Synaptojanin 1 is highly expressed in the brain, localizing to presynaptic nerve terminals and may represent the major PtdIns(3,4,5)P_3 5PTase in the brain (Woscholski et al., 1997). Synaptojanin 1 may have a role in certain neurological diseases as several studies have provided evidence of increased Synaptojanin 1 expression in Down's syndrome (Arai et al., 2002). Ts65Dn mice, commonly used as a model of Down's syndrome, and Synaptojanin 1 transgenic mice exhibit increased Synaptojanin 1 expression in the brain with a concomitant decrease in PtdIns(4,5)P_2 levels (Voronov et al., 2008). Both mouse strains also display defects in learning, suggesting that impaired PtdIns(4,5)P_2 regulation may play a role in the cognitive abnormalities observed in Down's syndrome (Reeves et al., 1995; Voronov et al., 2008).

II.2. Arabidopsis 5PTases

In 2001, our laboratory reported the initial characterization of the entire 5PTase protein family from *Arabidopsis thaliana* which contains 15 protein members encoded by 15 different genes (Berdy et al., 2001). By far the Arabidopsis 5PTases are the best characterized plant 5PTases. In fact, 5PTases from other plant species are poorly understood or characterized (DePass et al., 2001).

Arabidopsis 5PTases Domain Structure

Arabidopsis 5PTases all contain motif I and II of the conserved 5PTase catalytic domain as shown for the mammalian 5PTases. We classify the Arabidopsis 5PTases in two groups based on their domain structure. Group A is a large group of 11 small 5PTases (36-75 kD; 5PTase1 -11) that contain only the conserved 5PTase catalytic domain (Berdy et al., 2001). As such they have a simple domain structure since no other domains have been identified (Figure 6). Group B is a small group of 4 large 5PTases (110-150 kD; FRA3 and 5PTase12-14)(Berdy et al., 2001). Besides containing the conserved 5PTase catalytic domain, the Group B 5PTases also contains 5-6 WD40 repeats in their N-termini (Zhong and Ye, 2004) (Figure 6). The WD40 repeats function to facilitate protein-protein interactions (Li and Roberts, 2001). The mammalian 5PTases also contain domains that facilitate protein –protein interactions such as the proline rich domain (Erneux et al., 1998). These enzymes however, do not contain WD40 repeats which are found in plant and some fungal 5PTases. Thus, the presence of WD40 repeats in the Arabidopsis (plant) and certain filamentous fungal 5PTases is unique and likely reflects the addition of the WD40 region before the diversification of plants and fungi around 100 million years ago and results in a mechanism to allow Group B 5PTases to participate in protein complexes.

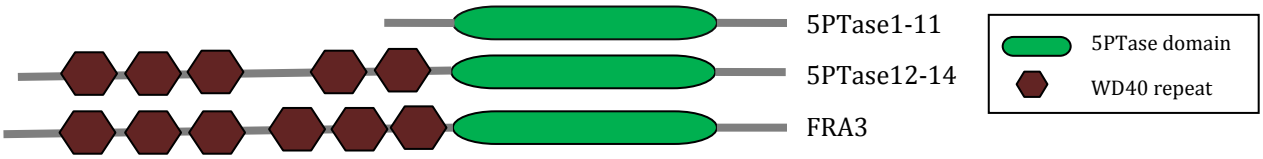

Figure 6. Domain organization of the Arabidopsis 5PTases. Each of the 5PTase family members contains a central conserved 5PTase catalytic domain. The 5PTase1 through 11 contain only the 5PTase catalytic domain whereas 5PTase12 through 14 as well as FRA3 (Fragile Fiber 3) contain 5-6 WD40 repeats in their N-termini. The WD40 domains facilitate protein-protein interactions.

Structure of the WD40 Domain

WD40 repeats are among the most abundant identifiable protein domains and are found in a wide variety of eukaryotic proteins that have a range of functions in signal transduction, pre-mRNA processing, cytoskeleton assembly, gene transcriptional activation, cell cycle control and apoptosis (Smith, 2008). Among the WD40 proteins are the β subunit of the G protein, the TAFII transcription factor, and the E3 ubiquitin ligase complexes (Li and Roberts, 2001). Within all these proteins the WD40 repeats are thought to have two common features: the domain folds into a β propeller; and the domains form a platform without any catalytic activity on which multiple protein complexes assemble reversibly (Li and Roberts, 2001; van Nocker and Ludwig, 2003; Smith, 2008).

The name WD40 is derived from the conserved tryptophan and aspartic acid residues (WD-Trp-Asp) and length of approximately 40 amino acids. The repeats typically end in Trp-Asp

but exhibit only limited amino sequence conservation. The specificity of the proteins is apparently determined by the sequences outside the repeats themselves (Smith, 2008).

When present in a protein, the WD40 domain is found as several (4-10) tandemly repeated units (blades) (Smith et al., 1999). As demonstrated by the crystal structure of the β subunit of G protein, it adopts a circularized β propeller structure made up of seven WD40 repeats (Wall et al., 1995; Sondek et al., 1996) (Figure 7A).

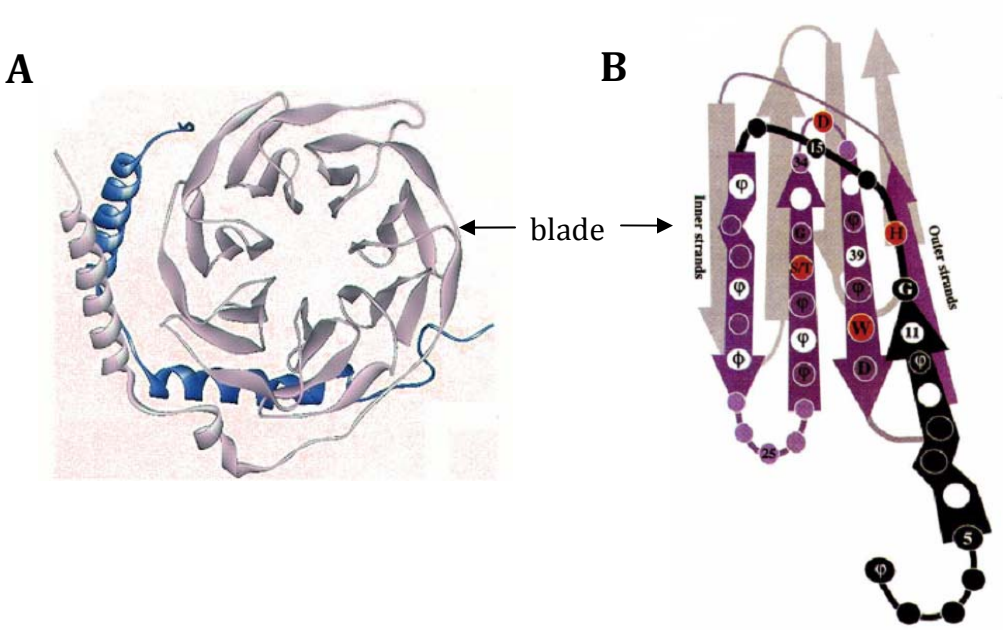

Figure 7. A diagrammatic view of the three-dimensional structure of the WD40 domain of G protein (β-subunit-in purple). A. Each WD40 repeat (blade) consists of four strands of a β sheet arranged around a central pseudosymmetrical axis into a circular β propeller with seven blades (Wall et al., 1995; Sondek et al., 1996; Li and Roberts, 2001). B. Each propeller blade contains the first three strands of the repeat unit and the last strand of the previous propeller blade. In each blade there are conserved residues important for protein interactions. Such residues are the hydrophobic Trp that interacts with Asp, His, Ser/Trn triad in the same repeat. The only invariant residue among the seven repeats is the Asp located in tight turn in the middle two strands of each β sheet (Sondek et al., 1996).

Each WD40 repeat comprises a four-stranded antiparallel β sheet. However, the repeat structure is not equivalent to each propeller blade; rather, the propeller blade contains the first three strands of the repeat unit and the last strand of the previous propeller blade. Thus, each propeller blade has only four strands, with the initial strand of each propeller blade being the last strand from the previous blade. This sharing of one strand between two blades is believed to stabilize the molecule (Figure 7B). The propeller structure provides extensive surface exposure of three surfaces: upper, lower, and the circumference (Wall et al., 1995; Sondek et al., 1996; Li and Roberts, 2001). The surfaces of this structure appear to provide a stable platform for several simultaneous protein-protein interactions.

A functional analysis revealed that there are 237 proteins that contain four or more recognizable copies of the WD40 domain in Arabidopsis (van Nocker and Ludwig, 2003). In some cases, sequences outside of the WD40 repeats may confer a new functional specificity to the protein even as conserved protein interactions are maintained through the WD40 repeats, potentially adapting basic cellular mechanisms to organism-specific processes. The presence of WD40 regions in the Arabidopsis 5PTases provides compelling evidence for protein: protein interactions in Ins(1,4,5)P_3 signal termination in plants. The four members of Group B 5PTases all have between 5 and 6 WD40 repeats and thus are speculated to function through protein –protein interactions.

Role of Arabidopsis 5PTases in Plant Growth, Development and Stress

Arabidopsis 5PTases have unique signal terminating abilities that could be exploited to better understand the impact of signal termination on plant responses to variety of stimuli. Recently, several Arabidopsis 5PTases have been shown to critically contribute to plant

growth, development and stress responses (Burnette et al., 2003; Carland and Nelson, 2004; Zhong et al., 2004; Lin et al., 2005; Jones et al., 2006; Gunesekera et al., 2007; Ananieva et al., 2008; Chen et al., 2008; Ercetin et al., 2008; Ananieva and Gillaspy, 2009).

Regulation of Seedling Growth- Role of 5PTase1, 2 and 11

The hypocotyls of dicotyledonous seedlings are widely used as a model for the physiological study of the mechanism of cell elongation and the variety of biological events that participate in its control. In order to explore the role of inositol signaling in seedling growth and development, Gunesekera et al., (2007) found that 5PTase1 (At1g34120) and 5PTase2 (At4g18010) are required for regulating seedling growth. When grown in the dark, seeds from *5ptase1* and *5ptase2* mutants germinate faster and have longer hypocotyls than WT seedlings. Seeds from these mutant lines also demonstrate an increase in sensitivity to the stress hormone ABA. These changes in early seedling growth are accompanied by mass increases in Ins(1,4,5)P_3, but not by changes in endogenous ABA content. By labeling the endogenous *myo*-inositol pool in *5ptase1* and *5ptase2* mutants, Gunesekera et al., (2007) detected increases in Ins(1,4,5)P_3 and a decrease in PtdIns, PtdIns(4)P, and PtdIns(4,5)$_2$ (Gunesekera et al., 2007). In 2008, Ercetin et al., (2008) showed that another 5PTase, called 5PTase11 (At1g47510), is also required for seedling growth. In contrast to *5ptase1* and *5ptase2*, seed from *5ptase11* mutants germinate slower and have decreased hypocotyl growth as compared to WT seedlings when grown in the dark. The hypocotyl growth changes correlate with a small increase in the 5PTase11 substrate, PtdIns(4,5)$_2$, and decreases in the potential products of 5PTase11, PtdIns(4)P and PtdIns(3)P (Ercetin and Gillaspy, 2004; Ercetin et al., 2008). However, *5ptase11* mutants also have a large increase in InsP_3 and InsP_2

species which may be Ins(4.5)P_2 (Ercetin et al., 2008). Taken together, these data indicate that the *5PTase1*, *5PTase2* and *5PTase11* genes have nonredundant roles in hydrolyzing inositol second-messenger substrates and that regulation of Ins(1,4,5)P_3 levels is important during germination and early seedling development.

Root Hair Morphogenesis- Role of MRH3 Protein

Root hairs are highly polarized cellular structures resulting from tip growth of specific root epidermal cells. Screening root-hair transcriptome for defects in root-hair morphogenesis lead to the identification of mutations in six genes one of which encodes 5PTase5 (At5g65090) and is called MRH3 (morphogenesis of root hair3). Root hairs of *mrh3* plants have wider root-hair initiation sites and hair bases than WT plants. Thus the *MRH3* gene is required for restricting both the size of the root-hair initiation site and the width of the root hairs during the transition to tip growth (Jones et al., 2006).

Leaf Development and Vascular Patterning – Role of CVP2 protein

The development of a complex vascular network that transports water, minerals, photosynthate, and signal molecules is essential to plants growing in nonaquatic environments. Vascular systems in most plants are comprised of several distinct cell and tissue types, including xylem and phloem. Xylem and phloem are organized in vascular bundles that are connected to form an integrated network in all parts of the plant (Carland et al., 1999).

The cotyledon vascular pattern 2 (*CVP2*) gene encodes 5PTase6 (At1g05470) and appears to regulate vascular strand propagation in cotyledons and rosette leaves. Mutation in

the *CVP2* gene ends the vascular strand propagation prematurely, resulting in an unclosed reticulum with open secondary and higher order veins. This mutant does not show perturbations in auxin content, response, or transport but has elevated Ins(1,4,5)P_3 and abscisic acid (ABA)-hypersensitive response. The authors attribute the open vascular network in *cvp2* mutants to unregulated *CVP2*-mediated Ins(1,4,5)P_3 production that elicits upregulation of otherwise tightly controlled response genes, presumably by an inappropriate release of Ca^{2+}. Misregulation of these genes prevents the specification of ground cells into vascular cell fate during vascular strand propagation (Carland and Nelson, 2004).

Auxin Homeostasis and Phototropin1 Signaling- Role of 5PTase13

Auxin is a plant hormone that plays roles in a number of plant processes such as apical dominance, root initiation and development, gravitropism and phototropism. The mechanism of phototropism includes the blue light as most effective and a flavoprotein called phototropin1 (PHOT1)(Christie, 2007).

In 2005, Lin et al., found that one of the members of Group B 5PTases, 5PTase13, plays a role in auxin homeostasis by using a mutant defective in the *5PTase13* gene (At1g05630). The *5ptase13-1* mutant had reduced auxin levels and altered expression of auxin regulated genes together with defects in vascular patterns (Lin et al., 2005). The cotyledon vascular pattern phenotype, however, was not confirmed by my experiments (Ananieva et al., 2008) and thereafter role of 5PTase13 in cotyledon vein development is not supported. In 2008, 5PTase13 was also found to play a role in PHOT1 signaling through a crosstalk between 5PTase13 and PHOT1 in the regulation of calcium under blue light (Chen et

al., 2008). Further connection between auxin and phototropin via 5PTase13 function was not identified.

Secondary Wall Synthesis and Strength of Fiber Cells- Role of FRA3 Protein

Arabidopsis inflorescence stems develop three to four layers of fiber cells between vascular bundles, and the mechanical strength of mature stems is largely attributable to these intervascular fibers (Zhong et al., 2001). To investigate the molecular mechanisms underlying fiber cell formation, Zhong et al., (2004) isolated a mutation in a *FRA3* (Fragile Fiber3) gene. The *FRA3* gene encodes a Group B 5PTase (At1g65580). The *fra3* mutation dramatically reduces secondary wall thickening, and this alteration is associated with abnormal actin organization in fiber cells. Moreover, the endogenous levels of PtdIns$(4,5)_2$ and Ins$(1,4,5)P_3$ are elevated in *fra3* stems. Together, these findings provide genetic evidence suggesting that the FRA3 5PTase plays an essential role in cell wall synthesis and actin organization (Zhong et al., 2004).

III. Nutrient Signaling and Energy Balance

Energy balance and metabolic homeostasis is a challenge for all organisms since it is important for normal cell growth and longevity as well as survival and stress response. In order to optimize their growth and development, organisms must constantly sense nutrient/energy- related internal and external stimuli. One important regulator of energy and nutrient sensing/ signaling is highly consereved in eukaryotes (Figure 8) and is called the AMPK (AMP-dependent protein kinase) in animals, the Snf1 (sucrose non-fermenting 1) in yeast and the SnRK1 (Snf1-related kinase) in plants (Polge and Thomas, 2007).

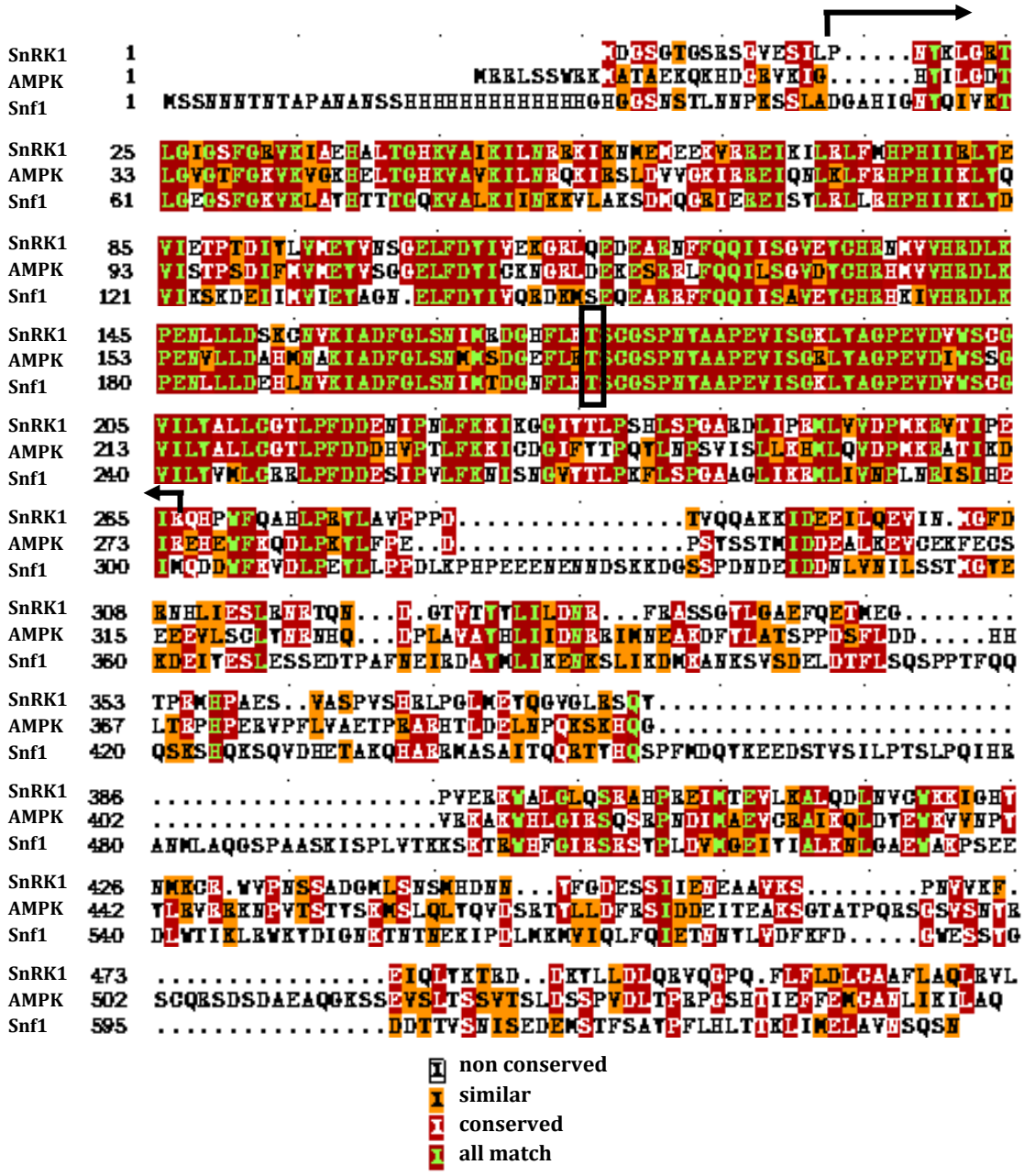

Figure 8. Amino acid alignment of SnRK1 and related proteins. Amino acid sequences corresponding to the α-subunits of the plant SnRK1, human AMPK and yeast Snf1 proteins were analyzed with ClustalX software. Arrows mark boundaries of the kinase catalytic domain, and a conserved threonine residue required for the kinase activation is framed.

Role of Mammalian AMPK in Cell and Whole Body Energy Homeostasis

AMPK is a heterotrimer complex comprised of a catalytic α-subunit, with a serine/threonine protein kinase domain, and two regulatory subunits, β and γ (Polge and Thomas, 2007). In mammals, each subunit is encoded by multiple genes ($\alpha 1$, $\alpha 2$, $\beta 1$, $\beta 2$, γ 1–γ 3), which results in 12 possible combinations of the AMPK complex (Hardie and Carling, 1997). The α-subunit contains an N-terminal kinase domain and a C-terminal domain involved in complex formation with β and γ subunits. The β-subunit is involved in the localization of the complex whereas the γ- subunit is involved in an allosteric activation of AMPK by AMP (Polge and Thomas, 2007). AMPK is also regulated by glucose starvation, upstream kinases and phosphatases (Polge and Thomas, 2007; Lage et al., 2008).
In mammals, AMPK is involved in sensing the cellular energy level. For example, during prolonged exercise AMPK is activated by AMP and it switches off ATP-consuming pathways such as the synthesis of fatty acids, cholesterol and proteins and switches on ATP-producing pathways such as fatty acid oxidation and glycolysis (Hardie, 2004, 2008).

AMPK is also important for whole body energy /glucose homeostasis. In muscle cells, activation of AMPK results in increased glucose uptake, a fact consistent with the role of skeletal muscles in maintaining glucose homeostasis (Hardie and Carling, 1997). AMPK is also important for the glucose homeostasis in the blood, because when the blood level glucose is low it participates in the inhibition of insulin production (da Silva Xavier et al., 2000; da Silva Xavier et al., 2003). Moreover AMPK might participate in the inhibition of glucose metabolism in the liver by controlling the expression of glycolitic and lipogenic enzymes (Leclerc et al., 1998). Finally, AMPK might regulate energy intake. In the hypothalamus, for instance, AMPK is inhibited by glucose, leptin, and insulin, which repress food intake, whereas

it is activated by ghrelin, a hormone that stimulates food intake (Andersson et al., 2004; Minokoshi et al., 2004).

Role of Yeast Snf1 in Adaptation to Energy Source

Snf1 in yeast is also a heterotrimeric complex composed of α-, β-, and γ-subunits (Carlson, 1998). The complex contains one of three β subunits, Sip1, Sip2 or Gal83 that binds to the catalytic α- subunit, Snf1 (a serine/threonine kinase). Snf1 contains regulatory and catalytic domains. It is known that the regulatory domain auto-inhibits the catalytic domain in high glucose media (McCartney and Schmidt, 2001). In low or no glucose this autoinhibition is relieved by the γ subunit, Snf4, that binds to the auto-inhibitory domain of Snf1, releasing its catalytic domain (Carlson, 1998; Polge and Thomas, 2007). Snf1 is also regulated by the AMP:ATP ratio, upstream protein kinases and phosphatases and other regulatory proteins such as STD1 (Wilson et al., 1996; McCartney and Schmidt, 2001; Kuchin et al., 2003).
Snf1 is important for the adaptation of yeast to varying sources of energy through the diauxic shift (Polge and Thomas, 2007). In the presence of glucose, ATP is produced by fermentation whereas Snf1 is inhibited via the hexokinase HXK2 (Schuller, 2003). Glucose is used as a carbon source during fermentation and genes involved in the utilization of non-fermentive carbon sources are repressed by the transcription factor MIG1 (Carlson, 1998). In the absence of glucose, Snf1 is activated by upstream kinases and it derepresses genes repressed by MIG1. Activated Snf1 phosphorylates MIG1, which is exported from the nucleus to the cytosol (Carlson, 1998). Snf1 also acts directly to activate transcriptional activators and not surprisingly 439 genes of the yeast genome are regulated by Snf1 (Polge and Thomas, 2007).

Role of Plant SnRK1 in Nutrient Sensing and Energy Deficit

The Snf1 homolog in plants, SnRK1, also shows remarkable structural and functional conservation. It is a heterotrimeric complex represented by three α-subunits (SnRK1.1, 1.2 and 1.3), three β-subunits (β3 is unique to plants) and 1 γ-subunit. The Arabidopis SnRK1 also contains a βγ-subunit that is plant specific (Polge and Thomas, 2007). SnRK1 is inhibited by glucose, sucrose, G6P (glucose 6-phosphate), T6P (trehalose 6-phosphate), upstream phosphatases and other proteins such as PRL1, AL2 and L2 (Bhalerao et al., 1999; Sugden et al., 1999; Halford et al., 2003; Lee et al., 2008; Zhang et al., 2009). On the other hand, SnRK1 is activated by AMP, upstream kinases, dark, energy deprivation and stress (Sugden et al., 1999; Rolland et al., 2006; Baena-Gonzalez et al., 2007; Baena-Gonzalez and Sheen, 2008). Additionally, SnRK1 is regulated by the proteasome since it is targeted to proteasomal degradation by two different E3 ligase complexes: the SCF -CUL1-E3 ligase complex (mediated by SKP1/ASK1) and the CUL4-based-E3 ligase complex (mediated by the PRL1 protein) (Farras et al., 2001; Lee et al., 2008).

SnRK1 was first identified to directly affect the activity of downstream target proteins such as 3-hydroxymehyl-3-methylglutaryl-CoA reductase (HMGR), nitrate reductase (NR), sucrose phosphate synthase (SPS) and trehalose-phosphate synthase 5 (TPS5) (Dale et al., 1995; Dale et al., 1995; Halford et al., 2003; Harthill et al., 2006). Recently, SnRK1 was identified as a master regulator of the plant transcriptome in response to darkness, starvation and multiple types of stress (Baena-Gonzalez et al., 2007; Baena-Gonzalez and Sheen, 2008). For instance, in response to energy deficit, SnRK1 triggers the induction of 288 genes and represses 320 other genes involved in wide variety of cellular processes. This metabolic switch induced by SnRK1 is important to provide alternative sources of metabolites and

energy upon starvation as a result of darkness or stress. Conversely, sugar availability regulates these genes in an opposite manner (Baena-Gonzalez et al., 2007; Baena-Gonzalez and Sheen, 2008). Thus SnRK1 is involved in transcriptional reprogramming as an important part of the convergent responses to stress, nutrient starvation and darkness.

Possible Links between Inositol Signaling/Metabolism and SnRK1-Mediated Energy Signaling

For more than a century, *myo*-inositol has been recognized as an important molecule with multifunctional roles in plants and its metabolic products have impacted plant growth and development (Loewus, 1969; Schneider et al., 2006). *Myo*-inositol can be incorporated in the second messenger Ins (1,4,5)P_3, methylated to the osmolyte pinitol or oxidized and thus converted to metabolite products important for cell wall synthesis or ascorbic acid synthesis (Lorence et al., 2004; Loewus, 2006; Schneider et al., 2006). *Myo*-inositol, and its derivatives, can also be seen as alternative source of energy since it plays an important role as a precursor in the synthesis of the nucleotide sugar uridine diphosphoglucuronic acid (UDP-GlcUA) and as a carrier of activated galactose (Gal) that is eventually transferred to sucrose (Suc) (Murthy, 1996). Moreover, phytic acid ($InsP_6$), the product of inositol phosphorylation represents a storage form for both inositol and phosphorus and may even represent a cellular energy currency (Raboy, 2003).

Recent microarray data indicates that SnRK1 as well as sugars regulate transcription of genes encoding key enzymes in *myo*-inositol metabolism and inositol signaling (Baena-Gonzalez et al., 2007; Ananieva et al., 2008; Ananieva and Gillaspy, 2009). In particular, glucose activates transcription of two genes required for *myo*-inositol synthesis

(*myo*-inositol-1-phosphate synthase, MIPS1 [At4g39800], and vitamin C4, VTC4 [At3g02870]), while repressing expression of the *myo*-inositol oxygenase 2 gene (At2g19800; MIOX2) that encodes an enzyme required for *myo*-inositol oxidation to D-glucuronic acid (DGlcA) (Lorence et al., 2004; Price et al., 2004). Glucose also represses transcription of three 5PTase genes. At the same time SnRK1.1 overexpression has the opposite effect on these genes, with MIPS1 and VTC4 undergoing repression, while transcription of MIOX2 and certain 5PTases increases (Baena-Gonzalez et al., 2007). These results indicate that energy and nutrient signals interconnect with *myo*-inositol metabolism and signaling in a complex signaling network that is now beginning to be understood.

CHAPTER II

OBJECTIVE I. Role of 5PTase13 in Sugar and Stress Signaling via Formation of a Protein Complex with SnRK1

"Interaction of the WD40 Domain of a *Myo*-inositol Polyphosphate 5-Phosphatase with SnRK1 Links Inositol, Sugar, and Stress Signaling"

Adapted from: **Elitsa A. Ananieva, Glenda E. Gillaspy, Amanda Ely, Ryan N. Burnette, and F. Les Erickson. Interaction of the WD40 Domain of a *Myo*-inositol Polyphosphate 5-Phosphatase with SnRK1 Links Inositol, Sugar, and Stress Signaling, December, 2008, Vol. 148, pp. 1868-1882. Copyright 2009, Plant Physiology. Used with permission of the American Society of Plant Biologist.**

ABSTRACT

In plants, *myo*-inositol signaling pathways have been associated with several stress, developmental, and physiological processes, but the regulation of these pathways is largely unknown. In our efforts to better understand *myo*-inositol signaling pathways in plants, we have found that the WD40 repeat region of a *myo*-inositol polyphosphate 5-phosphatase (5PTase13; At1g05630) interacts with the sucrose nonfermenting-1-related kinase (SnRK1.1) in the yeast two-hybrid system and *in vitro*. Plant SnRK1 proteins (also known as AKIN10/11) have been described as central integrators of sugar, metabolic, stress, and developmental signals. Using mutants defective in 5PTase13, we show that 5PTase13 can act as a regulator of SnRK1 activity and that regulation differs with different nutrient availability. Specifically, we show that under low-nutrient or sugar conditions, 5PTase13 acts as a positive regulator of SnRK1 activity. In contrast, under severe starvation conditions, 5PTase13 acts as a negative regulator of SnRK1 activity. To delineate the regulatory interaction that occurs between 5PTase13 and SnRK1.1, we used a cell-free degradation assay and found that 5PTase13 is required to reduce the amount of SnRK1.1 targeted for proteasomal destruction under low-nutrient conditions. This regulation most likely involves a 5PTase13-SnRK1.1 interaction within the nucleus, as a 5PTase13:green fluorescent protein was localized to the nucleus. We also show that a loss of function in 5PTase13 leads to nutrient level-dependent reduction of root growth, along with abscisic acid (ABA) and sugar insensitivity. *5ptase13* mutants accumulate less inositol 1,4,5-trisphosphate in response to sugar stress and have alterations in ABA-regulated gene expression, both of which are consistent with the known role of

inositol 1,4,5-trisphosphate in ABA-mediated signaling. We propose that by forming a protein complex with SnRK1.1 protein, 5PTase13 plays a regulatory role linking inositol, sugar, and stress signaling.

INTRODUCTION

Myo-inositol (inositol) signaling pathways are important for many different developmental and physiological processes in eukaryotes (Berridge, 2007). In plants, inositol signaling is used in the response to abscisic acid (ABA(Sanchez and Chua, 2001; Xiong et al., 2001; Burnette et al., 2003; Gunesekera et al., 2007; Lee et al., 2007), salt stress(DeWald et al., 2001; Takahashi et al., 2001), gravity (Perera et al., 2001; Perera et al., 2006), and pathogens (Ortega and Perez, 2001; Andersson et al., 2006). The inositol signaling pathway makes use of an inositol 1,4,5-trisphosphate ($Ins(1,4,5)P_3$; $InsP_3$) second messenger that triggers intracellular Ca^{2+} release from various sources within the cell (Berridge, 1993; Krinke et al., 2007; Tang et al., 2007), although the precise mechanism in plants is not yet known (Krinke et al., 2007). To terminate signaling events driven by $Ins(1,4,5)P_3$, cells utilize the *myo*-inositol polyphosphate 5-phosphatases (5PTases; EC 3.1.3.56) to remove the 5-phosphate, thus initiating messenger breakdown (Astle et al., 2007). Eukaryotes have a family of diverse 5PTases, with the Arabidopsis (*Arabidopsis thaliana*) genome containing 15 genes predicted to encode conserved 5PTases (Berdy et al., 2001). Of the 15 Arabidopsis 5PTase genes, four encode 5PTase enzymes with a large, N-terminal extension containing five to six WD40 repeat regions (Zhong and Ye, 2004). WD40 repeats are found in a number of eukaryotic regulatory proteins (Li and Roberts, 2001), where they are speculated to serve as a stable propeller-like platform to which proteins can bind either stably or reversibly. In some cases, sequences outside of the WD40 repeats may confer a new functional specificity to the protein even as conserved protein interactions are maintained through the WD40 repeats, potentially

adapting basic cellular mechanisms to organism-specific processes. WD40-containing 5PTases are unique to plants and certain fungi, as no other genomes contain candidate genes for these proteins (Zhong and Ye, 2004).

By examining plants containing either a gain or loss of function in specific 5PTases, investigators have established that 5PTases are critical in plant development and in ABA signaling. In particular, mutations in the *CVP2* (5PTase6; At1g05470) and *5PTase13* (At1g05630) genes have been linked to altered cotyledon vascular patterning and/or blue light responses and phototropin 1 signaling (Carland and Nelson, 2004; Lin et al., 2005; Chen et al., 2008). In contrast, *fra3* (At1g65580) and *mrh3* (5PTase5; At5g65090) mutants are altered in fiber cell development (Zhong et al., 2004) and root hair initiation (Jones et al., 2006), respectively. With regard to stress signaling, ectopic expression of either 5PTase1 or 5PTase2 has been shown to decrease ABA signaling by increasing hydrolysis of Ins(1,4,5)P_3 (Sanchez and Chua, 2001; Burnette et al., 2003). Loss-of-function mutants in these same genes result in ABA hypersensitivity in germinating seeds and increased seedling hypocotyl elongation in the dark, which is accompanied by an increase in Ins(1,4,5)P_3 levels (Gunesekera et al., 2007).

5PTases have been reported to play a role in Glc sensing/metabolism in animal cells (Sasaoka et al., 2001; Wada et al., 2001; Kagawa et al., 2008). Overexpression of an SH2-containing inositol phosphatase 2 (SHIP2) inhibited insulin-induced signaling leading to Glc uptake and glycogen synthesis via hydrolysis of phosphatidylinositol 3,4,5-trisphosphate (PtdIns-P3) in 3T3-L1 adipocytes and L6 myotubes (Sasaoka et al., 2001; Wada et al., 2001). On the other hand, loss of SHIP2 in mice resulted in increased sensitivity to insulin, which is characterized by deregulated expression of genes involved in gluconeogenesis and perinatal

death (Clement et al., 2001). Although there are recent reports delineating some relationship between inositol signaling and sugar sensing/metabolism in plant cells (Im et al., 2007; Lou et al., 2007), a specific role of 5PTases in sugar signaling has not yet been determined. The mechanisms by which plants sense sugars and regulate carbohydrate metabolism are complex and often facilitated by protein complexes. Therefore, we sought to identify 5PTase-interacting proteins involved in signaling and metabolic events.

We report here that the WD40 repeat region of the 5PTase13 gene interacts specifically with a Suc nonfermenting-1-related kinase (SnRK1.1, AKIN10; At3g01090), which functions as a sensor of energy and stress in plants (Baena-Gonzalez et al., 2007; Hardie, 2007; Hue and Rider, 2007). Using T-DNA insertion mutants in the *5PTase13* gene, we present evidence that 5PTase13 is a nuclear protein that can act as a regulator of SnRK1.1 under low-nutrient conditions by decreasing the amount of SnRK1.1 degraded by the proteasome.

RESULTS

5PTase13 Is a Member of a Unique Group of WD40-Containing Proteins

Besides containing a conserved inositol polyphosphate 5-phosphatase catalytic domain, 5PTase13 also contains five WD40 repeat regions in the N terminus that may allow for unique protein interactions. Three other genes in the Arabidopsis genome, *5PTase12* (At2g43900), *5PTase14* (At2g31830), and *FRA3* (At1g65580), encode similar proteins (Berdy et al., 2001; Zhong and Ye, 2004), and the amino acid identity of the WD40 repeat region varies from 45.5 % to 75.3 % among these proteins (Supplemental Table S1). We used the amino acid sequences corresponding to these WD40 repeat regions in BLASTp searches and obtained 12 related sequences with e-values less than 1. ClustalW and PAUP4.0 were used to generate phylogenetic trees using parsimony (Figure 9), which showed that the 5PTase WD40 repeat regions are contained on a separate branch, thus indicating that they are more similar to one another than to other WD40 repeat regions. The similarity of the 5PTases (Zhong and Ye, 2004) suggests that these proteins may function in a redundant manner. Microarray data from GENEVESTIGATOR (Zimmermann et al., 2004) indicates that *FRA3* is broadly and abundantly expressed compared with *5PTase12*, *5PTase13*, and *5PTase14* (Supplemental Figure S1A). We conclude that the WD40-containing 5PTases are a small group of proteins with the potential to form protein complexes and that functional redundancy may be present.

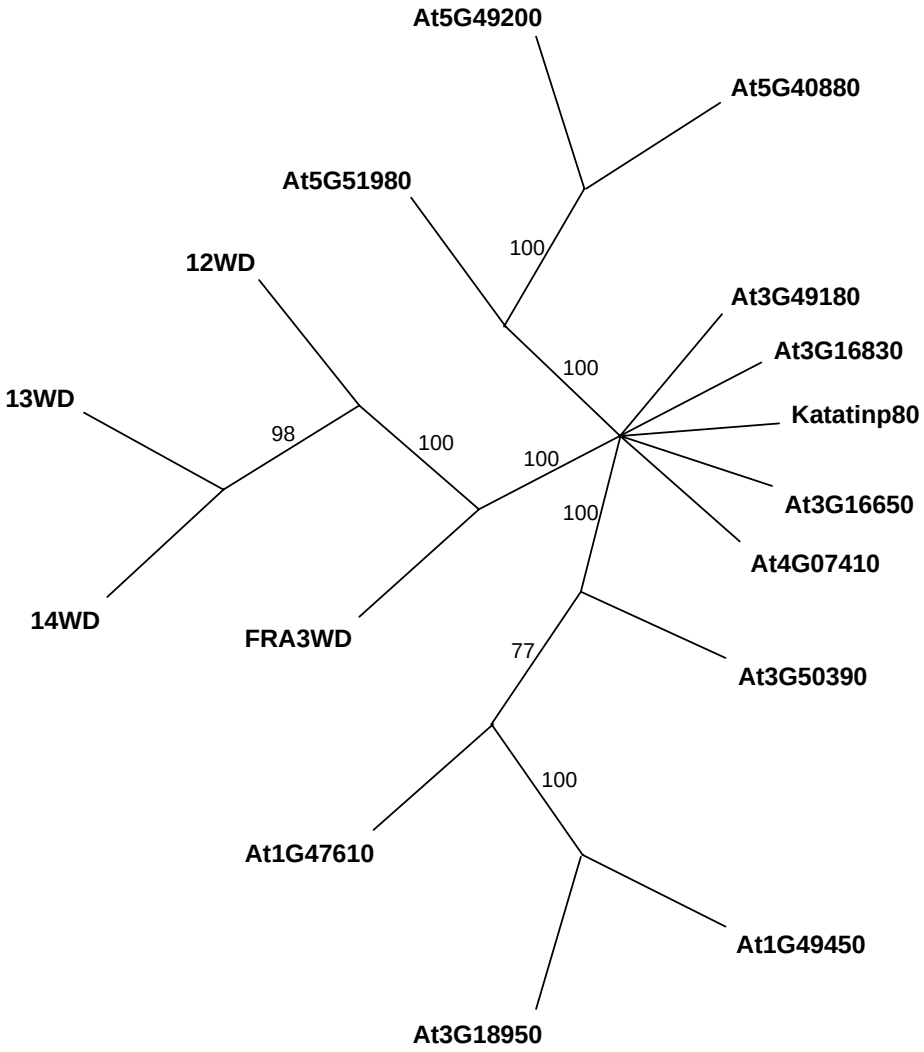

Figure 9. Phylogenetic tree of the WD40 regions from 5PTases and other WD40-containing Arabidopsis proteins. ClustalW and PAUP4.0 were used to generate a tree. Bootstrapping (1000 times) yielded a confidence level indicated at each branch. The results show that the WD40 region of 5PTase14 (14WD) is the closest relative to 5PTase13 (13WD). Further, the tree indicates that the 5PTase WD40 regions (12WD, 13WD, 14WD, FRA3WD) are more closely related to each other than to other WD40-containing proteins.

The WD40 Repeat Region of 5PTase13 Interacts with SnRK1.1

To investigate the ability of the WD40 regions of 5PTase13 to participate in protein complexes, we used the yeast two-hybrid system. The 533 N-terminal amino acids from 5PTase13 containing the WD40 repeats were used as bait in a yeast two-hybrid screen of an Arabidopsis 3d-old etiolated seedling cDNA library. We screened over 1 million yeast transformants and obtained a positive clone containing the C-terminal domain of the SnRK1.1 gene (At3g01090; also known as AKIN10). We retransformed this positive clone into yeast and verified the interaction (Figure 10). Negative controls, including the empty DNA binding domain and activation domain vectors, established that SnRK1.1 binds to the WD40 repeat region of the 5PTase13 protein in yeast. To examine the interaction between 5PTase13 and SnRK1.1 *in vitro*, we fused the sequence encoding the Xpress epitope tag to the N- terminus of the WD40 repeat region of 5PTase13 (13WDX) and the V5 epitope tag sequence to the C terminus of SnRK1.1 (SnRKV5) and expressed both proteins in Escherichia coli. The SnRKV5 construct directs the expression of a 61.7-kD protein detected by an anti-V5 monoclonal antibody, and in most cases we detected two SnRKV5 bands, perhaps as a result of phosphorylation or proteolytic cleavage (Figure 11, lane 1). The 13WDX construct directs the expression of a 65.9-kD protein detected by an anti- Xpress monoclonal antibody (Figure 11, lane 2). These interactions are specific, as SnRKV5 is not detected by the anti-Xpress antibody and 13WDX is not detected by the anti-V5 antibody (data not shown). To determine whether the SnRK1.1 recombinant protein can “pull down” 13WDX, immunoprecipitations using anti-V5:protein A-Sepharose beads were performed, and the resulting complex was then analyzed by western blotting with an anti-Xpress antibody (Figure 11, IP lanes). As shown in Figure 11, the WD40 repeat region from 5PTase13 (13WDX) is only detected in this pull-down assay

when it has been incubated in the presence of SnRKV5. We conclude that the WD40 repeat region from 5PTase13 and SnRK1.1 can form a protein complex *in vitro*.

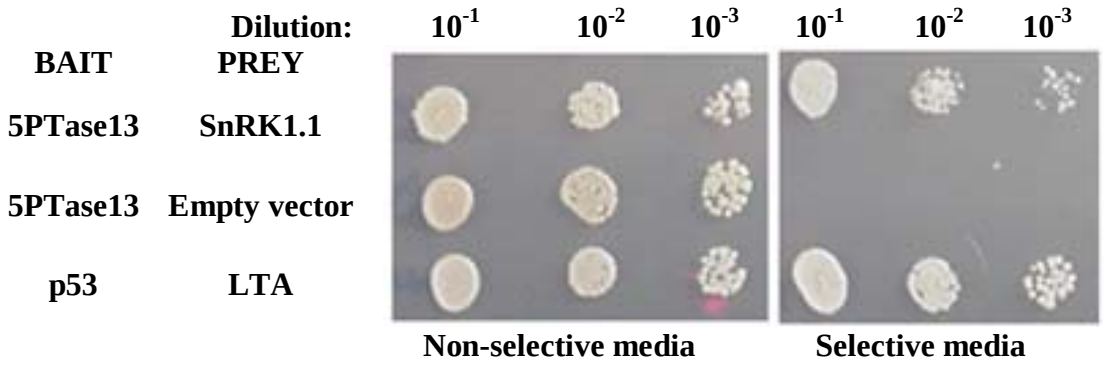

Figure 10. Yeast Two-Hybrid Screen. An Arabidopsis cDNA PREY library was screened using the WD40 region of 5PTase13 as a BAIT in the yeast two-hybrid system. Over 1 million yeast transformants were screened for reporter gene expression, which resulted in the isolation of a PREY plasmid expressing the C-terminal domain of SnRK1.1. Serially-diluted yeast strains were spotted onto agar plates that are either non-selective or selective for expression of the two hybrid reporter genes.

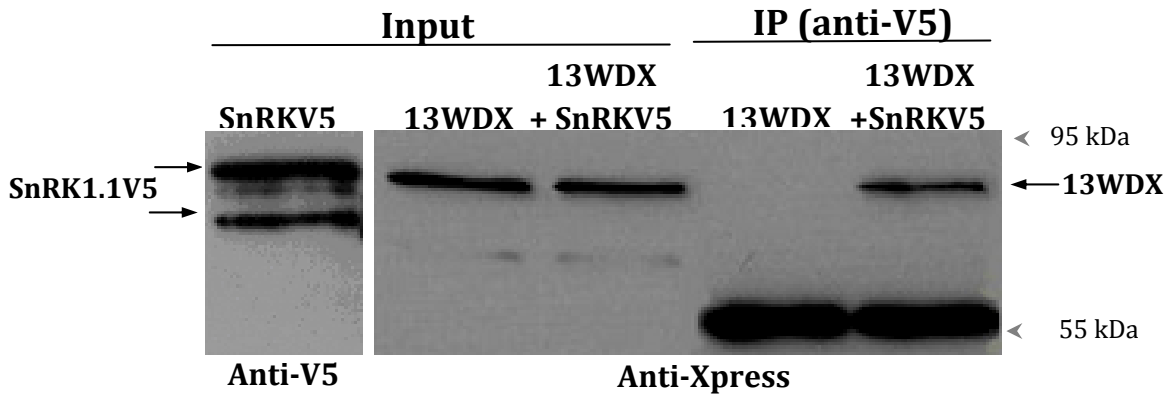

Figure 11. 13WD40-Xpress protein interacts with SnRK1.1-V5 *in vitro*. Immunoprecipitation (IP) was carried out using an anti-V5 antibody bound to a protein A sepharose (PAS). Purified and dialyzed proteins (13WDX and SnRKV5) were incubated for 2 hrs at room temperature in IP buffer before transferring to the antiV5:PAS complex. The resulting IP fractions were analyzed using a protein gel blotting: lane 1. Input fraction of SnRKV5 probed with an anti-V5 antibody; lane 2. Input fraction of 13WDX; lane 3. Input fraction of 13WDX in combination with SnRKV5; lane 4. Bound fraction of 13WDX alone; lane 5. Bound fraction of 13WDX in combination with SnRKV5. Lanes 2 through 5 were probed with an anti-Xpress antibody. The 55 kDa band is the immunoglobin heavy chain component of the anti-V5 antibody. The blot images are representative of four independent experiments.

SnRK1.1, along with its closely related gene family member SnRK1.2, encodes a Suc nonfermenting-1-related kinase implicated as a central integrator of energy signaling and metabolic regulation in yeast, plants, and animals. The interaction of 5PTase13 and SnRK1.1 is novel and is perhaps unique to plants in that yeast and animal 5PTases do not contain WD40 regions. This interaction may indicate that Ins(1,4,5)P_3 signal termination via 5PTase13 function affects the SnRK1 "energy sensor" in plants. Data obtained from the GENEVESTIGATOR database indicate that SnRK1.1, SnRK1.2, and 5PTase13 are detected in most plant tissues examined, although 5PTase13 expression levels are very low compared with SnRK1 gene expression (Supplemental Figure S1B).

5PTase13 Mutant Identification

To further explore the link between Ins(1,4,5)P_3 signaling and the energy sensor, SnRK1.1, we isolated two independent T-DNA insertion mutants in the *5PTase13* gene. Two potential mutants were identified in the SALK T-DNA database and named *5ptase13-1* (SAIL_350_F01) and *5ptase13-2* (SALK_081991) and were compared with their corresponding wild-type accessions (Figure 12A). The presence of the T-DNA insertion was verified by diagnostic PCR in each mutant using genomic DNA and primers specific for the T-DNA left border (LB) and gene-specific primers that flank the T-DNA insertion (Figure 12A and B). The resulting LB gene-specific fragments were sequenced, indicating that in *5ptase13-1* mutants, a second T-DNA insertion is found in tandem in the fourth exon (Figure 12A and B, LB-R band). This is in contrast to the previously reported analysis by Lin et al. (2005) showing that the *5ptase13-1* mutant contains a single T-DNA insertion. Using primers specific for the 3'end of 5PTase13, we detected a PCR product in both wild-type lines used (CS60000 and CS908) but

not in *5ptase13-1* and *5ptase13-2* mutants (5PTase13 in Figure 12C). Using primers that amplify the 5' end, we detected a 1.68- kb product in both wild-type lines and in the *5ptase13-1* mutant, but not in *5ptase13-2* (Figure 12C).We conclude that the *5ptase13-2* mutant is totally lacking 5PTase13 expression and that both *5ptase13-1* and *5ptase13-2* mutant lines do not express transcripts capable of encoding a full-length 5PTase13 protein.

To examine how the loss of 5PTase13 affects the expression of its binding partner SnRK1.1, we examined the expression of SnRK1.1 and its closely related isoform, SnRK1.2, in 7-d-old dark-grown *5ptase13* and wild-type seedlings. The results reveal that there are no large changes in SnRK1.1 and SnRK1.2 in *5ptase13* mutants (Figure 12D). As shown in Figure 12D, we found that FRA3 expression remains unchanged in *5ptase13* mutants, and 5PTase14 expression is barely detectable but also unchanged. In contrast, the expression of 5PTase12 is increased in both *5ptase13* mutant lines, revealing a possible means of compensation for the loss of 5PTase13 function (Figure 12D).

Under standard laboratory conditions, *5ptase13* did not exhibit any abnormalities in plant growth or development. Since Lin et al. (2005) previously reported that *5ptase13-1* mutants are altered in cotyledon vein development, we carefully examined both *5ptase13-1* and *5ptase13-2* mutants and their corresponding wild-type accessions for cotyledon vein development, as described by Carland and Nelson (2004). Using 7d-old light-grown seedlings of wild-type and *5ptase13* mutant soil-grown plants, we found no evidence for a cotyledon vein phenotype (Supplemental Tables S2 and S3). Our analysis revealed that 33.3 % of total WT1 cotyledons and 26.18 % of total *5ptase13-1* cotyledons have abnormal patterns and that only 15.9 % of total WT2 cotyledons and 19.4 % of total *5ptase13-2* cotyledons can be classified as abnormal (Supplemental Table S3). Thus, there is variation in cotyledon vein

development within different wild-type accessions, but not between *5ptase13* mutants and their matched wild-type accessions.

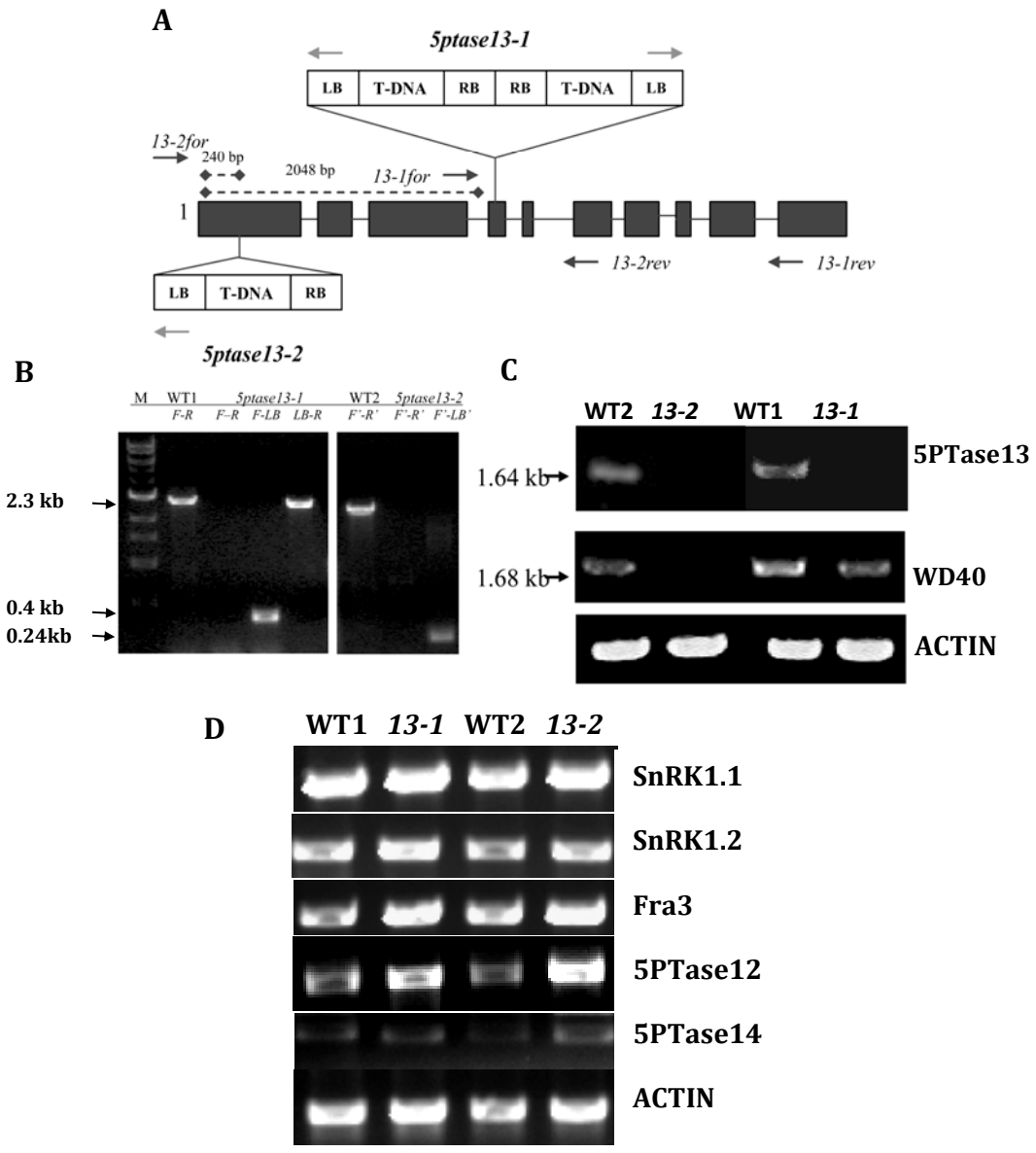

Figure 12. T-DNA insertions and gene expression in *5ptase13* mutant lines. A. T-DNA insertions in the 5PTase13 gene. Exons are dark gray boxes; light gray arrows indicate primers used to amplify the left border (LB) of the T-DNA; dark gray arrows indicate positions of gene-specific primers. B. PCR reactions performed with gene specific and left border (LB) primers confirm that both lines are homozygous. Gene specific primers that flank the T-DNA insertion (primers **F**orward: *13-1for* and **R**everse: *13-1rev*) in conjunction with the T-DNA LB primer amplify 0.4 kb and 2.3 kb fragments in *5ptase13-1* mutants, indicating the presence of two LB sequences in proximity to the 5PTase13 gene. C-D. Expression of genes in *5ptase13* mutants and WT seedlings. Total RNA (1-2 µg) was isolated and

semi-quantitative RT–PCR reactions were performed with the indicated primers as described (Supplemental Table S4). C. Verification of loss of 5PTase13 expression in 2 week-old leaves from soil-grown plants. D. SnRK1 and 5PTase expression from 7-day old WT and *5ptase13* (*13-1* and *13-2*) mutant seedlings grown on 0.5x MS salts, 0.8 % agar in the dark. The experiment was independently repeated two times.

SnRK1 Activity Is Altered in 5ptase13 Mutants and Varies with Nutrient Conditions

To determine whether 5PTase13 affects SnRK1 function, we measured the activity of SnRK1 in *5ptase13* mutants and wild-type seedlings grown under various nutrient conditions. It is well documented that SnRK1 regulates multiple transcription cascades in response to sugar or energy deprivation (Baena-Gonzalez et al., 2007); however, whether in planta SnRK1 activity changes under various nutrient conditions is not known. To address this, we measured SnRK1 activity from 7d-old wild-type seedlings grown under low light (40 μE) with different added nutrients to establish various "low-energy" conditions: no nutrients (agar and water alone), low nutrients (0.5x Murashige and Skoog [MS] salts and agar), and optimal nutrients (0.5x MS salts, agar, and 3 % Suc). In addition, we examined a stressful level of added sugar (0.5x MS salts, agar, and 6 % Glc). For this work, we used a well- established SnRK1 assay (Radchuk et al., 2006) and incubated a sucrose phosphate synthase (SPS) substrate peptide (Huang and Huber, 2001)**,** radiolabeled [γ-^{32}P]ATP, and 5 μg of plant protein extract for 30 min. Validation that these conditions are in the linear range of product accumulation is shown in Supplemental Figure S2. As expected from its role as a low-energy sensor, SnRK1 activity is higher in seedlings grown on low nutrients compared with extracts prepared from seedlings grown on optimal nutrients or 6 % Glc (Figure 13). Figure 14A shows that the activity of SnRK1 significantly increases in *5ptase13-1* and *5ptase13-2* mutants when seedlings are grown with no nutrients (8.1- and 11.3-fold increases, respectively). In contrast, SnRK1 activity decreases in *5ptase13-1* and *5ptase13-2* seedlings compared with wild-type seedlings when grown with low nutrients (Figure 14B). Furthermore, the decline in SnRK1 activity is even more dramatic when 6 % Glc is added (7.1- and 3.3-fold reduction, respectively; Figure 14C). We conclude that a loss of 5PTase13 function affects SnRK1 activity,

and the impact differs depending on nutrient availability. Our data support a role for 5PTase13 as a negative regulator of SnRK1 activity in the absence of nutrients and as a positive regulator when either low nutrients or 6 % Glc is present.

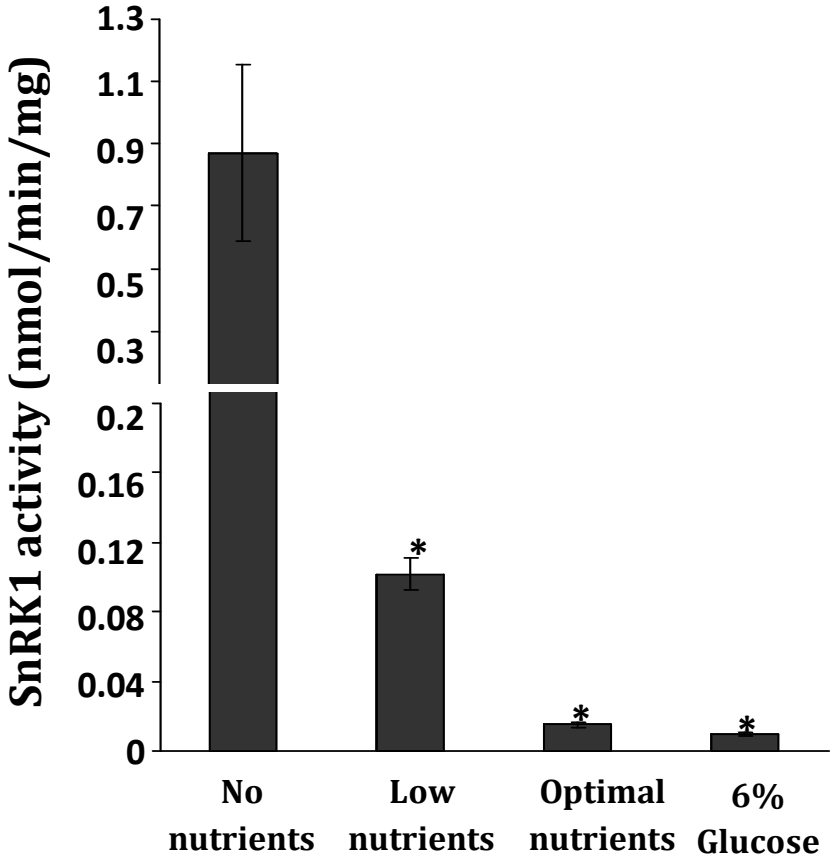

Figure 13. SnRK1 activity varies with different nutrient conditions. Seed from WT (WT2-CS60000) plants was grown on 0.8 % agar, no nutrients, low nutrients (0.5x MS), optimal nutrients (0.5x MS, 3 % sucrose) or 6 % glucose (0.5x MS, 6 % glucose) under low light for 7 days. The seed grown in 6 % glucose was allowed to germinate in a 0.5x MS media for 4 days and then transferred to a 6 % glucose media for 3 days. SnRK1 activity with an SPS peptide was measured from crude plant extracts precipitated with ammonium sulfate according to the method described (Radchuk et al., 2006). Bars represent the mean ± SE of 3 replicates. The experiment was independently repeated two times. * indicates a p value < 0.05 as compared to no nutrients.

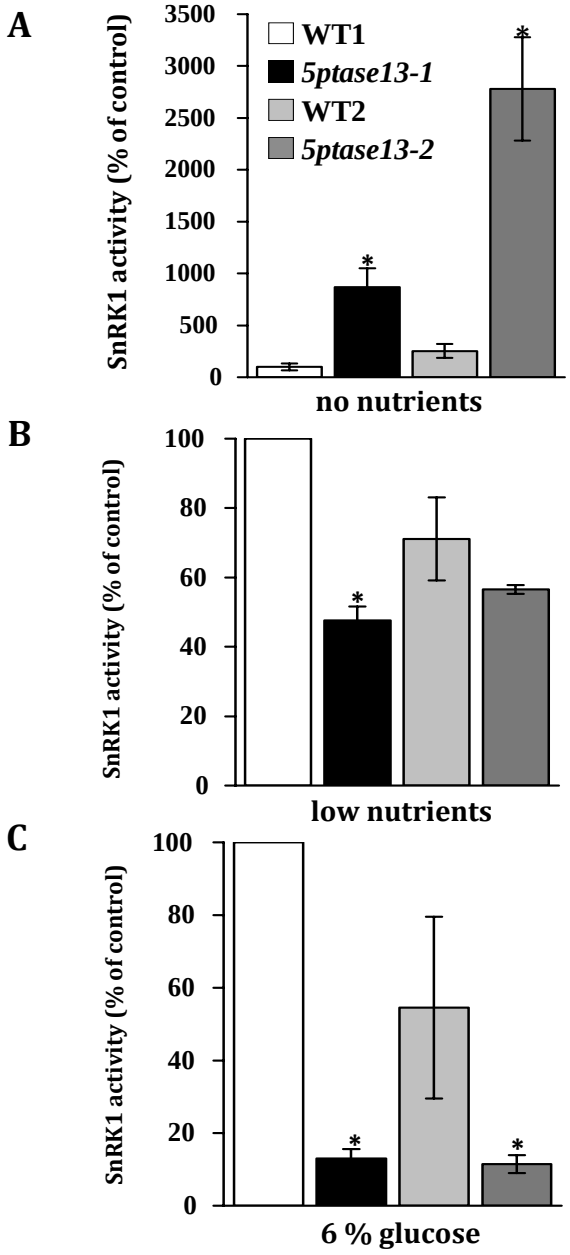

Figure 14. SnRK1 activity in *5ptase13* mutants. SnRK1 activity was measured in crude plant extracts from 7-day old seedlings precipitated with ammonium sulfate according to the method described (Radchuk et al., 2006) using an SPS peptide. Values for SnRK1 activity (nmoles Pi/min/mg protein) are normalized to WT1. Extracts are from seedlings grown in A. no nutrients; B. low nutrients (0.5x MS); C. 6 % glucose (0.5x MS, 6 % glucose). Bars represent the mean ± SE of 3 replicates. The experiment was independently repeated two times. * indicates a p value < 0.05 as compared to WT.

5PTase13 Affects SnRK1.1 Stability

To explore whether 5PTase13 regulates SnRK1.1 stability, we used a similar approach as Lee et al. (2008) to examine the stability of recombinant V5- tagged SnRK1.1 (SnRKV5) in a cell-free degradation assay with wild-type or *5ptase13* extracts. The time course of SnRKV5 degradation with wild-type seedling extracts indicated that SnRKV5 is mostly degraded within 60 min (Figure 15A). MG132, a proteasome-specific inhibitor, blocked SnRKV5 degradation in both *5ptase13* and wild-type extracts (Figure 15B), indicating that SnRKV5 is destroyed by the 26S proteasome pathway in these assays. To test the hypothesis that 5PTase13 destabilizes SnRK1.1 under the no-nutrient conditions, we examined a 30-min time point for analysis as a midpoint to total SnRKV5 degradation. The data indicate no difference in SnRKV5 stability in wild-type and *5ptase13* extracts under the no-nutrient conditions (Figure 15C). In contrast, when extracts are prepared from seedlings grown on low nutrients, we find less SnRKV5 accumulation in *5ptase13* extracts compared with wild-type extracts (Figure 15D). We conclude that under the low nutrient conditions, 5PTase13 is required to stabilize SnRKV5 protein and slow its degradation by the 26S proteasome pathway. Furthermore, the increased degradation of SnRKV5 seen with the low-nutrient conditions correlates well with the lower SnRK1 activity levels measured in *5ptase13* mutants under these same nutrient conditions (Figure 14B). In contrast, 5PTase13 is not required to stabilize SnRKV5 when seedlings are grown with no nutrients, and this is consistent with the switch in SnRK1 activity levels we found in *5ptase13* mutants grown with no nutrients (Figure 14A). However, since we did not observe an increase in SnRKV5 stability in *5ptase13* extracts prepared from the no-nutrient conditions, we speculate that there is an

additional mechanism that influences the elevated SnRK1 activity in *5ptase13* mutants under these conditions.

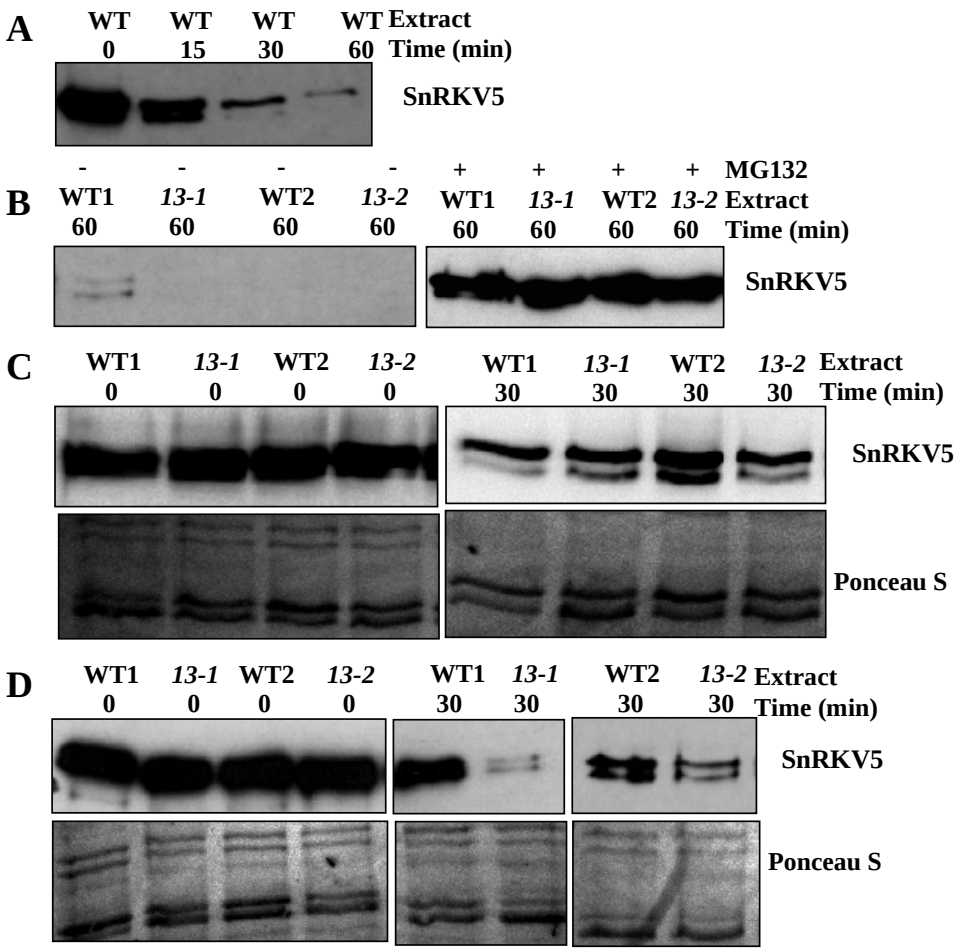

Figure 15. Degradation of V5-tagged SnRK1.1 in cell extracts from WT and *5ptase13* mutant seedlings grown under different nutrient conditions. SnRK1.1-V5 protein (SnRKV5; 500 ng) was incubated in extracts (30 µg) prepared from 7-day old light grown WT and *5ptase13* mutant seedlings for the indicated time at 30°C and was analyzed by a western blotting with an anti-V5 antibody. A,B. Extracts from seedlings grown on low nutrients were incubated in the presence or absence of 10 µM MG132. C. SnRKV5 protein degradation in extracts prepared from seedlings grown with no nutrients. D. SnRKV5 protein degradation in extracts prepared from seedlings grown with low nutrients (0.5x MS). Ponceau S stained filters are shown as controls for equivalent loading. The blot images are representative of two independent experiments.

Role of 5PTase13 in Root Growth under Different Nutrient Conditions

We compared *5ptase13* mutants with *snrk1.1* mutants, which have a small reduction in root growth under the low-nutrient conditions and exhibit enhanced root growth with 1 % to 3 % Suc (Baena-Gonzalez et al., 2007). *5ptase13-1* and *5ptase13-2* mutants exhibited reduced root growth under no-nutrient and low-nutrient conditions and no change in root growth when exogenously supplied with 3 % Suc (Figure 16A–C). A similar trend in nutrient-dependent root growth reduction of *5ptase13* mutants was also found when seedlings were grown in the dark (data not shown). This indicates that along with a decrease in SnRK1 activity (Figure 14B), *5ptase13* mutants grown on the low-nutrient conditions have the same root phenotype as the *snrk1.1* mutants (Baena-Gonzalez et al., 2007), suggesting that the decrease in root growth may be an outcome of decreased SnRK1 activity. However, since the *5ptase13* mutants grown with no nutrients have elevated SnRK1 activity (Figure 14A), we conclude that under these conditions the decrease in *5ptase13* mutant root growth cannot be a function of lower SnRK1 activity and most likely involves another mechanism.

5PTase13 Alterations Change Plant Sensitivity to Sugars and ABA

To test whether 5PTase13 is required for sugar and ABA responses, we analyzed age-matched seeds for germination in the presence of 0 %, 1 %, 3 %, or 6 % Glc or 0 %, 1 %, 2 %, 3 %, 6 %, or 11 % Suc. At low concentrations of sugar, there were no differences in the germination of wild-type and *5ptase13* seeds in the dark or light (data not shown). However, at a high exogenous sugar concentration (6 % Glc and 11 % Suc) in the dark, we found that *5ptase13* mutants were significantly less sensitive to sugar (Figure 16D; Supplemental Figures S3 and S4). We saw the same trend in sugar insensitivity when *5ptase13* mutant seeds were

germinated in the presence of 6 % Glc in the light, although the sugar insensitivity was less apparent (Supplemental Figure S3). This sugar insensitivity was also noted for *5ptase13-1* and *5ptase13-2* mutant seeds germinated in the presence of 11 % Suc, in which maximal increases of 2.5- and 2.2- fold for *5ptase13-1* and *5ptase13-2*, respectively, were noted compared with wild-type seeds (Supplemental Figure S4). Germination in the presence of mannitol, a nonmetabolizable sugar, was not altered, indicating that the sugar insensitivity of *5ptase13* mutants is not due to a general osmotic stress tolerance (Figure 16D). We also germinated *5ptase13* mutant seeds in the presence of 0, 1, 2, and 3 μM ABA and measured the impact on germination during a 6-d period. As expected, germination of wild-type seeds was delayed by ABA in a concentration-dependent manner during the 6-d period under light conditions (Figure 16E and F). In contrast, *5ptase13-1* and *5ptase13-2* mutant seeds were ABA insensitive, reaching 100 % germination on day 2 in the presence of 1μM ABA and 78 % to 90 % on day 6 in the presence of 3 μM ABA (Figure 16E and F). Since we did not find reduced seed dormancy in our mutants (data not shown), this ABA insensitivity of *5ptase13* mutants most likely does not correlate with changes in de novo synthesis of ABA (Gubler et al., 2005) and is in accordance with the previously reported results for ABA insensitivity of the *5ptase13-1* mutant (Lin et al., 2005).

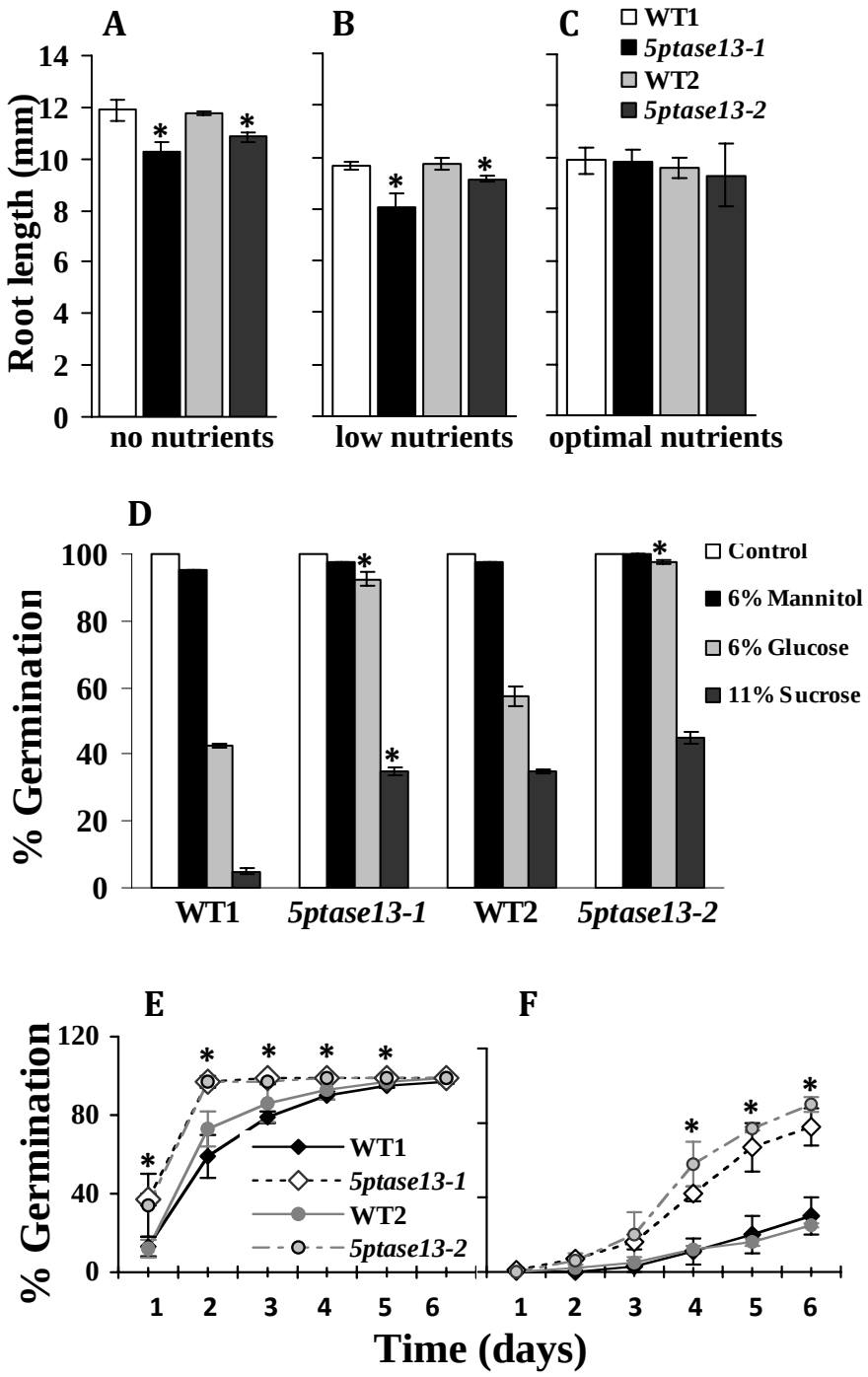

Figure 16. Phenotypes of *5ptase13* mutants. Role of 5PTase13 in root development under different nutrient conditions. WT and *5ptase13* mutant (*13-1* and *13-2*) seed were grown in low light for 6 days on 0.8 % agar plates and either no nutrients (A), low nutrients (0.5x MS) (B), or optimal nutrients (0.5x MS, 3 % sucrose) (C). The root length for each group of seedlings was measured on day

2, 4 and 6. The results in A, B and C represent the root length measured after 4 days. Values are means ± SE (n ≥ 40). The experiment was independently repeated two times. D. Comparison of germination of WT and *5ptase13* seeds grown on 0.5x MS salts and 0.8 % agar that were untreated (control) or treated with either 6 % glucose, 6 % mannitol or 11 % sucrose after 7 days in dark. Values are means ± SE (n = 50). The data are representative of three independent experiments. E, F. WT and *5ptase13* mutant seed were germinated in the light for 6 days on 0.5x MS salts, 0.8 % agar and either 1 μM ABA (E) or 3 μM ABA (F). The germination rate was scored for each group of seeds starting from day 1. Values are means ± SE (n =50). Significant differences from WT germination were noted at days 1 - 5 for *5ptase13-1* (1 μM ABA) and days 4 - 6 for both mutants (3 μM ABA). The experiment was independently repeated two times. * indicates p value of < 0.05 as compared to WT.

Expression of Glc- and ABA-Regulated Genes Is Altered in 5ptase13 Mutants

To determine whether there are differences in the expression patterns of Glc- and/or ABA-regulated genes (RD29A, KIN1, and CAB1 genes; Price et al., 2004) in *5ptase13* mutants, we examined their expression in 4d-old dark-grown wild-type and *5tase13* seedlings exposed to 6 % Glc for 3 d (Figure 17A). Treatment with 6 % Glc strongly induced the expression of RD29A and KIN1 in wild-type seedlings. In contrast, *5ptase13-1* and *5ptase13-2* mutants grown in 6 % Glc contained much smaller increases in RD29A and KIN1 transcript levels (Figure 17A), indicating that induction of these genes is diminished, but not abolished, in *5ptase13* mutants. The regulation of CAB1, on the other hand, was not significantly altered in *5ptase13* mutants.

Complementation of the 5ptase13-1 Mutant

To ensure that the alterations noted in *5ptase13* mutants are due to a loss of 5PTase13 expression, we expressed a 5PTase13:GFP fusion under the control of the 35S cauliflower mosaic virus promoter in wild-type and *5ptase13-1* plants (13:GFP and *13-1*/13:GFP plants, respectively). We examined two lines of *13-1*/ 13:GFP plants with good expression of the transgene (Figure 17B) along with wild-type and *5ptase13-1* plants in ABA-sensitivity assays. Both *13-1*/13:GFP lines exhibited more ABA sensitivity in germination assays compared with *5ptase13* mutants (Figure 17C). Since *5ptase13-1* mutants contain decreased SnRK1 activity under low-nutrient conditions compared with wild-type plants (47 %; Figure 14B), we also measured SnRK1 activity in the *13-1*/13:GFP-1 and *13-1*/13:GFP-2 lines and found, as expected, similar or increased SnRK1 activity compared with wild-type

plants (140 % ± 10 % for 13-1/13:GFP-1 and 102 % ± 5 % for 13-1/13:GFP-2). We conclude that expression of the 5PTase13:GFP transgene complements the *5ptase13-1* mutant.

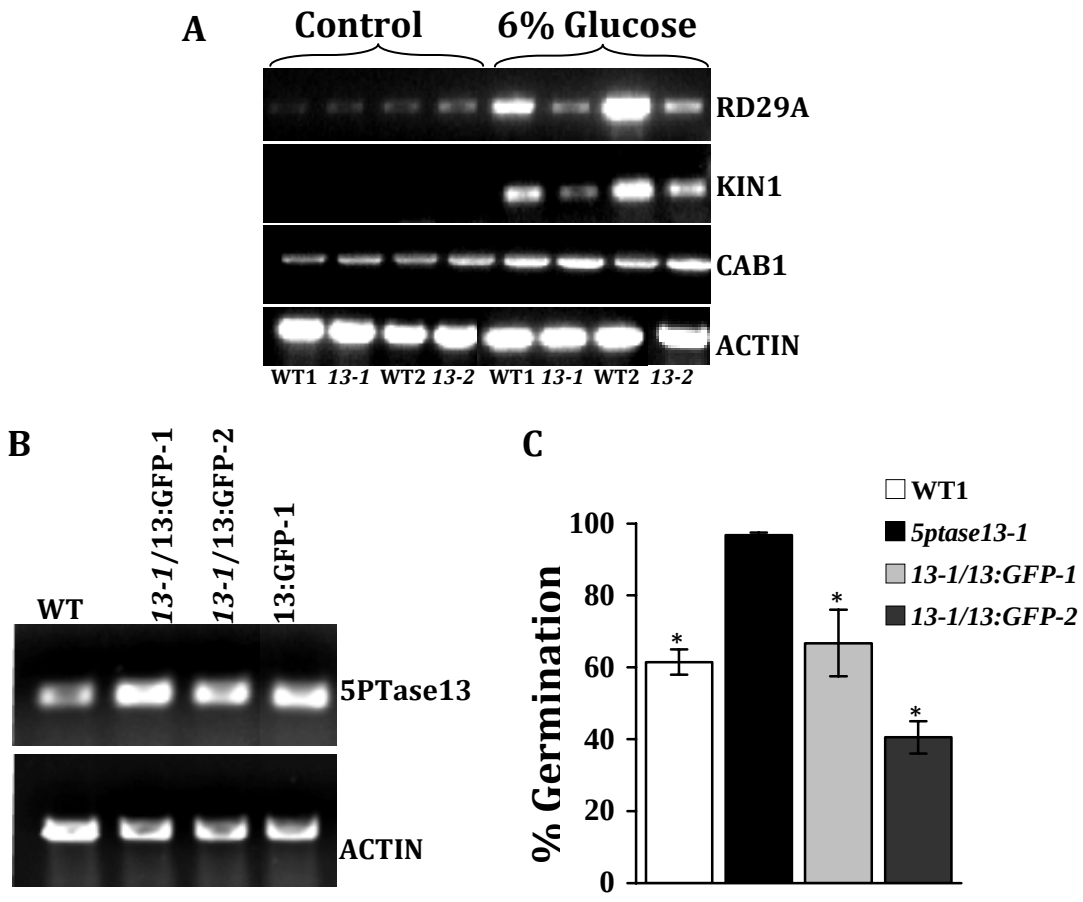

Figure 17. Expression of Glu- and ABA- inducible genes. A. Glu- and ABA-inducible genes in dark grown 4-day old WT and *5ptase13* mutant seedlings that were either untreated (control, 0.5x MS salts, 0.8 % agar) or treated with 6 % glucose (0.5x MS salts, 0.8 % agar) in the dark for 3 days. The experiment was independently repeated two times. B. Verification of overexpression of 5PTase13 in complemented lines and a 5PTase13:GFP line. Total RNA (1-2 µg) was isolated and semi-quantitative RT–PCR reactions were performed with the indicated primers as described in Supplemental Table S4. C. The 5PTase13:GFP gene complements the ABA-insensitive phenotype of *5ptase13-1* mutants. Seed from WT1, *5ptase13-1* and *5ptase13-1* mutants containing a 5PTase13:GFP transgene were germinated and grown in the light for 6 days on 0.5x MS salts, 0.8 % agar and 3 µM ABA. The germination rate was scored for each group of seeds at day 3. Values are means ± SE (n = 50). *

indicates a p value < 0.05 as compared to the *5ptase13-1* mutant. The experiment was independently repeated two times.

Glc-Stimulated Ins(1,4,5)P_3 Levels Are Altered in 5ptase13 Mutant Seedlings

We examined whether the Glc insensitivity of *5ptase13* mutants is accompanied by alterations in mass Ins(1,4,5)P_3 levels by measuring mass Ins(1,4,5)P_3 levels. The results in Figure 18 indicate that neither *5ptase13-1* nor *5ptase13-2* mutant seedlings differ significantly from wild-type seedlings in their Ins(1,4,5)P_3 mass levels under control conditions. When wild-type seedlings are exposed to 6 % Glc for 3 d, mass Ins(1,4,5)P_3 levels increase 2.8- to 3.7-fold, which is a statistically significant elevation. However, when *5ptase13* mutants are grown for 3 d in the presence of 6 % Glc, mass Ins(1,4,5)P_3 level changes are smaller, with an increase of 1.6- to 2-fold over basal levels, and statistically significant only in the *5ptase13-2* mutant. More importantly, the Glc-stimulated Ins(1,4,5)P_3 levels in both *5ptase13* mutants differ significantly from the Glc-stimulated Ins(1,4,5)P_3 levels in wild-type seedlings. We conclude that *5ptase13* mutants are impaired in their ability to accumulate Ins(1,4,5)P_3 in response to Glc and that this correlates with the sugar and ABA insensitivity noted in the germination assays.

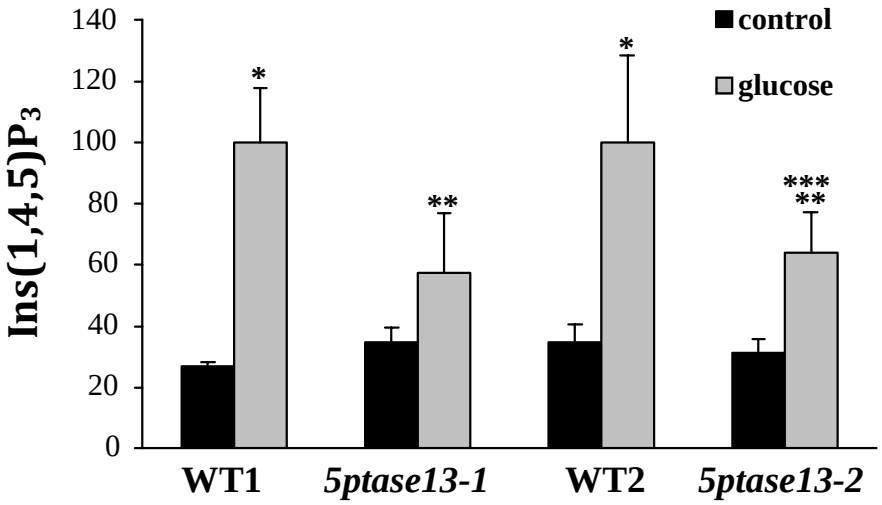

Figure 18. Comparison of mass Ins(1,4,5)P_3 levels in WT and *5ptase13* mutant seedlings. Dark-grown 4 day old WT and *5ptase13* mutant seedlings were untreated (control, 0.5x MS, 0.8 % agar) or treated with 6 % glucose and 0.5x MS for 3 days. The seedlings were frozen in liquid nitrogen, ground and analyzed for mass Ins (1,4,5)P_3 levels as described in the "Materials and Methods". Values for Ins (1,4,5)P_3 (pmols/gram tissue) were normalized to the matched WT glucose-treated sample; raw values are found in the "Materials and Methods". Bars represent the mean ± SE of 3 to 5 replicates. The experiment was repeated three times. * indicates a p value < 0.05 as compared to the control, untreated sample. ** indicates a p value < 0.10 as compared to the matched WT glucose sample. *** indicates a p value < 0.10 as compared to the control, untreated sample.

Subcellular Localization of the 5PTase13:GFP Fusion Protein

To investigate the subcellular location of the 5PTase13 protein, we performed imaging experiments with *5ptase13-1* mutants complemented with the 5PTase13:GFP construct (*13-1*/13:GFP plants) and wild-type plants containing the same 5PTase13:GFP construct. As the 5PTase13:GFP construct we used allowed for complementation of the ABA and sugar insensitivity phenotype in *5ptase13-1* mutants (Figure 17B and C), it is likely that this fusion protein undergoes the same posttranslational modifications and subcellular localization as the native 5PTase13 protein. We analyzed T2 progeny from two independent *13-1*/13: GFP lines with fluorescence deconvolution microscopy and found a similar pattern in both lines. GFP fluorescence was associated with the nucleus in many, but not all, cells in cotyledon epidermis (Figure 19B and C), hypocotyls (data not shown), and roots (Figure 19D–I). Nuclei from some but not all guard cells contained the 13:GFP protein (Figure 19C). To confirm the nuclear localization, we stained 13-1/13:GFP seedlings with the nuclear dye 4',6-diamidino-2-phenylindole (DAPI) and imaged GFP and DAPI fluorescence simultaneously (Figure 19D–I). Once again, we found 13:GFP fluorescence in only a portion of root nuclei, while DAPI fluorescence was present in all nuclei. We conclude that 5PTase13 protein is located in the nucleus of seedlings and that its presence in the nucleus is restricted in some cells.

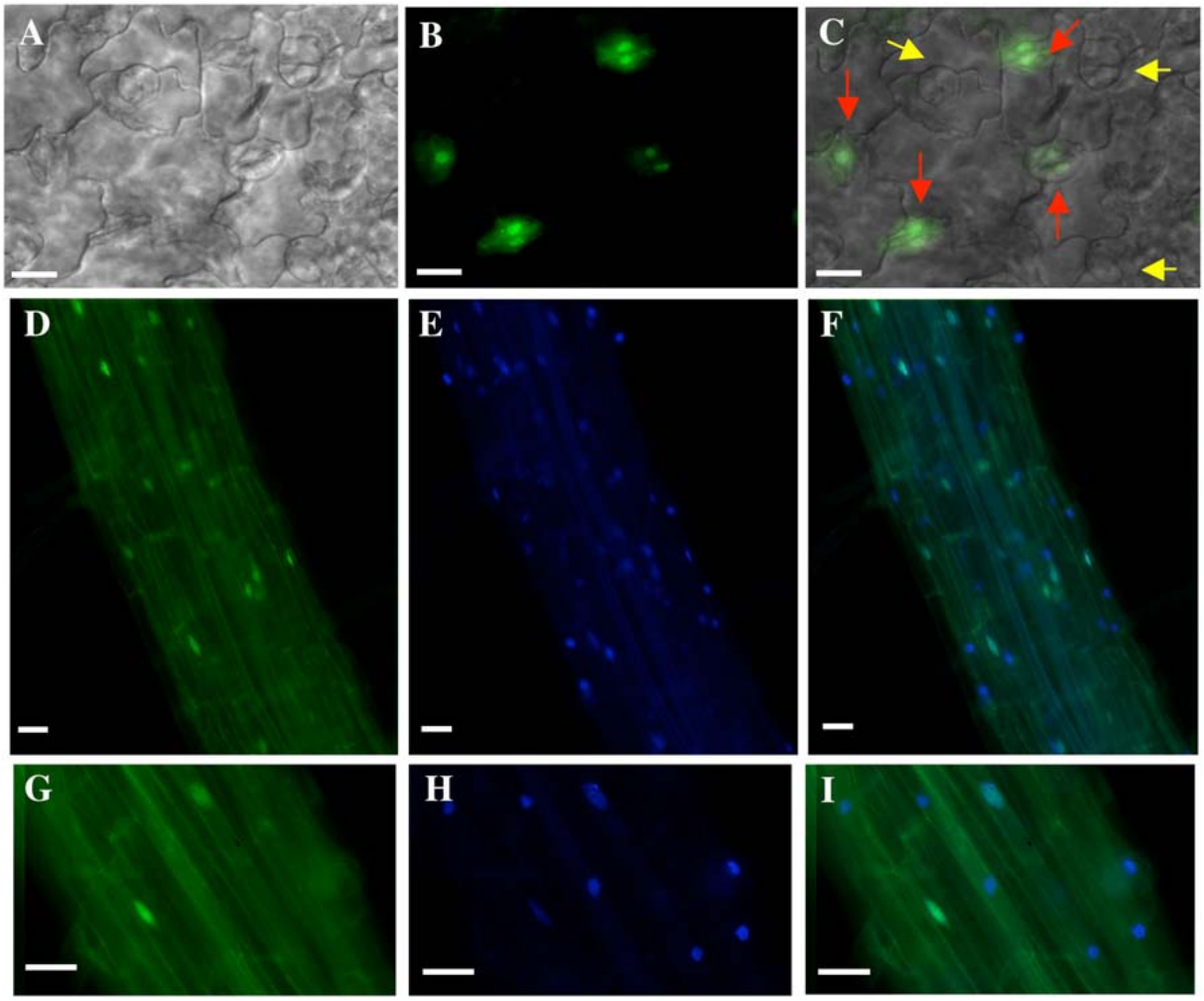

Figure 19. Subcellular localization of GFP tagged 5PTase13 in Arabidopsis seedlings. GFP-tagged 5PTase13 (13:GFP) was expressed in the *5ptase13-1* mutant background, and the subcellular location in cotyledons (A–C) and roots (D–I) from 7-d-old seedlings was examined with fluorescence deconvolution microscopy. A, Differential interference contrast. B, D, and G, GFP fluorescence. C, Overlay of A and B. E and H, Seedlings were stained with DAPI and examined with a standard UV fluorescence filter set. F and I, Overlay of GFPand DAPI fluorescence. Note that red arrows in C indicate nuclei from guard cells expressing 13:GFP, while yellow arrows correspond to nuclei lacking expression. Bars = 20 mm.

DISCUSSION

Since control of second messengers is critical for signaling, there is interest in determining how the plant cell regulates levels of second messengers such as Ins(1,4,5)P_3. We identified a potential regulator of Ins(1,4,5)P_3 signaling by isolating protein interactors of 5PTase13. We focused on 5PTase13 because it contains several conserved WD40 repeats (for review, see van Nocker and Ludwig, 2003) and the presence of WD40 repeats within 5PTase genes is unique to plants and certain fungi (Zhong and Ye, 2004). To date, the WD40 repeats of 5PTases have not been functionally characterized, and no potential protein partners have been identified.

We show here an important and novel interaction between the WD40 repeat region of 5PTase13 and the central metabolic regulator, SnRK1.1. SnRK1.1 and its orthologues in yeast and mammals is one subunit of a complex that modulates cellular metabolism in response to nutrient and environmental conditions (Baena-Gonzalez et al., 2007; Hardie, 2007; Hue and Rider, 2007). Recent work in Arabidopsis has elegantly delineated the role of SnRK 1.1 in the transcriptional activation of genes from catabolic pathways that provide routes for alternative energy sources and coordinate repression of a large number of anabolic genes (Baena-Gonzalez et al., 2007). Our discovery of a5PTase13:SnRK1.1 complex points to the novel interaction of this metabolic modulator and Ins(1,4,5)P_3 signaling.

It has been shown previously that a loss of function in the 5PTase13 gene leads to defects in auxin-regulated development (Lin et al., 2005) and in blue light responses (Chen et al., 2008). Because of the 5PTase13 interaction with SnRK1.1, we investigated the role of

5PTase13 in nutrient sensing and stress responses. Recent studies have shown that Arabidopsis plants overexpressing SnRK1.1 have greater Suc sensitivity and that mutants lacking SnRK1.1 use exogenous sugars more efficiently (Baena-Gonzalez et al., 2007). When virus-induced gene silencing is used to silence both SnRK1.1 and SnRK1.2, growth is severely affected, indicating the importance of the SnRK1 modulator to overall growth (Baena-Gonzalez et al., 2007). Repressing a pea (Pisum sativum) homolog of SnRK1 with antisense RNA results in seed maturation effects resembling ABA insensitivity (Radchuk et al., 2006), while a loss of function in SnRK1 in rice (Oryza sativa) delays seed germination and seedling growth (Lu et al., 2007). We report here that *5ptase13* mutants exhibit reduced root growth under limited nutrient conditions, but not when 3 % Suc is supplied. The variability of the root growth phenotype under different nutrient conditions is thus similar, although not identical, to growth responses of *snrk1.1* mutants. In addition, we documented that *5ptase13* mutants are altered in their responses to ABA and sugar stress (Figures 16–18). When *5ptase13* mutants are challenged with a sugar stress, alterations in germination, gene expression, and Ins(1,4,5)P_3 accumulation occur, indicating that *5ptase13* mutants are sugar insensitive. This sugar insensitivity is similar to that noted for the regulator of G-protein signaling1 mutant (Chen et al., 2006) but differs from the Glc-insensitive (Zhou et al., 1998; Arenas-Huertero et al., 2000; Moore et al., 2003; Lin et al., 2007) and sugar-insensitive (Laby et al., 2000; Gibson et al., 2001) mutants that are also insensitive to the developmental arrest induced by sugar that occurs over a period of 21 d. Since there are other WD40-containing 5PTases, we speculate that the sensitivity to developmental arrest noted in *5ptase13* mutants grown on high sugar may be due to this redundancy. Together, the data on nutrient and sugar stress responses of *5ptase13* mutants are consistent with the existence of a

5PTase13:SnRK1.1 complex that modulates seedling responses to nutrient conditions and stress. To understand how a 5PTase13:SnRK1.1 complex might regulate nutrient and stress signaling, we measured SnRK1 activity in *5ptase13* mutants and wild-type seedlings grown under different nutrient conditions. Our data show that the presence of 5PTase13 affects SnRK1 activity and that nutrient availability is an important switch in 5PTase13 regulation of SnRK1.1. Specifically, 5PTase13 is required to maintain wildtype levels of SnRK1 activity when low nutrient or high sugar is present (Figure 14B and C). In contrast, under the greatest starvation conditions of no added nutrients, 5PTase13 appears to be a negative regulator of SnRK1, as 5ptase13 mutants contain significantly elevated SnRK1 activity (Figure 14A). To further delineate the mechanism of 5PTase13 regulation of SnRK1.1, we used a cell-free degradation assay and showed that the decrease in SnRK1 activity in *5ptase13* mutants correlates with increased degradation of SnRK1.1 by the proteasome (Figure 15D).

Interestingly, another WD40 repeat-containing protein called PRL1 (for PLEITROPIC REGULATOR LOCUS1) also interacts with SnRK1.1 and is able to inhibit the activity of SnRK1.1 and SnRK1.2 (Bhalerao et al., 1999; Farras et al., 2001). Recent evidence shows that there is a decrease in SnRK1 degradation in *prl1* mutant extracts, and additional evidence suggests that PRL1 acts in delivering SnRK1 to the CUL4-DDB1 complex for proteasomal degradation (Lee et al., 2008). Thus, we predict that 5PTase13 and PRL1 have opposing functions regarding SnRK1 stability under low nutrient and sugar-stress conditions. The fact that *prl1* mutants are ABA and sugar hypersensitive (Bhalerao et al., 1999), which is the opposite of *5ptase13* mutants, also supports opposing roles for 5PTase13 and PRL1 in regulating SnRK1 degradation.

Our data reported here, along with data from other groups, support the model of SnRK1 as a sensor of low nutrient status and cellular stress. Under low-nutrient or sugar-stress conditions, 5PTase13 acts as a positive regulator of SnRK1.1 activity by reducing the amount of SnRK1 targeted for proteasomal destruction. This regulation most likely involves a 5PTase13-SnRK1.1 interaction within the nucleus, as that is where we find 5PTase13:GFP (Figure 19), and SnRK1 is most likely nuclear as well (Thelander et al., 2004; Pierre et al., 2007). A loss of 5PTase function, therefore, results in a lack of response, or insensitivity, to stress conditions. In contrast, nuclear PRL1 acts as a negative regulator of SnRK1.1 and facilitates its proteasomal destruction. Thus, the increased SnRK1 levels found in *prl1* mutants could potentiate low-nutrient and/or stress signaling, resulting in the hypersensitivity to sugar and ABA found in this mutant. Nemeth et al. (1998) showed that PRL1 is located in the nucleus, as are CUL4 and other SnRK1-interacting proteasomal components such as SKP/ASK1 and a4/PAD1 (Farras et al., 2001; Chen et al., 2006).

While data support this model, we currently do not know how the second messenger Ins(1,4,5)P_3 affects the SnRK1 pathway. We have shown that Ins(1,4,5)P_3 levels increase when seedlings are given a sugar stress, implicating Ins(1,4,5)P_3 as a second messenger under high-sugar conditions (Figure 18). Given that the 5PTase13 enzyme has been shown to hydrolyze Ins(1,4,5)P_3 in vitro (Zhong and Ye, 2004), we expected that a loss of 5PTase13 function would elevate Ins(1,4,5)P_3. However, *5ptase13* mutants have, instead, lower Ins(1,4,5)P_3 levels upon sugar stress (Figure 18). The lack of increase in Glc-stimulated Ins(1,4,5)P_3 accumulation in *5ptase13* mutants may indicate a more complex role for Ins(1,4,5)P_3 in 5PTase13 function and/or could be the result of compensatory actions of the other 5PTase enzymes. Elevated Ins(1,4,5)P_3 levels have been found in other *5ptase* mutants,

and this increase in Ins(1,4,5)P_3 is sometimes associated with ABA hypersensitivity (Carland and Nelson, 2004; Gunesekera et al., 2007). It should be noted that *5ptase13* mutant seeds are also ABA insensitive, a trait they share with other sugar-insensitive mutants. It is currently thought that the sugar-induced delay of germination involves the action of ABA, as ABA synthesis mutants are also resistant to the effects of sugars (Price et al., 2003). There have been previous reports that inositol signaling and sugar sensing/metabolism are linked. Im et al. (2007) found that expressing a human phosphatidylinositol 4-phosphate 5-kinase (PIP5K) gene in tissue culture cells dramatically elevated phosphatidylinositol 4,5-bisphosphate (PtdInsP_2) and Ins(1,4,5)P_3 and resulted in increased sugar use and oxygen uptake. This work importantly defined the PIP5K enzyme as the flux-limiting enzyme for PtdInsP_2 production and Ins(1,4,5)P_3 signaling in plant cells. In separate studies, Lou et al. (2007) found that one member of the PIP5K gene family, At3g09920, negatively regulates a cytosolic invertase by direct protein interactions. These investigators found that a gain of function in this same PIP5K gene results in less invertase activity and a resulting sugar insensitivity in transgenic seedlings. Additional evidence supporting the importance of PtdInsP_2 in sugar sensing/metabolism comes from transcriptional studies. A rigorous correlative analysis of gene expression shows that a different PIP5K gene (At4g17080) is one of 278 genes coactivated by SnRK1.1 and sugar starvation and down-regulated by sugar treatment (Baena-Gonzalez et al., 2007). Together, these studies indicate that PIP5K-catalyzed production of PtdInsP_2 may play a critical role in mediating the response of plant cells to sugar. In addition to transcriptional changes in PIP5K, protoplasts overexpressing SnRK1.1 repress two genes required for inositol synthesis (At4g39800 and At3g02870) and activate three genes encoding other 5PTases (5PTase1, 5PTase12, and FRA3; Baena-Gonzalez et al., 2007). These

alterations indicate the likelihood that the SnRK1 modulator decreases the energy-consuming synthesis of inositol but increases the ability of the plant cell to hydrolyze inositol containing second messengers such as Ins(1,4,5)P_3. Together, the data presented here support a unique role for 5PTase13, functioning as a binding partner and regulator of the SnRK1.1 modulator of energy and stress signaling. Given the previously established role of 5PTase13 in blue light signaling (Chen et al., 2008), this work identifies a new connection between inositol signaling and the sensing of cellular metabolism, energy, light, and stress.

APPENDIX TO CHAPTER II

SUPPLEMENTAL DATA

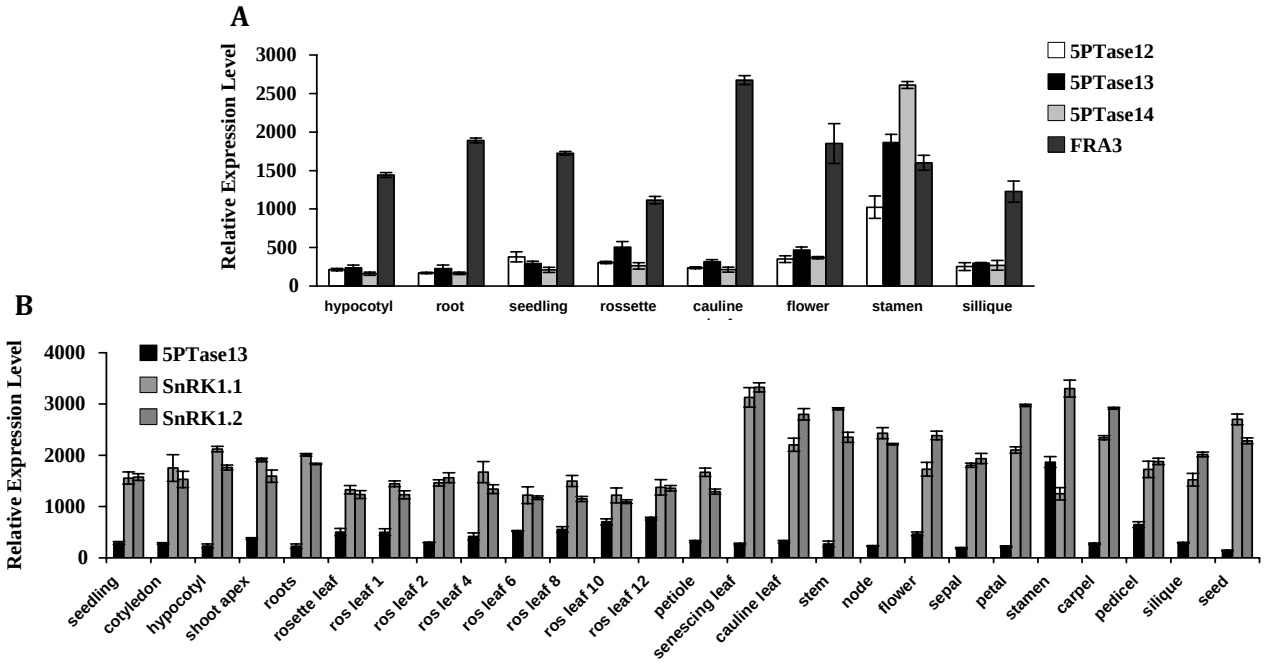

Supplemental Figure S1. GENEVESTIGATOR expression analysis. A. Genevestigator Expression Analysis of 5PTase12, 13, 14 and FRA3. Data from the Genvestigator web site was analyzed and plotted. B. Genevestigator Expression in tissues of 5PTase13 as compared to SnRK1.1 and SnRK1.2. Error bars are standard deviation.

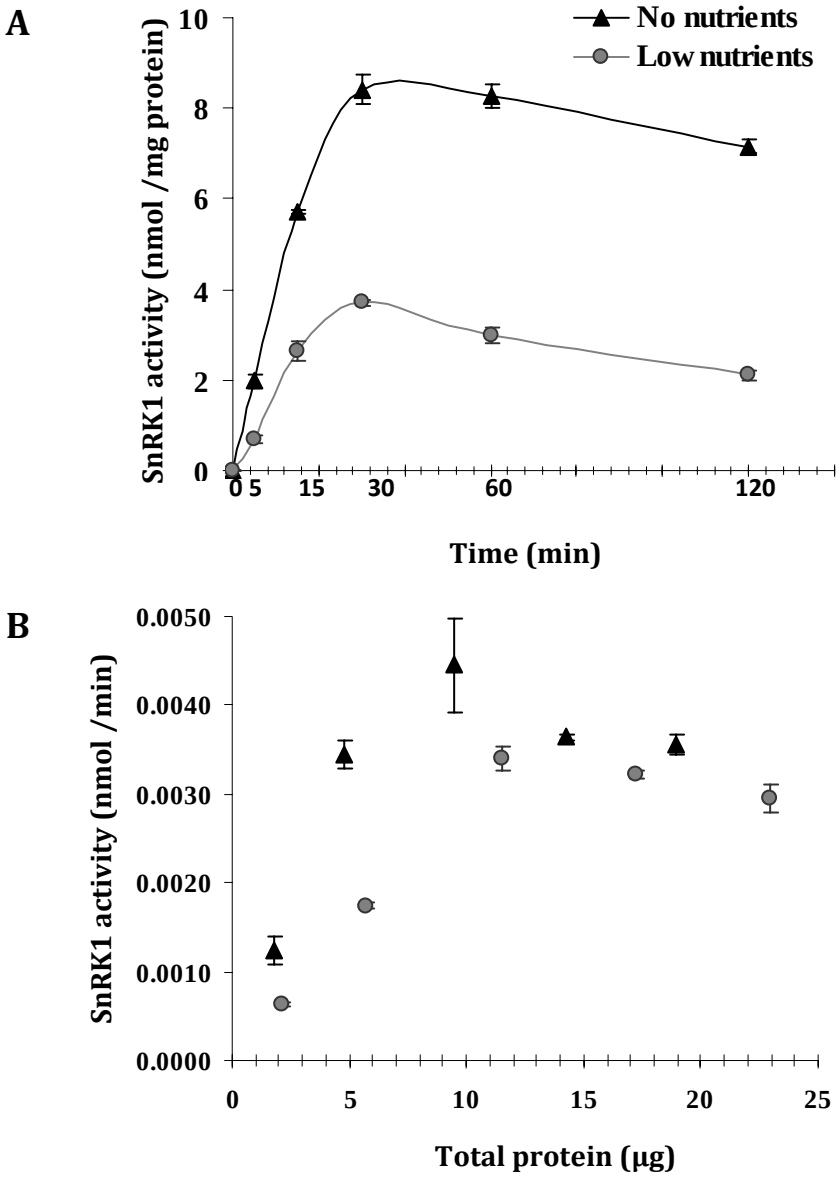

Supplemtantl Figure S2.Validation of SnRK1 activity assay. Seed from wild-type (WT2-CS60000) plants was grown on 0.8 % agar and either no nutrients (black triangles) or low nutrients (gray circles, 0.5x MS) under low light for 7 days. SnRK1 activity was measured from crude plant extracts precipitated with ammonium sulfate according to the method described (Radchuk et al., 2006). A. Time course of the incorporation of nmoles Pi in the SPS peptide per miligram of protein at 30°C. For two different nutrient conditions, SnRK1 activity is linear over 30 min but declines after a longer incubation time. B. Protein amount dependent incorporation of nmoles Pi in the SPS peptide per min in 20 µl reaction at 30°C. SnRK1 activity is linear with up to 9.48/11.48 µg total protein (no

nutrients/low nutrients) respectivley. An average of 5 µg protein was used in SnRK1 activity assay in Figures 5 and 6. Bars represent the mean ± SE of 3 replicates, a p value < 0.05 as compared to no nutrients.

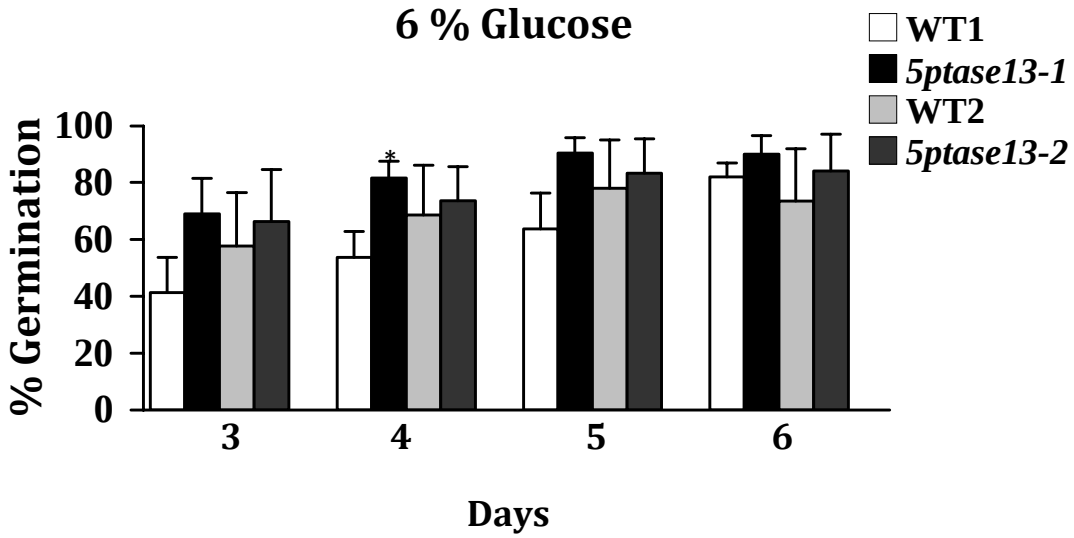

Supplemental Figure S3. *5ptase13* mutants are less sensitive to 6 % glucose under light. WT and *5ptase13* mutant seed was germinated and grown in the light for 6 days on 0.5x MS salts, 0.8 % agar, and 6 % glucose. Germination rate was scored for each group of seeds starting from day 3. Values are means ± SE (n = 50). * indicates p value of < 0.05 as compared to WT. The experiment was independently repeated three times.

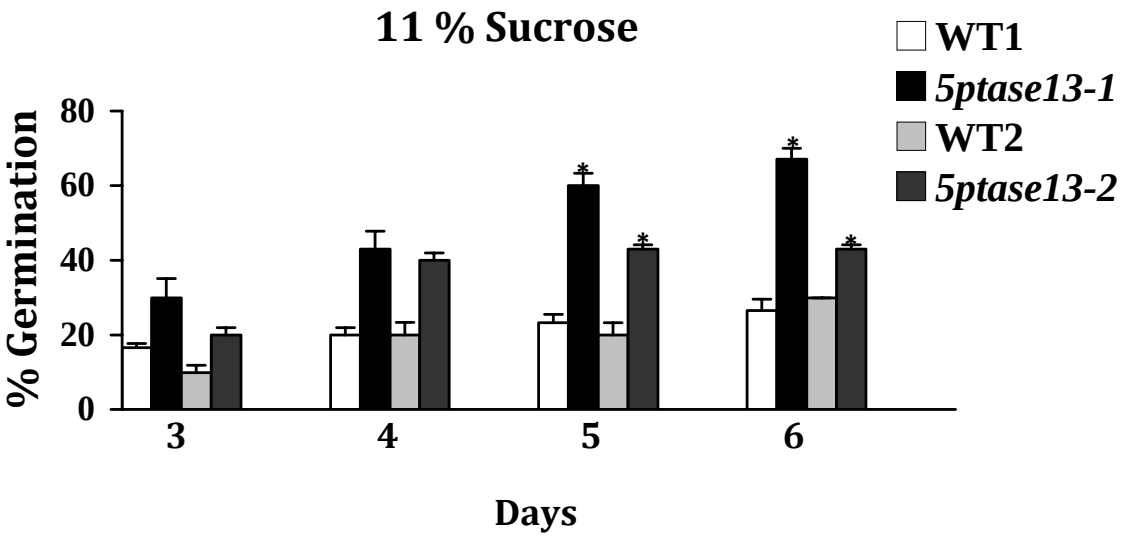

Supplemental Figure S4. *5ptase13* mutants are less sensitive to 11 % sucrose under light. WT and *5ptase13* mutant seed were germinated and grown in the light for 6 days on 0.5x MS salts, 0.8 % agar, and 11 % sucrose. Germination rate was scored for each group of seeds starting from day 3. Values are means ± SE (n = 50). * indicates p value of < 0.05 as compared to WT. The data are representative of three independent experiments.

Table S1. ***Identity of the WD40 regions of 5PTases in Arabidopsis.*** The identity values are obtained by using ALIGN for optimal global alignment of two WD40 sequences each time.

5PTases	Identity (%)			
	5PTase12 (At2g43900)	5PTase13 (At1g05630)	5PTse14 (At2g31830)	FRA3 (At1g65580)
5PTase12	-	62.4	59.5	46.4
5PTase13	62.4	-	75.3	46.5
5PTase14	59.5	75.3	-	45.5
FRA3	46.4	46.5	45.5	-

Table S2. *Normal cotyledon vein development patterns*. Various normal cotyledon vein development patterns were observed and compared in Wild-type (WT1 and WT2) and *5ptase13* mutant (*13-1* and *13-2*) plants. A. 4 closed loops; B. 3 closed loops; C. 3 closed 1 open loops; D. 2 closed 2 open loops; E. 2 closed 1 open loops; Data represented are in % of total cotyledons counted (n=50).

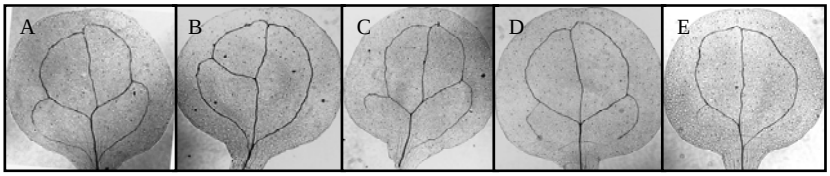

Plant line	4 closed loops	3 closed loops	3 closed 1 open loop	2 closed 2 open loops	2 closed 1 open loops	Total % normal patterns
WT1	16.66	2.38	38. 09	4.76	4.76	66.7
5ptase13-1	26.18	11.9	26.19	7.14	2.38	73.8
WT2	31.81	4.54	31.81	15.9	0	84.1
5ptase13-2	27.77	2.77	33.33	16.66	0	80.5

Table S3. *Abnormal cotyledon vein development patterns**. Various abnormal cotyledon vein development patterns were observed and compared in Wild-type (WT1 and WT2) and *5ptase13* mutant (*13-1* and *13-2*) plants. A. altered vein number; B. wrong orientation; C. additional loops; D. branches. Data represented are in % of total cotyledons counted (n=50).

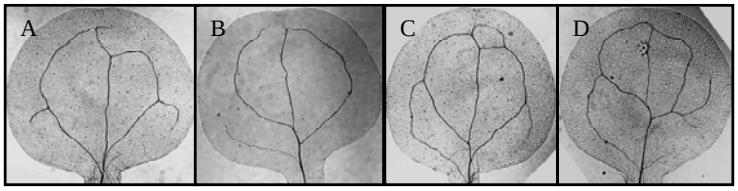

Plant line	Altered vein number	Wrong orientation	Additional loops	Branches	Total % abnormal patterns
WT1	4.76	23.8	2.38	2.38	33.3
5ptase13-1	2.38	21.42	0	2.38	26.18
WT2	0	15.9	0	0	15.9
5ptase13-2	8.33	11.11	0	0	19.4

*The abnormal patterns are as described by Lin at el. (2005) for comparison.

Table S4. Primers used for PCR/RT-PCR.
Primer Sequence (5' to 3')
SALK LB -TTCATAACCAATCTCGATACAC
SAIL LB - GCGTGGACCGCTTGCTGCAACT
13-1for - GCCATGGACAATGTTAGAATTTAATTGGTACCAATGTTGGTCAAGGAAGGGC
13-1rev -CCGGCTTTTACCTC GTCT
13-2for - TCGAAGAAGAAGACGAAGAGGC
13-2rev- CTGCTGCAACATCAAGATCTCC
13WD40for- CATATGGATTCGCTAATTATCGAAGAAGAAGACGAAGAGGCG
13WD40rev - GGATCCTCAGTCTTGTCTGGCATATAAAG
CAB1for - TCAATGGCCGCCTCAACAATGG
CAB1rev - CCTCTGGGTCG GTAGCCAAACC
SnRK1.1for - ACTGGACAATCGTTTCCGTGCCTCTAGTGG
SnRK1.1rev - TCAGAGGACTCGGAGCTGAGCAAGAAAAGC
SnRK1.2for - GCTTATAGTTGACCCGGTGAAACG
SnRK1.2rev - CTGAAGTCCAAGAGCCCATTTTCG
FRA3for - GAAAAGAAGCGGATTCCTGCCTGG
FRA3rev - ATTGTGCCAGTTCCTGGAGACACC
5PTase12for - AGAAAGTCAGAGCGTTGCTCAACG
5PTase12rev - TCTTCTTCTGTGACTTGGAGCAGG
5PTase13for - TTTTGGCCGTGCCATTGGCAAC
5PTase13rev - TTTGTCCTCGGGAAAAGACC
5PTase14for - AAAGTGCCCTGTAGTTTCGTCGAC
5PTase14rev - ATGAACCTTCACCTGCAGTGAAGC
SnRK1.1pFor - ATGTTCAAACGAGTAGATG
SnRK1.1pRev - GAGGACTCGGAGCTGAGC
WD40For - CATATGGATTCGCTAATTATCGAAGAAGAAGACGAAG AGGCG
WD40Rev - GGATCCTCAGTCTTGTCTGGCATATAAAG

CHAPTER III

OBJECTIVE II. Identification and Functional Role of Atp80, a Novel Protein Partner of 5PTase13

ABSTRACT

In this study I identified the Arabidopsis homolog (Atp80) of the human WDR48 protein (HsWDR48, Hsp80) as a novel interactor of 5PTase13. Atp80 is encoded by a single gene in Arabidopsis that is abundantly expressed in most plant tissues with high levels in vascular tissue and senescent leaves. Like its human counterpart, Atp80 contains 7 WD40 repeats in its N-terminal half. Disruption in the Atp80 gene resulted in dramatic defects in rosette leaf development including abnormal leaf emergence and differentiation and premature leaf senescence. The *atp80* mutant plants were small in size and displayed arrested root growth under no nutrient and low-nutrient conditions, but root growth was rescued when 3 % sucrose was added to the growth media. Atp80 was found to physically associate with SnRK1.1 and PINOID binding protein1 (PBP1). While SnRK1.1 is well-known for its interaction with 5PTase13, PBP1, a co-factor of PINOID kinase that regulates auxin transport, is a newly discovered protein partner of Atp80 that introduces a role for Atp80 in auxin transport regulation. My results indicate that Atp80 plays roles in nutrient and inostiol signaling and could be involved in auxin transport regulation as well.

INTRODUCTION

Members of a conserved family of *myo*-inositol polyphosphate 5-phosphatases (5PTases; EC 3.1.3.56) regulate diverse cellular processes in eukaryotes such as cell differentiation and proliferation, protein trafficking, and actin organization and play essential roles in growth, development, stress and disease (Burnette et al., 2003; Carland and Nelson, 2004; Zhong et al., 2004; Jones et al., 2006; Gunesekera et al., 2007; Ananieva et al., 2008; Ercetin et al., 2008; for review see Astle et al., 2007; Ooms et al., 2009). Each 5PTase enzyme contains a conserved 5PTase catalytic domain which removes the 5-position phosphate from the inositol ring of phosphorylated InsPs and PIs (Berdy et al., 2001; Zhong and Ye, 2004; Ooms et al., 2009). Besides containing highly conserved 5PTase catalytic domain, the 5PTases also contain numerous other domains important for their subcellular localization and/ or protein-protein interactions (Astle et al., 2006; Ooms et al., 2009). In *Arabidopsis thaliana* there are 15 members of the 5PTase family, the majority of which comprise of a single 5PTase catalytic domain (Berdy et al., 2001). Four members of the Arabidopsis 5PTase family, however, have a unique protein domain structure with several N-terminal WD40 domain and a single C-terminal 5PTase catalytic domain (Berdy et al., 2001; Zhong and Ye, 2004).

The WD40 domain folds into a highly symmetrical structure called a β propeller that serves as a platform for multiple protein-protein interactions (Li and Roberts, 2001; Smith, 2008). WD40-repeat proteins are diverse regulatory proteins found in all eukaryotes and are implicated in a variety of functions ranging from signal transduction and transcription regulation to cell cycle control, proteasomal degradation and apoptosis (Li and Roberts, 2001;

van Nocker and Ludwig, 2003; Lee et al., 2008). The underlying common function of all WD40-repeat proteins is coordinating multi-protein complex assemblies, where the repeating units serve as a scaffold for protein-protein interactions (Smith, 2008). There are several examples of such proteins, such as the E3 ubiquitin lagase family that includes COP1 (constitutive photomorphogenesis 1), a nuclear repressor of photomorphogeniesis that controls seedling development and contains a C-terminal WD40 domain (Torii et al., 1998; Yu et al., 2008; Wang et al., 2009). A variety of DDB1(DNA damage-binding protein1)-binding WD40 proteins exist that associate with the DDB1-CUL4 E3 ligase complexes through a conserved DWD box motif and are targeted for proteasomal degradation (Lee et al., 2008). Finally, WD40 proteins such as the human WDR5, RbBP5 and RbAp48/46 are components of histone-modifying complexes (Suganuma et al., 2008). A recent study also demonstrated that the WD40 domain can serve as a RNA binding domain since the human Gemin5 was shown to bind to the small nuclear ribonucleoprotein (snRNP) complex via its WD40 domain. The authors mapped a discrete region of the WD40 domain that contacts snRNAs and demonstrated that specific amino acids in this region are crucial for Gemin5-snRNA binding (Lau et al., 2009).

Recently, I have investigated the function of the WD40 domains of the Arabidopsis 5PTases, and have identified potential protein partners (Ananieva et al., 2008). I found that the WD40 domain of one of the members of the Arabidopsis 5PTases, 5PTase13, forms a protein complex with a sucrose (Suc) nonfermenting-1-related kinase1 (SnRK1.1, AKIN10; At3g01090). SnRK1 protein is a nutrient sensor/ metabolic modulator that was recently identified as a central regulator of the transcriptome in response to darkness and multiple types of stress signals (Baena-Gonzalez et al., 2007; Ananieva et al., 2008; Baena-Gonzalez and

Sheen, 2008). My identification of a 5PTase13:SnRK1.1 complex pointed to the novel interaction of this metabolic modulator and inositol signaling as 5PTase13 is implicated in inositol signal termination. I found that a loss of 5PTase13 function affects SnRK1 activity, and the impact differs depending on the nutrient availability. *5ptase13* mutants contain significantly elevated SnRK1 activity in the absence of nutrients, suggesting that 5PTase13 functions in this context to downregulate SnRK1. In contrast, SnRK1 activity deceases in *5ptase13* mutants when either low nutrients or 6 % Glc is present indicating that 5PTase13 functions in this condition as a positive regulator of SnRK1. Further analysis of the mechanism of this interaction, revealed that 5PTase13 stabilizes SnRK1.1 under low nutrient conditions and protects SnRK1.1 from proteasomal degradation (Ananieva et al., 2008).

In this study, I identified a novel 5PTase13-binding protein partner and named it Atp80 (*Arabidopsis thaliana* homolog of the human p80 [Hsp80; HsWDR48], At3g05090). The Atp80 protein is encoded by a single gene in Arabidopsis and contains 7 WD40 repeats in its N-terminus. A loss-of function *atp80* mutant has a light-inducible growth retardation phenotype and premature senescence of rosette leaves. This mutant develops short siliques and dark-brown seed and its root growth is differently impacted by nutrients. Atp80 also interacts with SnRK1.1 and another protein partner called PBP1 (PINOID binding protein1) in the yeast two hybrid system and in vitro. Further analysis reveals that Atp80 and 5PTase13 affect PBP1 stability in opposing ways in a nutrient dependent manner.

RESULTS

Atp80 Interacts with the WD40 Region of 5PTase13

My collaborator, Les Erickson of Salisbury University, identified the Arabidopsis homolog (Atp80) of the human WDR48 (HsWDR48 or Hsp80) as a novel protein interactor of 5PTase13. Dr. Erickson used the 533 N-terminal amino acids from 5PTase13 containing the WD40 repeats as bait in a yeast two-hybrid screen of an Arabidopsis 3 d-old etiolated seedling cDNA library. Over 1 million yeast transformants were screened and two positive clones were identified: one containing the C-terminal domain of the SnRK1.1 gene (At3g01090; also known as AKIN10) as previously characterized (Ananieva et al., 2008), and a second one containing the C-terminal portion of the Atp80 gene (At3g05090). The Atp80 positive clone was re-transformed into yeast to verify the interaction (Figure 20). Negative controls, including the empty DNA binding domain and activation domain vectors, established that Atp80 binds to the WD40 repeat region of the 5PTase13 protein in yeast.

To examine the interaction between 5PTase13 and Atp80 *in vitro*, I fused the sequence encoding the Xpress epitope tag to the C terminus of the WD40 repeat region of 5PTase13 (13WDX) and the V5 epitope tag sequence to the C terminus of Atp80 (Atp80V5) and expressed both proteins in *E coli*. The Atp80V5 construct directs the expression of a 70 kDa protein detected by an anti-V5 monoclonal antibody and in most cases we detected two Atp80V5 bands, perhaps as a result of proteolytic cleavage (Figure 21, lane 1). The 13WDX construct directs the expression of a 65.9 kDa protein detected by an anti- Xpress monoclonal antibody (Figure 21, lane 2). These interactions are specific, as Atp80V5 is not detected by the

anti-Xpress antibody and 13WDX is not detected by the anti-V5 antibody (data not shown). To determine whether the Atp80V5 recombinant protein can "pull down" 13WDX, immunoprecipitations using anti-V5:protein A-Sepharose beads were performed, and the resulting complex was then analyzed by western blotting with an anti-Xpress antibody (Figure 21, IP lanes). As shown in Figure 21, the WD40 repeat region from 5PTase13 (13WDX) is only detected in this pull-down assay when it has been incubated in the presence of Atp80V5. I conclude that the WD40 repeat region from 5PTase13 and Atp80 can form a protein complex *in vitro*.

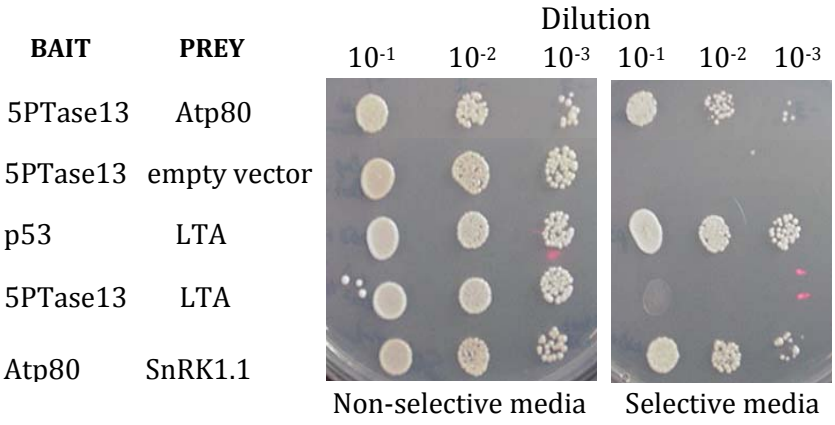

Figure 20. Yeast Two-Hybrid Screen. An Arabidopsis cDNA PREY library was screened using the WD40 region of 5PTase13 and the C-terminal region of Atp80 as BAITs in the yeast two-hybrid system. When 5PTase13 was used as bait over 1 million yeast transformants were screened for reporter gene expression, which resulted in the isolation of a PREY plasmid expressing the C-terminal domain of Atp80. When Atp80 was used in a direct yeast two hybrid screen it was found to interact with the PREY plasmid expressing the SnRK1.1 gene. Serially-diluted yeast strains were spotted onto agar plates that are either non-selective or selective for expression of the two hybrid reporter genes.

P53 and LTA (a viral large T-antigen) are positive control clones and encode a DNA-binding domain and transcriptional activation domain respectively.

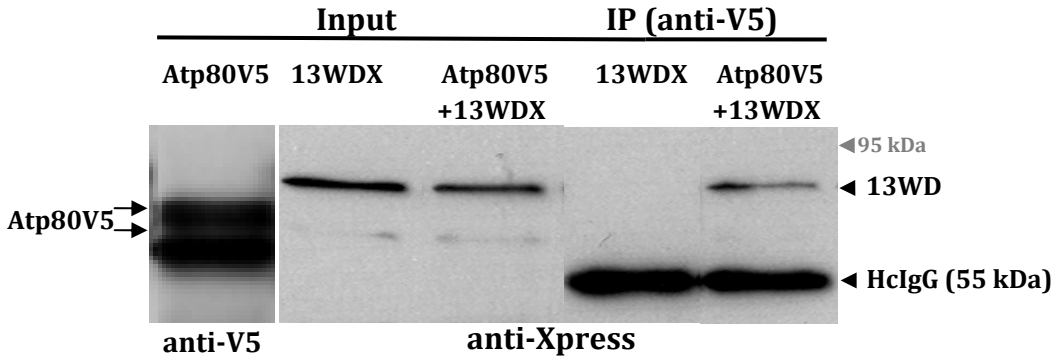

Figure 21. Atp80V5 interacts with the 13WD40-Xpress protein *in vitro*. Immunoprecipitation (IP) was carried out using an anti-V5 antibody bound to a protein A sepharose (PAS). Purified and dialyzed proteins (13WDX and Atp80V5) were incubated for 2 hours at room temperature in IP buffer before incubation with the antiV5:PAS complex. The resulting IPs were analyzed using protein gel blotting: lane 1. Input fraction of Atp80V5 probed with an anti-V5 antibody; lane 2. Input fraction of 13WDX; lane 3. Input fraction of 13WDX in combination with Atp80V5; lane 4. Bound fraction of 13WDX alone; lane 5. Bound fraction of 13WDX in combination with Atp80V5. Lanes 2 through 5 were probed with an anti-Xpress antibody. The 55kDa band is the immunoglobin heavy chain (HcIgG) component of the anti-V5 antibody. The blot images are representative of four independent experiments.

Atp80, an Arabidopsis Homolog of the Human WDR48

The open reading frame of Atp80 encodes a 753 amino acid (AA) protein with a predicted molecular weight of 84.2 kDa. Analysis of conserved domains by Pfam (http:pfam/sanger.ac.uk) reveals 6 WD40 repeats in the N-terminal half (AA 34-68, 74-111, 116-155, 203-241, 245-283, and 287-325) with e values ranging from 7.9 e^{-06} to 1.9 e^{-10}. A seventh WD40 repeat is present at AA 435-441 and has a higher e value (7.8), thus this WD40 repeat has less statistical significance. Pfam identified additional domains with lower confidence including a YaeQ protein domain (AA 343-366; putative specialized transcription elongation function, e value 0.86), and a Gar1 RNA binding domain from AA 620-639 (e value 0.11). Submission of the Atp80 sequence to the COILS prediction server (http://www.ch.embnet.org/software/COILS_form.html) revealed elevated coiled-coil potential in the C-terminal half of Atp80 (AA 420-580).

In an effort to identify homologues of Atp80 in plants as well as in other species, I used the entire 753 AA sequence of Atp80 as a query in BLASTp searches and analyzed related sequences with e-values less than 2 e^{-105}. In plants, I found several potential homologues of Atp80 containing 64-70 % AA identity over the entire protein and 66-76 % identity within the N-terminal half (425 AAs). Arabidopsis did not contain any other genes that could encode related proteins, thus Atp80 appears to be encoded by a single gene in this species. I found that rice (*Oryza sativa*) and grape (*Vitis Vinifera)* also contain a single p80 gene, while poplar (*Populus trichorcarpa*) contains two p80 genes. Additionally, I found three homologues of Atp80 in the moss *Physcomitrella patens,* which suggests that expansion of the p80 gene family has occurred in this lower plant.

In animals, I found a single p80 homologue represented in most species including the invertebrate lancelet (*Branchiostoma floridae*), and vertebrates chicken (*Gallus gallus*), horse (*Equus caballus*), dog (*Canis familiaris*), rat (*Rattus norvegicus*) and humans (*Homo sapiens*). The animal p80 proteins share 33-34 % AA identity with Atp80 across the entire protein, and a slightly higher identity (42-44 %) within the WD40 repeat-containing N-terminal half. The human p80 homologue has been previously identified as WDR48, a protein with 7-8 WD40 repeats in its N-terminal region which plays a role in vesicular transport of proteins targeted for lysosomal degradation (Park et al., 2002). Human p80 (WDR48) binds to herpesviral and papillomaviral proteins (Cote-Martin et al., 2008), and a recent report details binding of Hsp80 to deubiquinating enzyme complexes where it regulates enzymatic activity (Cohn et al., 2009).

In collaboration with my advisor, I used ClustalW to generate an amino acid alignment which was submitted to the Mobyle server (http://mobyle.pasteur.fr) for analysis by the PhyML program (a likelihood method) to generate a phylogenetic tree with 1000 bootstraps. TreeDyn 198.3 was used to produce a cladogram which is shown in Figure 22. This cladogram indicates that Atp80 and all plant homologues are contained on a branch with Atp80 being most related to the poplar and grape proteins. A separate branch containing the animal p80 proteins is also evident (Figure 22). A different cladogram constructed with a neighbor-joining method gave similar results (data not shown). We conclude that Atp80 is encoded by a single gene in Arabidopsis and that it has one or two homologues in some plant species, while animals appear to contain a single p80 gene.

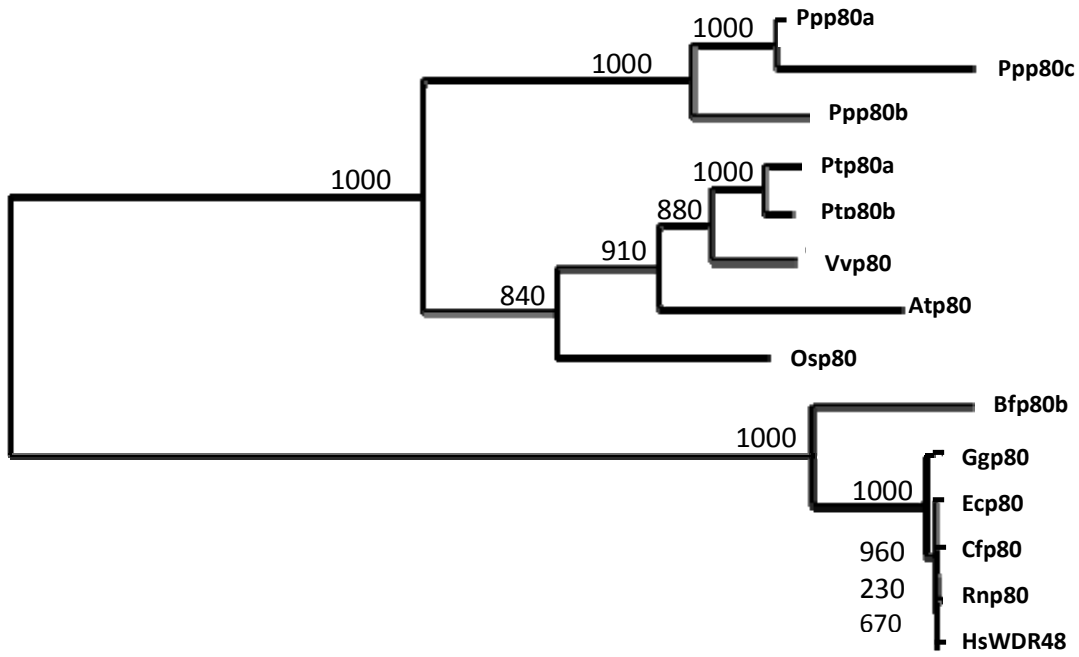

Figure 22. Phylogenetic tree of putative Atp80 homologues. Putative Atp80 homologues were identified with BLASTp search and the predicted amino acid sequences were aligned with ClustalW. The resulting alignment was analyzed with PhyML to generate 1000 bootstrapped phylogenetic trees. TreeDyn 198.3 was used to generate a cladogram. The tree has 2 major branches containing plant (upper) and animal (lower) p80s. The tree also consists of a separate moss branch. The results indicate that the Arabidopsis p80 is most related to the *Populus*, *Vitis* and *Rice* (Os) proteins, as expected. Abbreviations: moss, *Physcomitrella patens* (Pp); plant species, *Populus Trichorcarpa* (Pt), *Vitis Vinifera* (Vv), *Oriza Sativa* (Os); animal species, *Branchiostoma floridae* (Bf), *Gallus gallus* (Gg), *Equus caballus* (Ec); *Canis familiaris* (Cf); *Rattus norvegicus* (Rn); *Homo sapiens* (Hs).

Another clue to the function of Atp80 could exist in the WD40 repeat region. To examine whether the WD40 repeat region of Atp80 shares high homology with other Arabidopsis proteins, I used the first 492 amino acids from Atp80 as a query in a BLASTp search to identify similar WD40 proteins in Arabidopsis. The BLASTp search revealed 48 related sequences with e-values less than 1. Among them were the WD40 regions of PRL1, PRL2, and katanin p80 (for a complete list see Supplemental Table S5). As a group, these proteins share 24- 36 % AA identity with Atp80. ClustalW and PhyML were used to generate a phylogenetic tree as before, which showed low bootstrap values and support for individual branches and/or clades (data not shown). For example, At5g13480 encodes the FY protein involved in flowering time control and is the most closely related protein to Atp80 based on the phylogenetic tree. However, the bootstrap value of 240 does not support a strong evolutionary relationship between Atp80 and At5g13480. Therefore, individual WD40 repeats of the most closely related proteins were aligned with ClustalW-XXL and Quicktree was used to determine if individual WD40 repeats were strongly conserved in these proteins. The results in Figure 23 indicate that the WD40 repeats within Atp80 are most closely related to those from the p80 homologues (grape and human only are shown). Together these analyses support the idea that Atp80 is a unique protein and does not have redundant function with other Arabidopsis WD40-containing proteins.

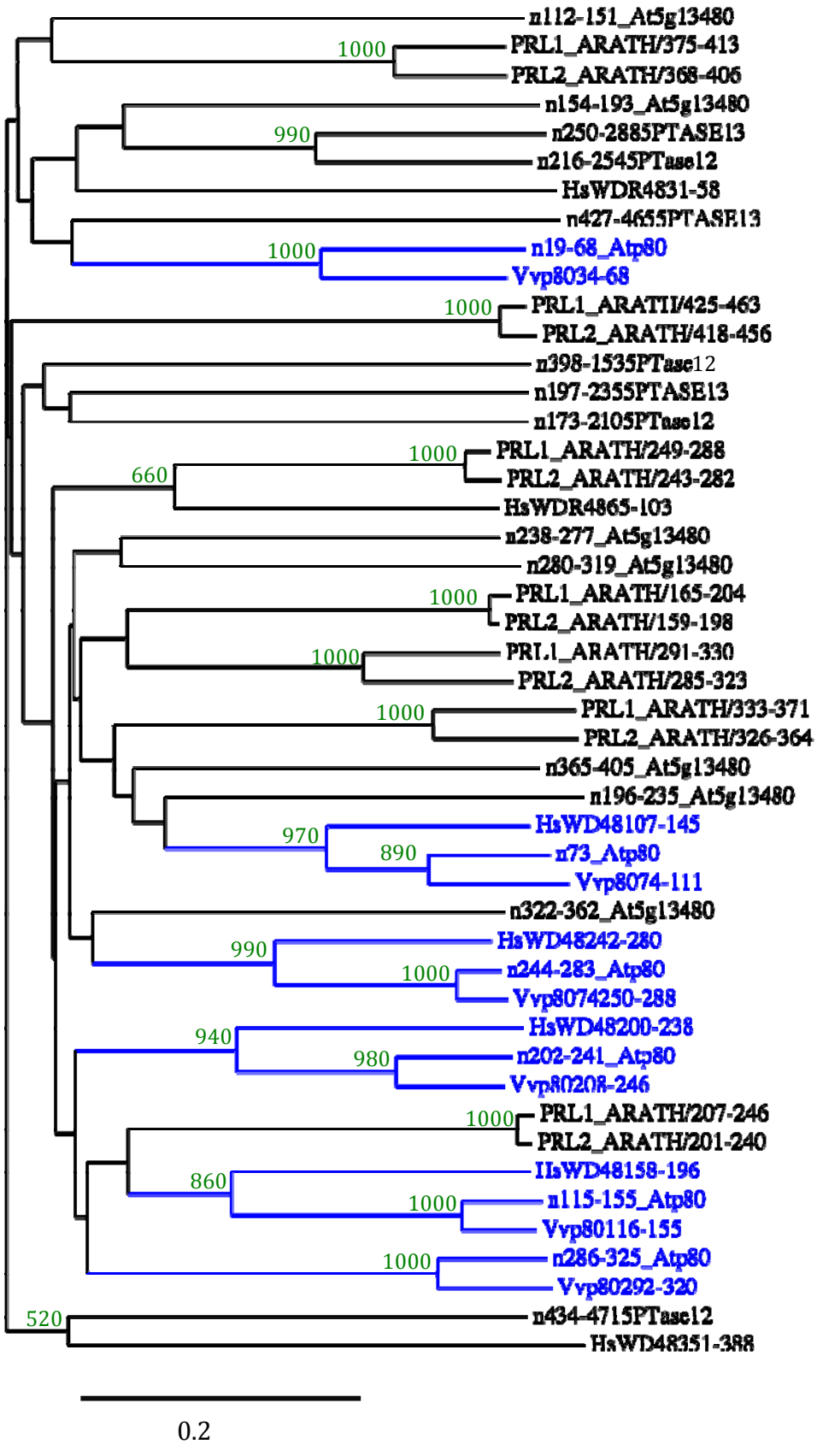
n112-151_At5g13480
1000
PRL1_ARATH/375-413
PRL2_ARATH/368-406
n154-193_At5g13480
990
n250-2885PTASE13
n216-2545PTase12
HsWDR4831-58
n427-4655PTASE13
1000
n19-68_Atp80
Vvp8034-68
1000
PRL1_ARATH/425-463
PRL2_ARATH/418-456
n398-1535PTase12
n197-2355PTASE13
n173-2105PTase12
1000
PRL1_ARATH/249-288
660
PRL2_ARATH/243-282
HsWDR4865-103
n238-277_At5g13480
n280-319_At5g13480
1000
PRL1_ARATH/165-204
PRL2_ARATH/159-198
1000
PRL1_ARATH/291-330
PRL2_ARATH/285-323
1000
PRL1_ARATH/333-371
PRL2_ARATH/326-364
n365-405_At5g13480
n196-235_At5g13480
HsWD48107-145
970
890
n73_Atp80
Vvp8074-111
n322-362_At5g13480
HsWD48242-280
990
1000
n244-283_Atp80
Vvp8074250-288
HsWD48200-238
940
980
n202-241_Atp80
Vvp80208-246
1000
PRL1_ARATH/207-246
PRL2_ARATH/201-240
IIsWD48158-196
860
1000
n115-155_Atp80
Vvp80116-155
1000
n286-325_Atp80
Vvp80292-320
520
n434-4715PTase12
HsWD48351-388
0.2

Figure 23. Phylogenetic analysis of individual WD40 repeats from Atp80 and relatives. The indicated regions of amino acid sequences from Atp80 and homologues from *Vitis vinifera* (Vvp80) and Humans (HsWDR48) along with the most closely related WD40 domain-containing proteins were aligned with Clustal W-XXL. The alignment was analyzed by quicktree and 1000 bootstraps were performed. TreeDyn 198.3 was used to generate a cladogram. Atp80 branches are shown in blue, bootstrap values greater than 500 are in green.

Atp80 is Localized in the Nucleus

To investigate the subcellular location of the Atp80 protein, I generated Atp80:GFP expressing plants in wild-type under the control of the 35S cauliflower promoter and performed imaging experiments with four independent homozygous lines containing the Atp80:GFP construct. I analyzed T2 progeny from all lines with fluorescence deconvolution microscopy and found a similar pattern in three of the lines. GFP fluorescence was associated with nuclei in guard cells in the cotyledon epidermis (Figure 24A, B) and root cells (Figure 24C, D). To confirm the nuclear localization, I stained Atp80:GFP seedlings with the nuclear dye 4',6-diamidino-2-phenylindole (DAPI) and imaged the GFP and DAPI fluorescence in nuclei from the same root cells (Figure 24E, F). The nuclear location of Atp80 was also observed in *atp80* mutant plants expressing the Atp80:GFP construct (*atp80*/Atp80:GFP lines) (data not shown).

Two of the lines (Atp80/Atp80:GFP-1, Atp80/Atp80:GFP-2) were used in a genomic PCR experiment to confirm presence of the transgene in the genome by using primers Atp80For1 and Atp80Rev1 (Figure 25A and Supplemental Table S6). Additionally, the Atp80:GFP fusion protein was detected in both lines with anti-GFP antibody as a single band with a size of 110-kDa (Figure 25B). I conclude that the Atp80 protein is located in most of the nuclei from guard cells and roots.

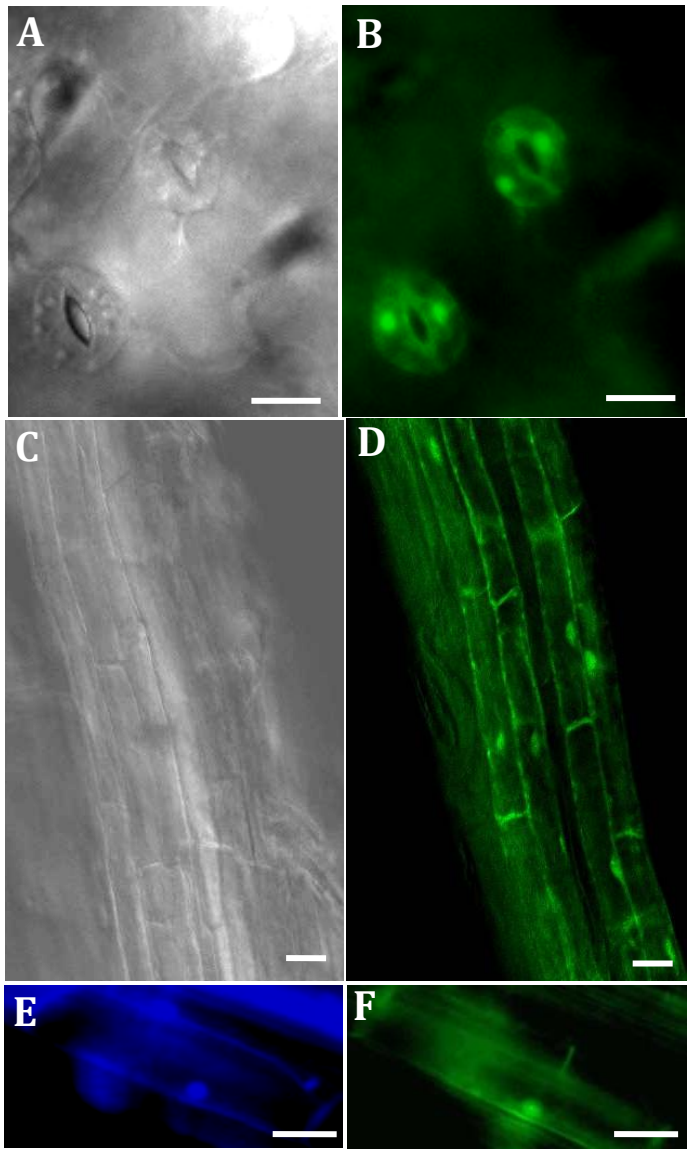

Figure 24. Subcellular localization of GFP-tagged Atp80 in Arabidopsis seedlings. GFP-tagged Atp80 (Atp80:GFP) was expressed in a wild-type background, and the subcellular location in cotyledons (A,B) and roots (C,D) from 2 weeks-old seedlings was examined with fluorescence deconvolution microscopy. A. Differential interference contrast of guard cells. B. GFP fluorescence in nuclei of guard cells. C. Differential interference contrast of root cells. D. GFP fluorescence in nuclei of

root cells. E, F. Seedlings were stained with DAPI and examined with a standard UV fluorescence filter set. DAPI (E) and GFP (F) fluorescence in a nucleus from a root cell. Bar = 20 μm.

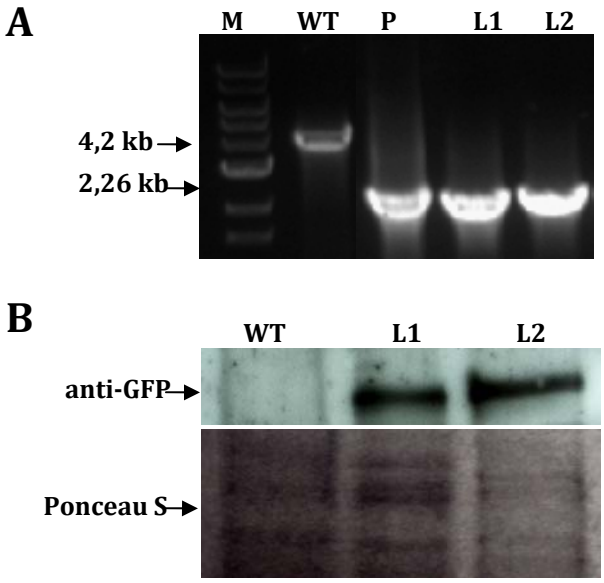

Figure 25. Genomic PCR and western blot analysis of Atp80 transgenic plants. A. Genomic PCR reactions performed with Atp80 gene specific primers confirm that both lines (L1=Atp80/Atp80:GFP-1; L2=Atp80/Atp80:GFP-2) contain the transgene (a 2,26 kb fragment); P= Atp80 plasmid DNA used as a positive control. B. Western Blot. Denatured seedling extracts from WT, L1 (Atp80/Atp80:GFP-1) and L2 (Atp80/Atp80:GFP-2)were separated by SDS-PAGE, transferred to a nitrocellulose membrane, and blotted with an anti-GFP antibody. Ponceau S stained filters are shown as controls for equivalent loading.

Atp80 Interacts with SnRK1.1 and PBP1

Atp80 is a WD40–containing protein and is likely to have more than one protein binding partners. As such I consider Apt80 as a possible subunit of a larger protein complex containing 5PTase13 and SnRK1.1. To test this hypothesis my collaborator Les Erickson used the C-terminal region of Atp80 as bait in the yeast two hybrid system. First he performed direct yeast two hybrid screen with the Atp80 and SnRK1.1 pray plasmids and found that Atp80 and SnRK1.1 interact (Figure 20). Next he used the C-terminal region of Atp80 as bait and obtained a second clone containing a gene encoding the pinoid binding protein (PBP1, At5g54490). Dr. Erickson retransformed the Atp80 positive clones into yeast and I verified the interactions *in vitro* (Figure 26A,B).

To examine the interactions between Atp80 and either SnRK1.1 or PBP1 *in vitro*, I fused the V5 epitope tag sequence to the C-terminus of Atp80 (Atp80V5) and the sequence encoding the GST epitope tag to the C-terminus of SnRK1.1 (SnRKGST) or the N-terminus of PBP1 (GST-PBP1) and expressed all proteins in *E. coli*. The Atp80V5 construct directs the expression of an 82 kDa protein detected by an anti-V5 monoclonal antibody (Figure 26B, lanes 1-6). The SnRK-GST and GST-PBP1 constructs direct the expression of 83.3 kDa and 41 kDa proteins, respectively, detected by an anti- GST monoclonal antibody (Figures 26B, lanes 2 and 3 respectively). To determine whether the Atp80V5 recombinant protein can "pull down" SnRKGST and/or GST-PBP1, immunoprecipitations using anti-V5:protein A-Sepharose beads were performed, and the resulting complexes were then analyzed by western blotting with an anti-GST antibody (Figure 26B, IP lanes). As shown in Figure 26B, SnRKGST and GST-PBP1 are detected in the pull-down assay when either of them has been incubated in the presence of Atp80V5 (Figure 26B, lanes 5 and 6 respectively). It should be noted that the pull-

down efficiency of SnRK-GST by Atp80V5 is much less as compared to that of GST-PBP1 which may indicate differences in the interactions between these proteins. As a negative control, I used a GUS-GST construct that directs the expression of a 97 kDa protein (Figure 26B, lane 1). When incubated with Atp80V5, GUS-GST does not appear in the IP fraction (Figure 26B, lane 4). Input and bound fractions of each protein alone were anaylsed to ensure that the interactions are valid. As expected no band was detected in the IP fractions of SnRKGST, GUS-GST or GST-PBP1 when incubated with anti-V5-agarose beads alone (Supplemental Figure S6). I conclude that Atp80 and either SnRK1.1 or PBP1 but not the GUS protein can form protein complexes *in vitro*.

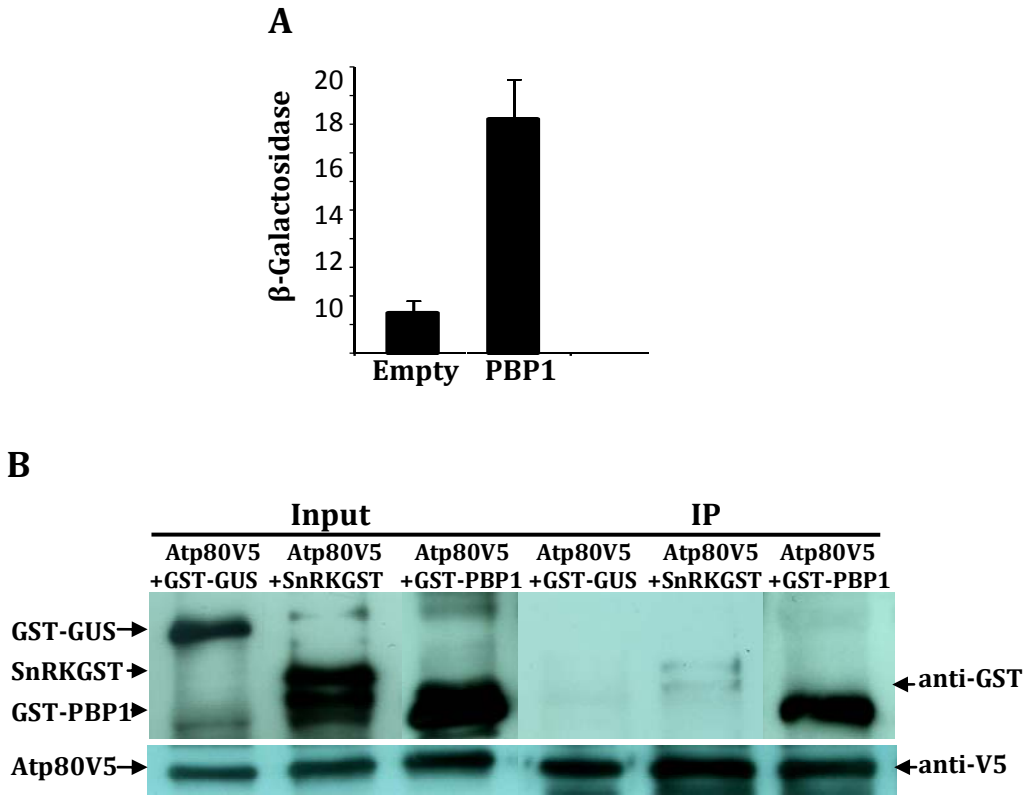

Figure 26. β -Galactosidase Assay. A. An Arabidopsis cDNA prey library was screened using the C-terminal region of Atp80 as bait in the yeast two-hybrid system. Over 1 million yeast transformants were screened for reporter gene expression (β-galactosidase). This resulted in the isolation of a PREY plasmid expressing the PBP1 gene. Independent PBP1 yeast transformants (e.g. three separate colonies that are recovered after a directed-interaction) are assayed with β -galactosidase assay, each in triplicate. The PBP1 prey plasmid was isolated, retested and sequenced. B. Atp80V5 interacts with SnRK1.1 and PBP1 *in vitro*. Immunoprecipitation (IP) was carried out using an anti-V5 antibody bound to a protein A sepharose (PAS). Purified and dialyzed recombinant proteins, Atp80V5 (Atp80) SnRKGST (SnRK1.1), GST-PBP1 (PBP1) and GUS-GST (GUS) were incubated for 2 hrs at room temperature in IP buffer before transferring to the antiV5:PAS complex. The resulting IPs were analyzed using a protein gel blotting. Lanes 1-3: Input fractions of Atp80V5 in combination with GUS-GST (lane 1), SnRKGST (lane 2) or GST-PBP1 (lane 3); Lanes 4-6: Bound (IP) fractions of Atp80V5 in combination with GUS-GST (lane 4), SnRKGST (lane 5) or GST-PBP1 (lane 6). GUS-GST was used as a negative control. The blot images are representative of three independent experiments.

Gene Expression Patterns of Atp80, 5PTase13 and PBP1

I previously compared available microarray data on expression patterns of 5PTase13 and SnRK1.1 and found that SnRK1.1 is highly expressed in most plant tissues examined (Ananieva et al., 2008), while 5PTase13 appears to have overall less expression. To determine whether 5PTase13, Atp80 and PBP1 are co-expressed in similar tissues and throughout development, I used two independent approaches: comparison of microarray data from GENEVSTIGATOR and analysis of transgenic plants containing promoter-reporter gene constructs.

Microarray data from GENEVESTIGATOR (Zimmermann et al., 2004) indicates that Atp80 is broadly and abundantly expressed during different developmental stages as compared to 5PTase13, and PBP1 (Supplemental Figure S5A). 5PTase13 and PBP1 are also broadly expressed but thier their transcripts are not as abundant as Atp80. In addition, PBP1 expression is high in young rosette leaves (Supplemental Figure S5B). In seedlings, Atp80 is abundantly expressed while 5PTase13 and PBP1 expression levels are lower. The three genes are expressed at similar expression levels in roots (Supplemental Figure S5B). I conclude that Atp80, 5PTase13 and PBP1 are detected in all plant tissues examined although 5PTase13 and PBP1 expression levels are lower, in general, as compared to Atp80.

To further examine the expression patterns of Atp80 and its protein partners, I produced promoter:reporter gene constructs using the β-glucuronidase (GUS) gene. Atp80Prom:GUS, 5PTase13Prom:GUS and PBP1Prom:GUS gene fusions were constructed by cloning up to 2,000 bp of DNA upstream of the predicted start site of transcription and fusing this to the GUS reporter gene. Constructs were introduced into plants and stably transformed

plants were obtained. A GUS staining protocol was used to examine the spatial and temporal expression of the three genes as described in "Materials and Methods" (Jefferson et al., 1987). As seen in Figure 27, all three promoter:GUS constructs direct moderate expression in cotyledons with Atp80Prom:GUS and PBP1Prom:GUS directing strong expression in vascular tissues (Figure 27A-C). In roots, 5PTase13Prom:GUS directs low level expression while Atp80Prom:GUS and PBP1Prom:GUS plants show intense staining indicative of high level expression (Figure 27D-F). Specifically, Atp80Prom:GUS shows highest expression in the root tip zone (Figure 27E) while PBP1Prom:GUS is detected in the root hairs as well (Figure 27F). In rosette leaves, 5PTase13Prom:GUS directs moderate level expression mostly detected in the base of the leaf and some in the vascular tissues (Figure 27G). Atp80Prom:GUS and PBP1Prom:GUS are detected in the vascular tissues of the rosette leaves with PBP1Prom:GUS showing the most intensive staining (Figure 27I). I conclude that the three promoter:GUS constructs show similar expression patterns in all organs examined.

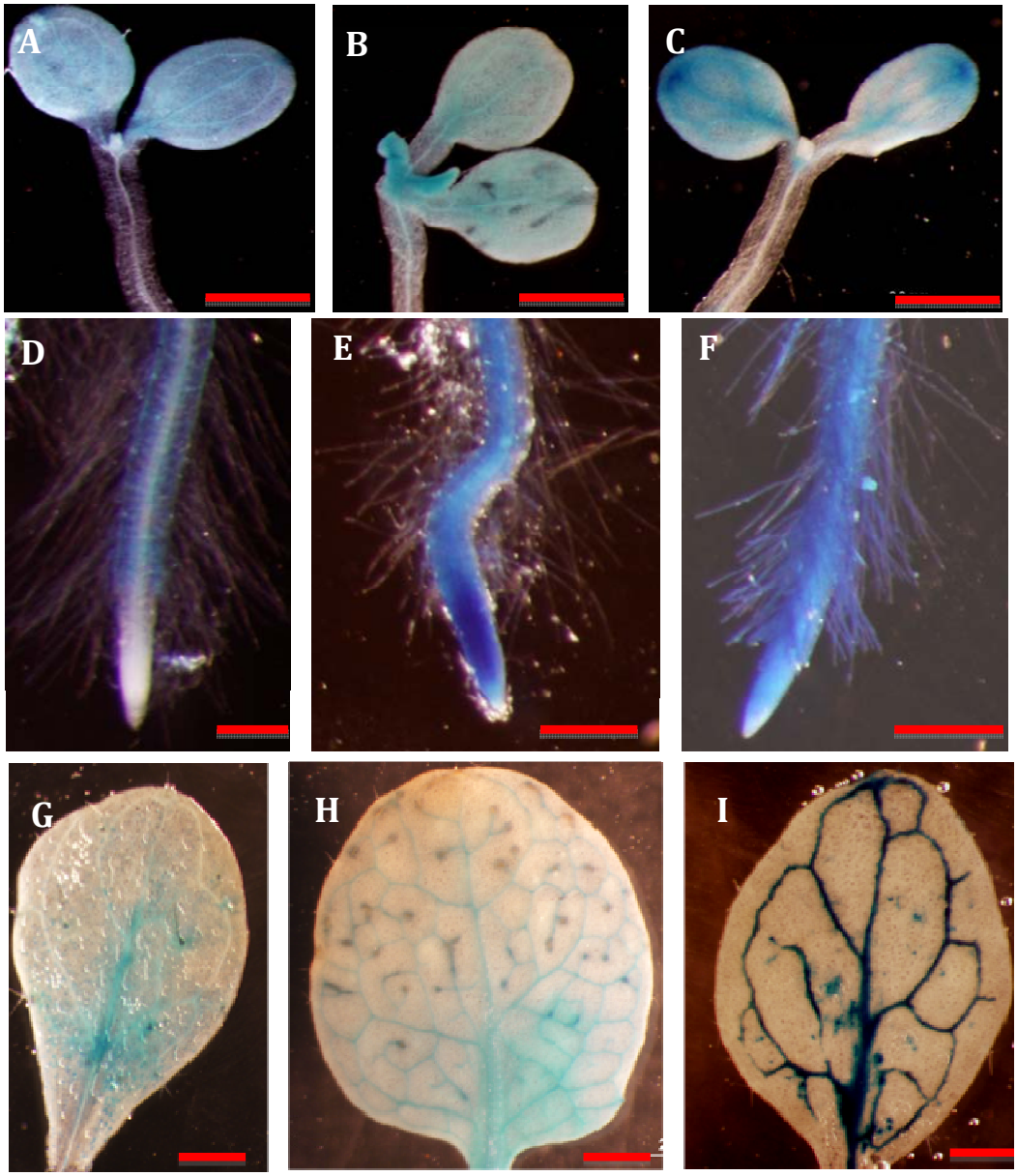

Figure 27. Spatial Expression Analysis of Atp80 and its protein partners 5PTase13 and PBP1. Promoter GUS staining of 10 days-old seedlings screened on Basta (30 µg mL^{-1}) plates containing 0.8 % agar, 0.5x MS and 1 % sucrose. A-C. Images of cotyledons from 5PTase13Prom:GUS (A), Atp80Prom:GUS (B) or PBP1Prom:GUS (C) plants; D-F. Images of roots from 5PTase13Prom:GUS (D), Atp80Prom:GUS (E) or PBP1Prom:GUS (F) plants. G-I. Images of rosette leaves 5PTase13Prom:GUS (G), Atp80Prom:GUS (H) or PBP1Prom:GUS (I) plants. Pictures are representative of similar staining pattern in ≥10 samples. Bar is 1 mm in A, B, C, G,H, I; bar = 0.5 mm in D, E, F.

Atp80 Mutant Identification

To explore the function of Atp80 and characterize the relationship of Atp80 with its protein partners, I isolated a T-DNA insertion mutant in the Atp80 gene. A potential mutant was identified in the SALK T-DNA database, named *atp80* (At3g05090, Gabi-Kat 007H09) and compared with its corresponding wild-type accession (Figure 28A, B). The presence of the T-DNA insertion was verified by diagnostic PCR using genomic DNA and primers specific for the T-DNA left border (LB, Gabi-Kat LB primer) and gene-specific primers (Atp80For, Atp80Rev) that flank the T-DNA insertion (Figure 28A and B and Supplemental Table S6). Using primers specific for the 3'end of Atp80 (Atp80For3, Atp80Rev3), I detected a PCR product in wild-type but not in the *atp80* mutant (Figure 28C). I also used this analysis to determine the fold increase in the expression of the Atp80 transcripts in Atp80/Atp80-GFP-1 and Atp80/Atp80-GFP-2 overexpressors as compared to wild-type (Figure 28C, the last two lanes). I conclude that the *atp80* mutant does not express transcripts capable of encoding a full-length Atp80 protein and that the Atp80/Atp80-GFP-1 line is a low expressor line whereas Atp80/Atp80-GFP-2 line is a high expressor line.

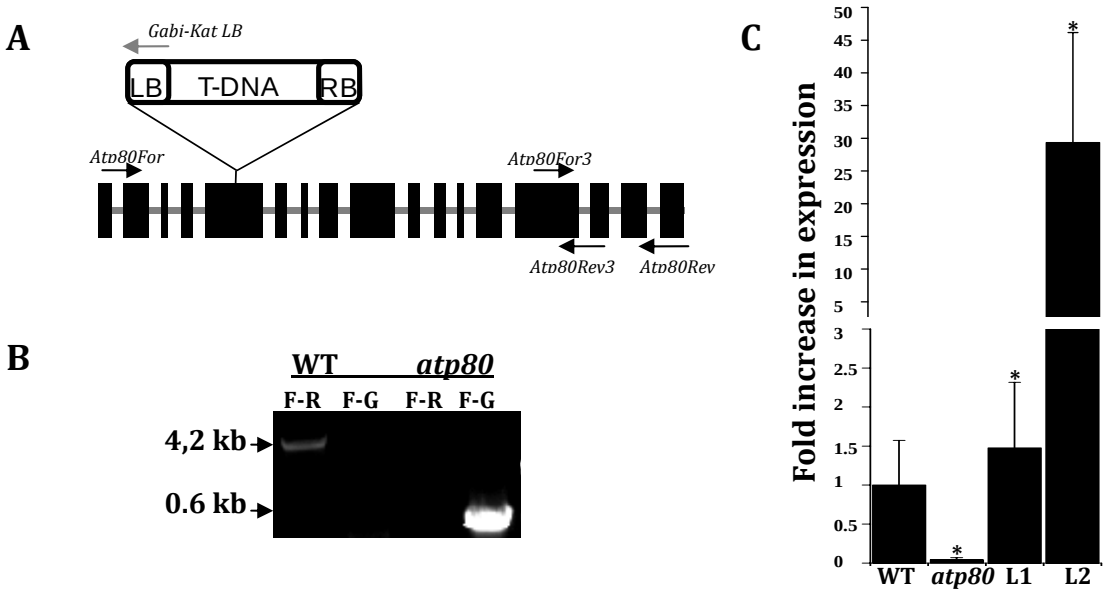

Figure 28. T-DNA insertions and gene expression in the *atp80* mutant line. A. Map of the T-DNA insertion in the Atp80 gene. The Atp80 gene has 17 exons shown as black boxes; the light gray arrow indicates the Gabi-Kat primer used to amplify the left border (LB) of the T-DNA; black arrows indicate positions of gene-specific primers. B. PCR reactions performed with gene specific and left border (LB) primers confirm that the *atp80* mutant line is homozygous. A gene specific primer that flanks the T-DNA insertion (primer **F**orward: *Atp80For*) in conjunction with the T-DNA LB (**G-**Gabi-Kat primer) primer amplify 0.6 kb fragment in the *atp80* mutant indicating the presence of one LB sequence in proximity to the Atp80 gene. C. Verification of loss of Atp80 expression in 3 week-old leaves from soil-grown WT, *atp80* mutant or two independent transgenic lines expressing the Atp80:GFP construct in wild-type background (L1= Atp80/Atp80:GFP-1; L2=Atp80/Atp80:GFP-2). Total RNA (2 µg) was isolated and quantitative RT–PCR (qPCR) reactions were performed with primers Atp80For3, Atp80Rev3, PEX4For and PEX4Rev as described in the "Materials and Methods" (see supplemental Table S6 for primer sequences). * indicates a p value < 0.05 as compared to WT.

The atp80 Mutant Exhibits Light-Dependent Rosette Leaf Defects and Premature Senescence

Soil-grown *atp80* mutant plants were grown in a growth chamber with a visible radiation between 100-130 μE and long day conditions (16 hrs light). Under these conditions, *atp80* mutants exhibit a severe growth retardation phenotype (Figure 29). I compared rosette leaf development of the *atp80* mutant and wild-type plants and observed that the *atp80* mutant develops normal cotyledons and the first pair of rosette leaves (Figure 29A-C). However, the further growth and development of *atp80* mutant rosette leaves is severely impacted. These mutant leaves fail to develop to full size and have a more rounded shape as rgy Metabolism/drug effects/*genetics</keyword><keyword>G-B*ox Bi*nding m</keyword><keyword>Gene Expression Profiling</keyword><keyword>*Gene Expression , Pette leaves have senesced (Figure 29D-F). The majority of *atp80* mutant plants are able to bolt, flower and develop siliques although their overall size is smaller and flowering time is delayed as compared to wild-type plants (Figure 29G). It is important to note that senescence and flowering time have been previously linked with nutrient sensing in plants (Baena-Gonzalez et al., 2007).

Under standard laboratory growth conditions I made the observation that nutrient solutions such as Miracle-Gro highly improve Arabidopsis growth and plants grow robust, develop more rosette leaves and accumulate more leaf biomass. To determine whether a nutrient solution can improve the growth and development of the *atp80* mutant, I watered *atp80* mutant and wild-type plants with distilled water only or distilled water and a nutrient solution. As shown in Figure 29, the *atp80* mutants show symptoms of growth retardation

with and without the added nutrient solution (Figure 29B, C and I, J) indicating that added nutrients can not “rescue” the growth retardation phenotype of *atp80* mutants.

To test whether the light period impacts the development of growth retardation symptoms in *atp80* mutants I grew *atp80* mutant and wild-type plants under short day (8 hr light) and visible radiation of 100-130 μE. Likewise, I watered half of the plants with a nutrient solution as described above. Under short day growth conditions, *atp80* mutants do not show the growth retardation phenotype in either the presence or absence of the nutrient solution (Figure 30A). Under these conditions, the rosette leaves of *atp80* mutants develop normally and do not show signs of senescence as compared to wild-type plants (Figure 30A). When wild-type plants are watered with a nutrient solution, the size and number of leaves increases (Figure 30A, B). In contrast, the *atp80* mutant leaf development does not change when a nutrient solution is added, with leaf size and number remaining the same as with no added nutrient solution (Figure 30A, B). I conclude that under short days and normal visible radiation the *atp80* mutants do not show a growth retardation phenotype and appear to be unresponsive to an added nutrient solution. These data indicate that day length and possibly light signaling plays a major role in the growth retardation phenotype of *atp80* mutants.

To confirm whether light intensity impacts the severe growth retardation symptoms in *atp80* mutants, I placed a plastic barrier called a humidity dome over *atp80* mutant and wild-type plants to limit light. These plants were grown in the same growth chamber under long day conditions and 100-130 μE of light as described before (Figure 31A, B). My results revealed that the *atp80* growth retardation symptoms are rescued to a great extent by lessening the light intensity, but not entirely since I measured a lower number of rosette leaves on *atp80* mutants as compared to wild-type plants grown in these conditions (Figure

31A-C). These results suggest that the functional role of the Atp80 gene is complex and that there are factors other than light that also impact the development of the *atp80* mutants.

An ongoing goal is to confirm that the loss of *atp80* function causes the light dependent growth retardation phenotype by complementing the *atp80* mutant with an Atp80:GFP transgene. My analysis so far reveals that the Atp80:GFP transgene partially complements the *atp80* mutant growth phenotype in the T1 generation (a heterozygous stage) (Figure 31E-G). Different transgenic lines I have analyzed show phenotype variations from severe to mild leaf developmental defects (Figure 31 F, G). A likely explanation for this result is that the heterozygous stage does not provide enough expression to complement the retardation phenotype completely. I will continue to analyze the next generation of potential complemented lines to obtain homozygous plants and examine their light dependent phenotypes.

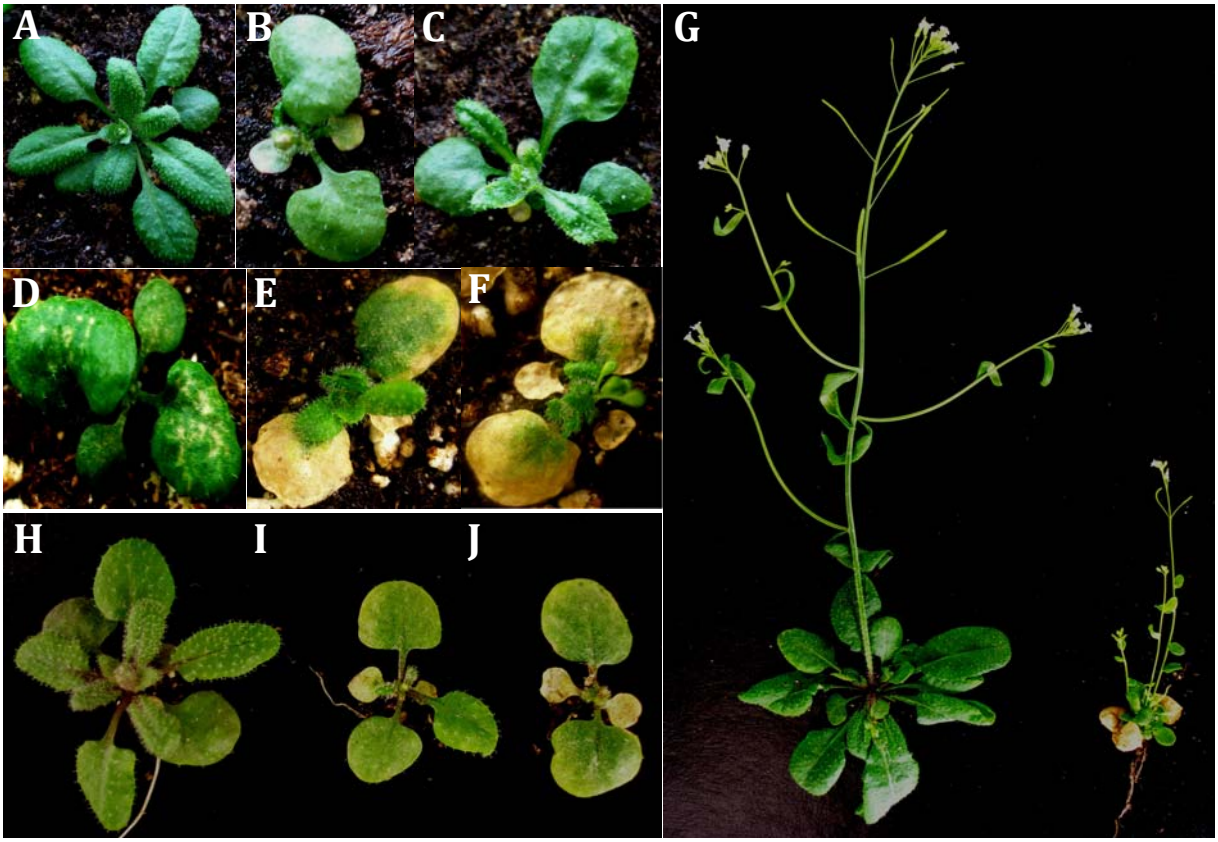

Figure 29. Light-inducible rosette leaf phenotypes of the *atp80* mutant. Wild-type and *atp80* mutant plants are grown on soil in a growth chamber with visible radiation between 100-130 µE, 50 % humidity and long days (16 hrs light). A-G. Plants watered with a nutrient solution: A. Wild-type plant; B, C. *atp80* mutant plants with severely retarded rosette leaves; D-F. *atp80* mutant plants undergoing different stages of premature senescence of their rosette leaves. G. Fully grown wild-type plant (left) as compared to a small and developmentally delayed *atp80* mutant plant (right). H-J. Plants watered with distilled water only. H. Wild-type plant; I,J. *atp80* mutant plants with severely retarded rosette leaves. The light-inducible growth retardation phenotypes of the *atp80* mutant were observed in two consecutive generations of plants.

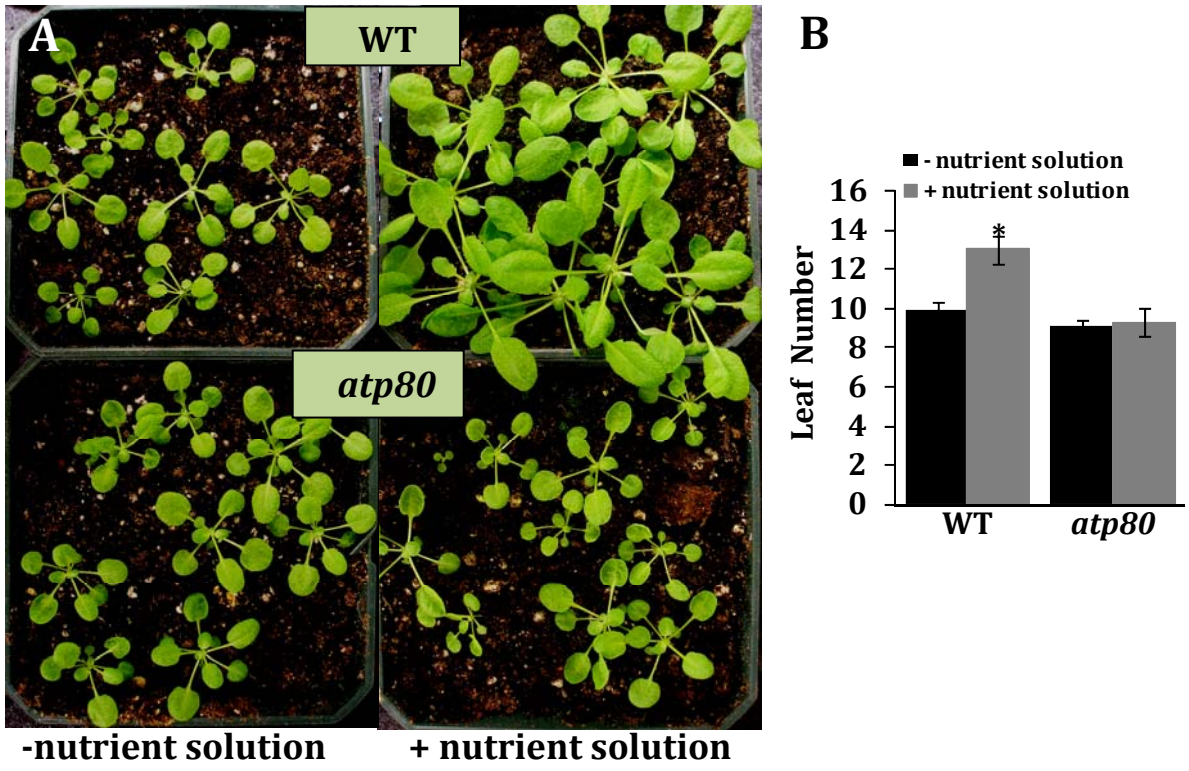

Figure 30. *Atp80* mutant phenotype under short day growth conditions. Wild-type and *atp80* mutant plants are grown on soil in a growth chamber with visible radiation between 100-130µE, 50 % humidity and short day (8 hrs light). A. Images of 5-weeks old wild-type and *atp80* mutant plants watered without (left panel of pots) or with a nutrient solution (right panel of pots). B. Leaf Number. Rosette leaves from 5-weeks old soil grown wild-type and *atp80* mutant plants watered with or without a nutrient solution were counted. Bars represent the mean ± SE of 4-5 pots per variant. The experiment was independently repeated two times. * indicates a p value < 0.05.

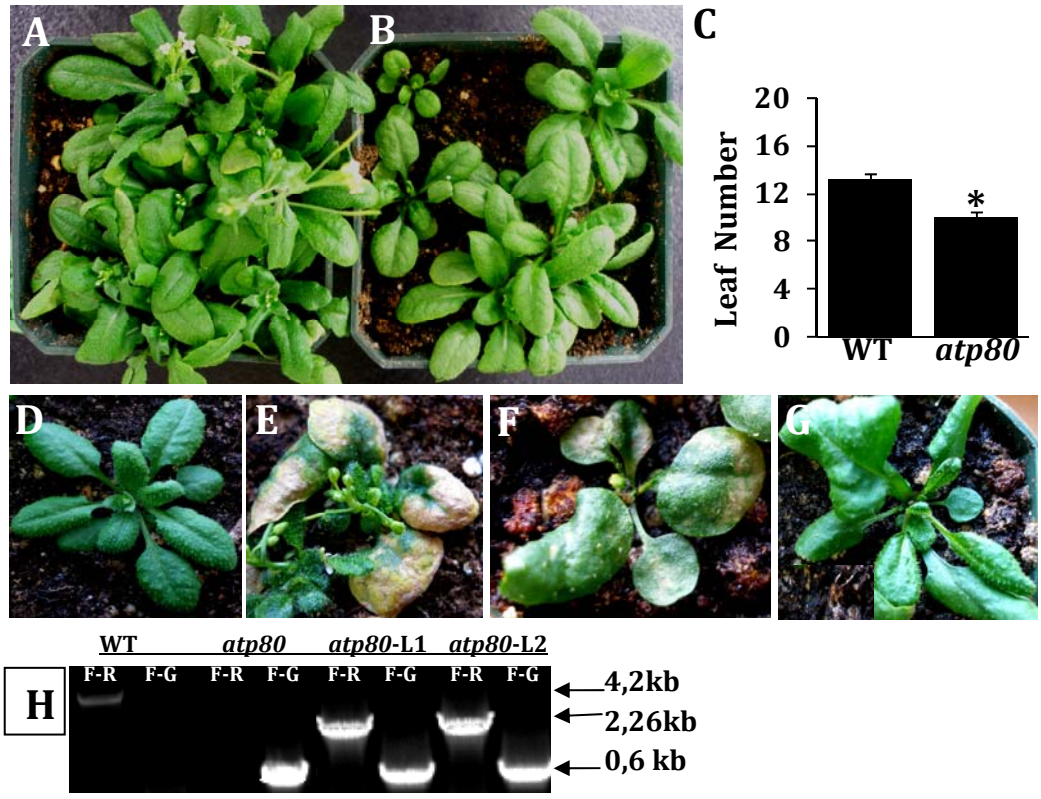

Figure 31. Complementation of the *atp80* mutant phenotype under long day growth conditions. Wild-type and *atp80* mutant plants are grown on soil in a growth chamber with visible radiation between 100-130 µE, 50 % humidity and long days (16 hrs light). A, B. Images of wild-type (A) and *atp80* mutant (B) plants watered with a nutrient solution and covered with a dome for the entire period of 4 weeks. C. The leaf number of dome covered *atp80* mutant plants is smaller than that of WT. Rosette leaves from 4-weeks old soil-grown wild-type and *atp80* mutant plants watered with a nutrient solution and covered with a dome were counted. Bars represent the mean ± SE of 4-5 pots per variant. * indicates a p value < 0.05. D-G. Images of wild-type (D), *atp80* mutant (E) and *atp80* mutant plants expressing the Atp80:GFP construct (F, G) watered with a nutrient solution and grown under long day conditions. My segregation analysis shows transgenic plants with severe growth retardation phenotype (F, *atp80*/Atp80:GFP-1, [*atp80*-L1]) or with a mild growth retardation phenotype (H, *atp80*/Atp80:GFP-2 [*atp80*-L2]). I. Genomic PCR confirmation that the two transgenic lines (*atp80*-L1 and *atp80*-L2) contain the transgene (a 2.3 kb fragment) and the mutant specific band (a 0.6kb fragment). Primers F- Atp80For; R-Atp80Rev; G-Gabi-Kat (Supplemental Table S6).

The atp80 Mutant Produces Smaller Siliques and Dark Brown Seeds

I studied the seed development of the *atp80* mutant and compared it with that of wild-type plants. As seen in Figure 32, seeds from *atp80* mutant plants are dark brown as compared to the light brown seeds from wild-type plants (Figure 32 A, B). Additionally, I observed that *atp80* mutants produce smaller siliques as compared to wild-type siliques which may be related to the overall reduction in organ size in the *atp80* mutant plants (Figure 32 C, D see also Figure 29 G).

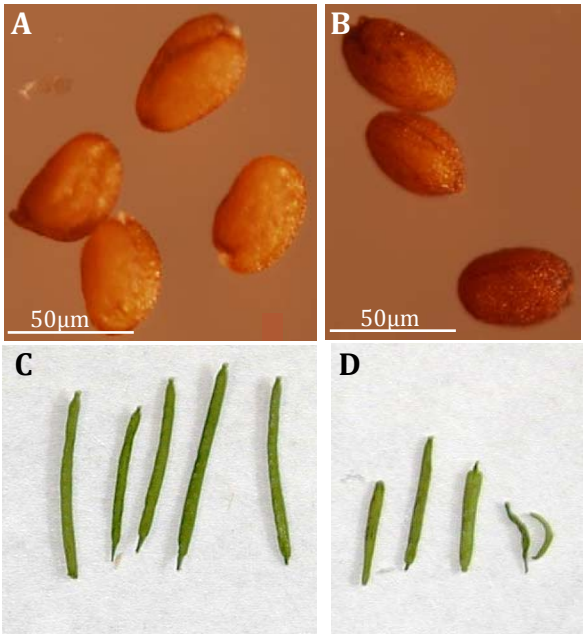

Figure 32. The *atp80* mutant produces smaller siliques and dark-brown seed. Wild-type and *atp80* mutant plants are grown on soil in a growth chamber with visible radiation between 100-130 µE, 50 % humidity and long day (16 hrs light). A,B. Images of light brown seeds from wild-type plants (A) and dark-brown siliques from *atp80* mutant plants (B). C,D. Images of siliques from wild-type plants (C) and *atp80* mutant plants (D).

The Root Growth Response of atp80 is Similar to that of 5ptase13 and snrk1.1 Mutants

As described in the previous section, the *atp80* mutant is smaller in size and has a reduced number of rosette leaves as compared to wild-type plants when stimulated with a nutrient solution (see Figure 30 A, B). This suggests a role of Atp80 function in nutrient sensing or signaling. To test this hypothesis, I measured the root length of *atp80* mutant plants grown under no- and low-nutrients and 3 % sucrose conditions for 6 days (Figure 33 A-C). I then compared *atp80* mutant root growth with that of *5ptase13* and *snrk1.1* mutants, which have a small reduction in root growth under the no-nutrient and low-nutrient conditions and exhibit no change or enhanced root growth with 1 % to 3% Suc, respectively (Baena-Gonzalez et al., 2007; Ananieva et al., 2008, see Figure16 A-C Chapter II). The a*tp80* mutant exhibited 1.4-1.6 fold reduced root growth on day 2 and a 2.5-3.2 fold reduction on day 6 under no-nutrient and low-nutrient conditions, respectively. There was no change in *atp80* root growth as compared to wild-type when supplied with exogenous 3 % Suc (Figure 33 A–C), indicating that *atp80* root growth alterations can be "rescued" by sucrose supplementation. In contrast, plants overexpressing Atp80 (Atp80/Atp80:GFP-1) showed enhanced root growth under no and low nutrient conditions as compared to wild-type plants after 6 days (Figure 33 A-C). This increase in root growth in Atp80/Atp80:GFP-1 seedlings is not present when 3 % Suc is supplied exogenously, thus the gain-of-function phenotype is also impacted by carbon supplementation.

The loss of Atp80 function root growth phenotypes described here are similar to those found in *5ptase13* mutants (Chapter II) and to those found by others in *snrk1.1* mutants (Baena-Gonzalez etal., 2007) with the *atp80* mutant showing more severe root growth inhibition in response to no- and low-nutrients as compared to *5ptase13* and *snrk1.1* mutants.

This may indicate that Atp80, 5PTase13 and SnRK1.1 work together in providing critical control over energy and nutrient sensing.

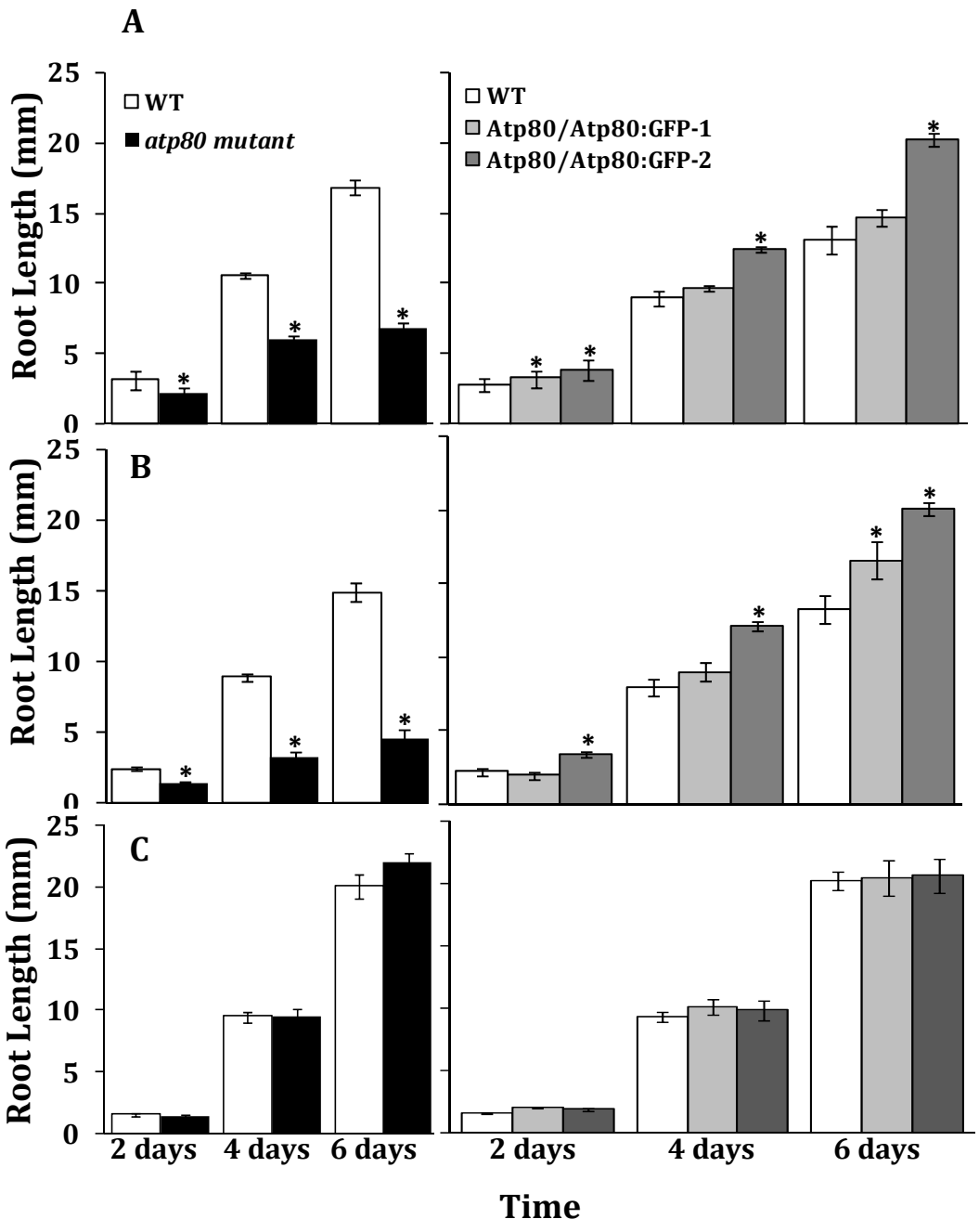

Figure 33. Nutrient-mediated root growth of the *atp80* mutants. Seed from WT, *atp80* mutant and two independent transgenic lines expressing the Atp80:GFP construct in wild-type background (Atp80/Atp80:GFP-1 and Atp80/Atp80:GFP-2) were grown in low light for 6 days on 0.8 % agar plates and either no nutrients (A), low nutrients (0.5x MS) (B), or optimal nutrients (0.5x MS, 3 % sucrose) (C). The root length for each group of seedlings was measured on day 2, 4 and 6. Values are means ± SE ($n \geq 40$). The experiment was independently repeated three times. * indicates a p value < 0.05 as compared to WT.

Atp80 and 5PTase13 Affect PBP1 Stability in Opposing Ways

I have previously shown that 5PTase13 can stabilize the SnRK1.1 protein, most likely by limiting SnRK1.1 proteasomal destruction (Chapter II). Since 5PTase13 also binds to Atp80 and Atp80 binds to SnRK1.1 and PBP1, I tested whether Atp80 regulates SnRK1.1 and PBP1 stability. For this work I used a similar approach as Lee et al. (2008) to examine the stability of recombinant V5- tagged SnRK1.1 (SnRKV5) and GST-PBP1 proteins in a cell-free degradation assay with wild-type, *apt80* or *5ptase13-1* mutant extracts grown under three different nutrient conditions: no-, low-nutrient and 3 % sucrose conditions. I performed a similar assay with recombinant Atp80V5 in wild-type and *5ptase13-1* mutant extracts to examine Atp80 stability.

The time course of SnRKV5 degradation with wild-type seedling extracts was previously determined (Ananieva et al., 2008), while the time course of GST-PBP1 and Atp80V5 indicated that these proteins are mostly degraded within 120 min and 2 min respectively (Figure 34). Accordingly, I chose a 15-min time point for analysis of SnRKV5 and GST-PBP1 degradation and a 2 min time point for analysis of Atp80V5. MG132, a proteasome-specific inhibitor, blocked SnRKV5, GST-PBP1 or Atp80V5 degradation in all extracts examined indicating that all proteins are destroyed by the 26S proteasome pathway in these assays (data not shown).

I found no difference in SnRKV5 stability between wild-type and *atp80* extracts under the three different nutrient conditions (Figure 35). Similar results were obtained for Atp80V5 stability in wild-type and *5ptase13-1* extracts regardless of the nutrient condition applied (Figure 36). In contrast, when I examined stability of GST-PBP1 in extracts prepared from either *atp80* or *5ptase13-1* mutant seedlings grown on no nutrients, I found changes in

GST-PBP1 stability as follows: there was less GST-PBP1 accumulation in *atp80* extracts as compared with wild-type extracts and there was more GST-PBP1 accumulation in *5ptase13-1* extracts as compared with wild-type extracts (Figure 37). This indicates an antagonistic relationship between Atp80 and 5PTase13 with respect to PBP1 stability. I did not observe any changes in GST-PBP1 stability when the *atp80* or *5ptase13* mutant extracts were grown under low nutrient or 3 % sucrose conditions. I conclude that under the no nutrient conditions, Atp80 is required to stabilize the GST-PBP1 protein while 5PTase13 acts in an opposing way by increasing GST-PBP1 degradation by the 26S proteasomal pathway.

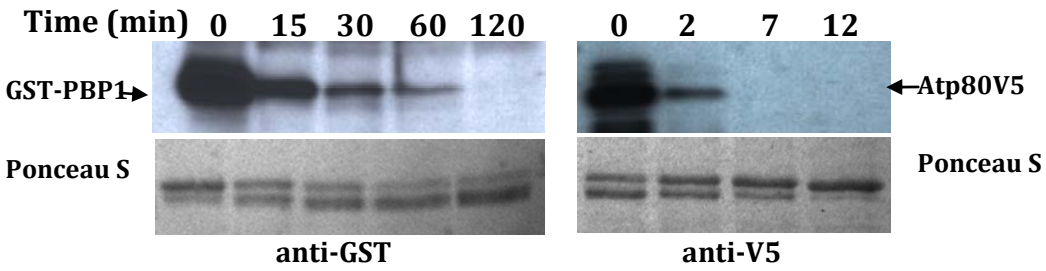

Figure 34. Time course of GST-PBP1 and Atp80V5 degradation in wild-type extracts. GST-PBP1 (500 ng) and Atp80V5 (500 ng) were incubated in extracts (20 µg) prepared from light grown WT seedlings for the indicated time at 30°C and were analyzed by a western blotting with an anti-GST and anti-V5 antibody respectively. The WT extracts were from seedlings grown on low nutrients. Ponceau S stained filters are shown as controls for equivalent loading. The band in the ponceau S filters is the big subunit of Rubisco from the plant extracts.

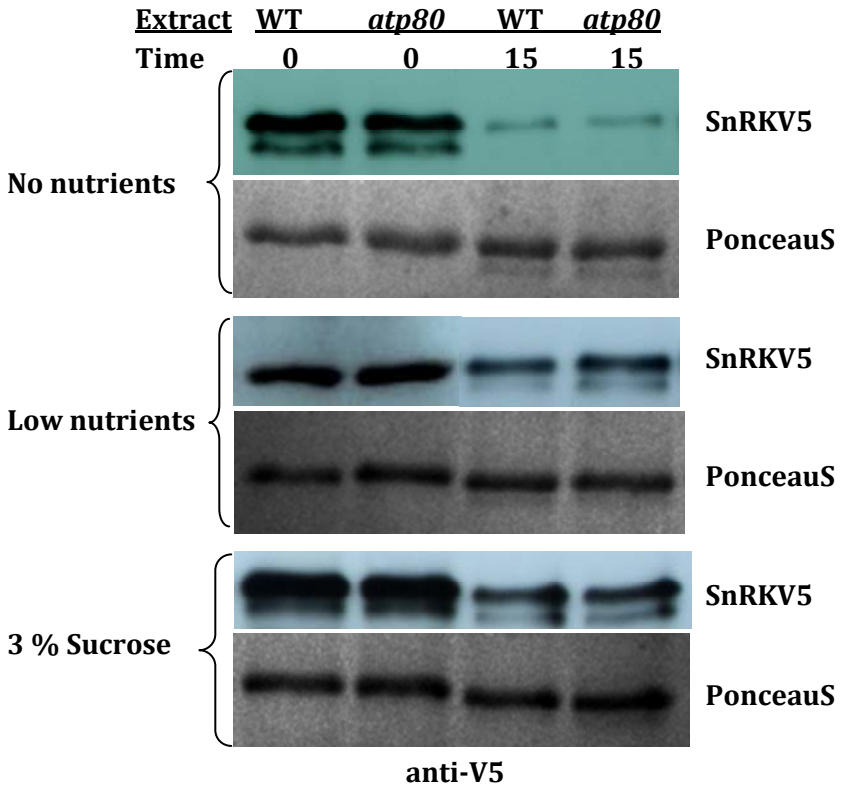

Figure 35. Degradation of V5-tagged SnRK1.1 in cell extracts from WT and *atp80* mutant seedlings grown under different nutrient conditions. SnRK1.1-V5 protein (SnRKV5; 500 ng) was incubated in extracts (20 µg) prepared from 15-day old low light grown WT and *atp80* mutant seedlings for the indicated time at 30°C and was analyzed by a western blotting with an anti-V5 antibody. Upper blot image shows SnRKV5 protein degradation in extracts prepared from seedlings grown with no nutrients; middle blot image shows SnRKV5 protein degradation in extracts prepared from seedlings grown with low nutrients (0.5x MS); and lower blot image shows SnRKV5 protein degradation in extracts prepared from seedlings grown with 3 % sucrose (0.5x MS; 3 % sucrose). Ponceau S stained filters are shown as controls for equivalent loading. The band in the ponceau S filters is the big subunit of Rubisco from the plant extracts.

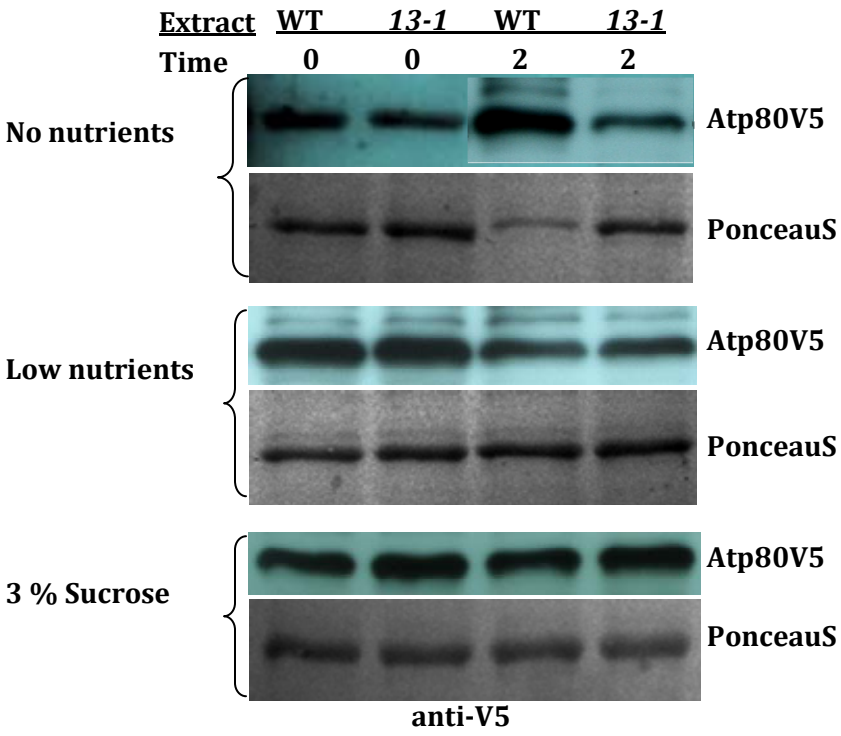

Figure 36. Degradation of V5-tagged Atp80 in cell extracts from WT and *5ptase13-1* mutant seedlings grown under different nutrient conditions. Atp80V5 protein (500 ng) was incubated in extracts (20 µg) prepared from 15-day old low light grown WT and *5ptase13-1 (13-1)* mutant seedlings for the indicated time at 30°C and was analyzed by a western blotting with an anti-V5 antibody. Upper blot image shows Atp80V5 protein degradation in extracts prepared from seedlings grown with no nutrients; middle blot image shows Atp80V5 protein degradation in extracts prepared from seedlings grown with low nutrients (0.5x MS); and lower blot image shows Atp80V5 protein degradation in extracts prepared from seedlings grown with 3 % sucrose (0.5x MS; 3 % sucrose). Ponceau S stained filters are shown as controls for equivalent loading. The band in the ponceau S filters is the big subunit of Rubisco from the plant extracts.

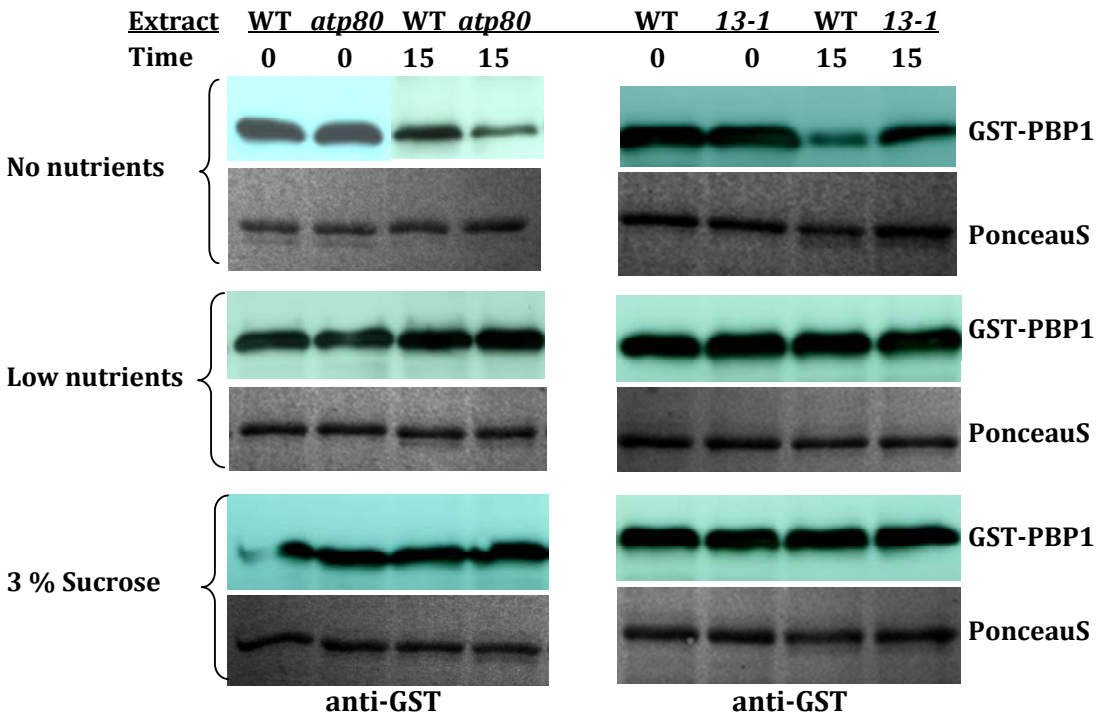

Figure 37. Degradation of GST-tagged PBP1 in cell extracts from WT, *atp80* and *5ptase13-1* mutant seedlings grown under different nutrient conditions. GST-PBP1 protein (500 ng) was incubated in extracts (20 µg) prepared from 15-day old low light grown WT, *atp80* and *5ptase13-1 (13-1)* mutant seedlings for the indicated time at 30°C and was analyzed by a western blotting with an anti-GST antibody. Upper blot images show GST-PBP1 protein degradation in extracts prepared from seedlings grown with no nutrients; middle blot images show GST-PBP1 protein degradation in extracts prepared from seedlings grown with low nutrients (0.5x MS); and lower blot images show GST-PBP1 protein degradation in extracts prepared from seedlings grown with 3 % sucrose (0.5x MS; 3 % sucrose). Ponceau S stained filters are shown as controls for equivalent loading. The band in the Ponceau S filters is the big subunit of Rubisco from the plant extracts.

The *atp80 Mutant is Insensitive to ABA*

Previously I have shown that *5ptase13* mutants are ABA-insensitive (Ananieva et al., 2008). To explore the ABA germination response of Atp80, I germinated WT, *atp80* mutant and Atp80/Atp80-GFP transgenic seeds in the presence of 1 and 3 μM ABA and measured the impact on germination during a 6-d period. As expected, germination of wild-type seeds was delayed by ABA in a concentration-dependent manner during the 6-d period under light conditions (Figure 38A-D). In contrast, *atp80* mutant seeds were ABA-insensitive and they showed a 1.5 fold increased germination rate on day 2 as compared to WT when treated with 1 μM ABA (Figure 38A). The fold difference was even more dramatic when *atp80* mutants were treated with 3 μM ABA with a maximal increase in germination of 2.3 fold after 4 days (Figure 38C). In contrast, there were no significant differences in the germination rate of the two transgenic lines (Atp80/Atp80:GFP-1, Atp80/Atp80:GFP-2) and WT plants with either 1 or 3 μM ABA (Figure 38B,D). I conclude that the *atp80* mutant is ABA-insensitive and that the overexpression of the Atp80 gene does not have an effect on the ABA response of the transgenic lines.

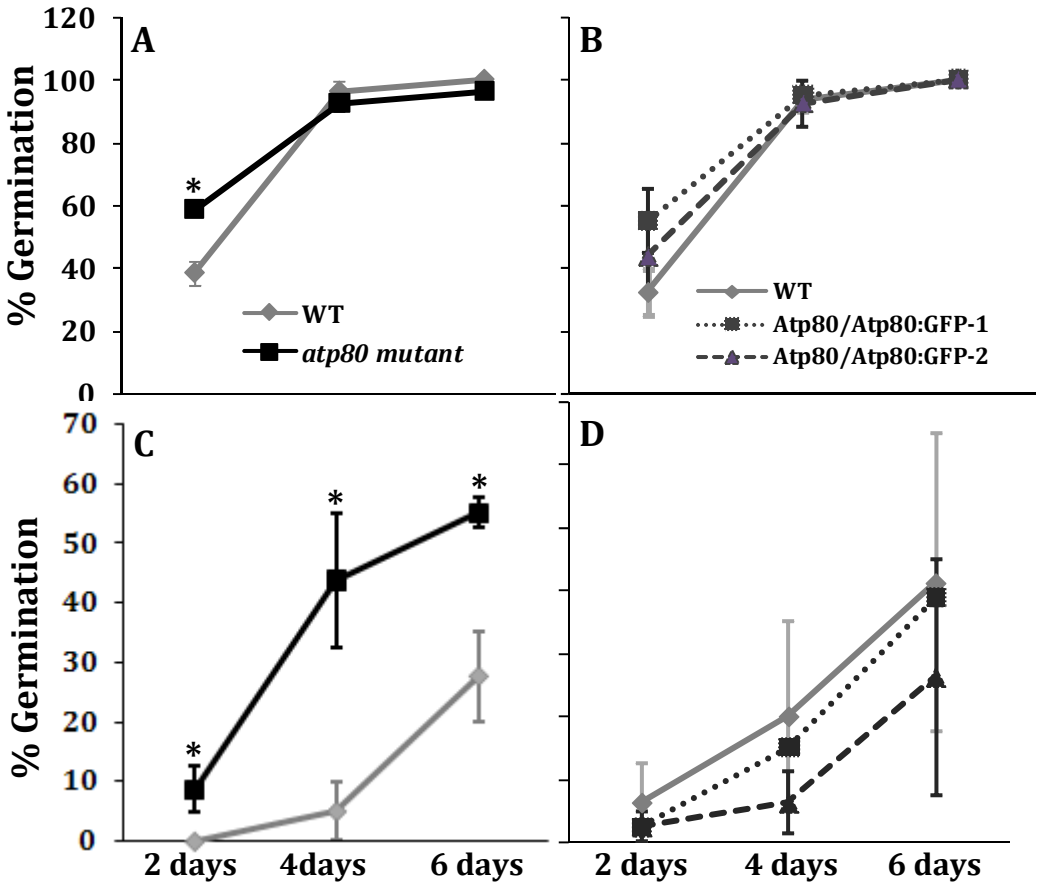

Figure 38. The *atp80* mutant is ABA insensitive. Seed from WT, *atp80* mutant and two independent transgenic lines expressing the Atp80:GFP construct in wild-type background (Atp80/Atp80:GFP-1 and Atp80/Atp80:GFP-2) were grown in light for 6 days on 0.8 % agar plates with 0.5x MS salts and either 1 µM ABA (A, B) or 3 µM ABA (C, D). The germination rate for each group of seeds was measured on day 2, 4 and 6. Values are means ± SE (n ≥ 80). The experiment was independently repeated two times. * indicates a p value < 0.05 as compared to WT.

DISCUSSION

The WD40-containing Arabidopsis 5PTases have a unique structural architecture, predicted to exist in other plant species but not in animals (Zhong et al., 2004; Zhong and Ye, 2004). This indicates a new plant specific functional role for the WD40 containing 5PTases that likely occurs via coordination of multi-protein complex assemblies, where the WD40 repeats serve as a scaffold for protein-protein interactions.

In my effort to characterize the function of the WD40 repeats of one Arabidopsis 5PTase (5PTase13), I identified potential protein partners and found that the WD40 region of 5PTase13 interacts with a sucrose (Suc) nonfermenting-1-related kinase (SnRK1.1) in a yeast two hybrid experiment and *in vitro* (Ananieva et al., 2008). SnRK1.1 has been identified as a central regulator of the transcriptome in response to darkness and multiple types of stress signals (Baena-Gonzalez et al., 2007; Baena-Gonzalez and Sheen, 2008). My identification of a 5PTase13:SnRK1.1 complex points to the novel interaction of this metabolic modulator and inositol signaling/metabolism. Thus, I consider 5PTase13 an important regulator of SnRK1 function that acts as a rheostat in balancing inositol metabolism and signaling (Ananieva et al., 2008; Ananieva and Gillaspy, 2009). 5PTase13 likely plays a regulatory role in other plant specific processes as well, since it has a previously established role in blue light signaling and auxin homeostasis (Lin et al., 2005; Chen et al., 2008). Together these data indicate that 5PTase13 may have more than one protein partner and might participate in multiple signaling pathways.

Using the yeast two hybrid system and an *in vitro* approach I identified a novel protein partner of 5PTase13 and named it Atp80 (Figures 20-21). Atp80 is the plant homolog of the human WDR48 (p80) (Figure 22). The main structural features of the human p80 are the presence of seven or eight WD40- repeats in the N-terminal half of the protein and of a putative coiled-coil domain in the C-terminal part (Cote-Martin et al., 2008). The human p80 was first shown to associate with a tyrosine kinase-interacting protein (Tip) from the lymphotropic Herpesvirus saimiri (Park et al., 2002; Park et al., 2003). Tip interacts with the WD40 domain of p80 to facilitate lysosomal vesicle formation and subsequent recruitment of a lymphocyte-specific tyrosine kinase (Lck) into lysosmes for degradation (Park et al., 2002). Recently, the WD40 region of p80 was shown to interact with the E1 helicase from a human papillomavirus, an interaction important for viral life cycle completion in its host (Cote-Martin et al., 2008).

After searching the conserved domain database, I found that Atp80 shares similar structural features with the human p80, since it also contains 7 WD40 repeats in its N-terminal half. A phylogenetic analysis revealed that Atp80 is encoded by a single gene with homologues in several plant and animal species (Figure 22). The sequence conservation raises the possibility that Atp80 has a similar function in all eukaryotes. In this study, I demonstrate that Atp80 is important for the establishment, development, and senescence of rosette leaves in Arabidopsis plants. Our *atp80* mutant shows light-dependent growth retardation and premature senescence phenotypes of rosette leaves (Figure 29). The light intensity and duration of light period are critical for the development of the observed phenotypes since visible radiation below 100 μE or short days (8hr light) does not impact the growth, development or senescence of the *atp80* mutant plants (Figure 30).

Under short days, however, *atp80* leaves (a source tissue) do not respond to added nutrient solution (Figure 30A,B). These results imply that the *atp80* mutants are defective in either nutrient uptake and/or nutrient response. The developmental delay, deformity and premature senescence of *atp80* rosette leaves observed under long day and visible radiation higher than 100 μE indicates a critical role for Atp80 in leaf establishment, development and senescence. In support of this, Genvestigator microarray expression analysis shows that Atp80 is highly expressed in rosette and senescent leaves (Supplemental Figure S5). Disruption in the WD40-containing cyclophilin71 (CYP71) gene that functions in gene repression and organogenesis in Arabidopsis shows defects in rosette leaf morphology and organogenesis that are similar to those observed in the *atp80* mutants (Li et al., 2007). The *cyp71* mutant plants display dramatic defects, including reduced apical meristem activity, delayed and abnormal lateral organ formation, and arrested root growth but do not show symptoms of premature senescence (Li et al., 2007). The *cyp71* mutant plants are small and developmentally retarded and thus they are reminiscent of the *atp80* mutant plants (Figure 29). The CYP71 protein interacts with H3 histone and it is proposed to serve as a histone remodeling factor involved in chromatin-based gene silencing (Li et al., 2007). Although, the Atp80 gene seems to impact the rosette leaves in a similar way during development it is unlikely that Atp80 has a histone remodeling function since H3 was not indentified as an interactor in the yeast two hybrid system.

My protein-protein interaction approach revealed that Atp80 interacts with the WD40 domain of 5PTase13 in the yeast two hybrid assay and *in vitro* (Figures 20 and 21). Since 5PTase13 forms a protein complex with SnRK1.1, I wondered whether Atp80 also interacts with SnRK1.1 (Ananieva et al., 2008; Ananieva and Gillaspy, 2009). To test this

hypothesis, Atp80 was used as a bait in the yeast two hybrid assay which revealed that SnRK1.1 interacts with the C-terminal half of Atp80 (Figure 20). I confirmed this interaction *in vitro* with recombinant protein pull-down assays, however I was able to pull down only a very small amount of the SnRK-GST recombinant protein with Atp80 (Figure 26B). Moreover, during the cell free degradation assay I did not observe any changes in the SnRKV5 stability under three different nutrient conditions in an *atp80* mutant background (Figure 35). In contrast, my previous work has shown that 5PTase13 stabilizes SnRK1.1 under low nutrient conditions (Ananieva et al., 2008). One possible explanation of the pull-down results is that Atp80 interaction with SnRK1.1. may require eukaryotic post-translational modifications, such as phosphorylation, that do not occur in *E. coli.* In addition, Atp80 could be involved in regulating SnRK1.1 activity instead of controlling its stability.

Several lines of evidence support my hypothesis that Atp80 is a subunit of the 5PTase13:SnRK1.1 complex. First, the complex likely resides in the nucleus since all protein partners have been found to localize in the nucleus (Figure 24)(Farras et al., 2001; Ananieva et al., 2008). Second, the *atp80* mutants exhibit severely reduced root growth when grown under no nutrient and low-nutrient conditions and show no change in root growth when 3 % sucrose is added to the growth medium (Figure 33). Similar root growth phenotypes have been described for *5ptase13* and *snkr1.1* mutants (Baena-Gonzalez et al., 2007; Ananieva et al., 2008). Third, the *atp80* mutant is insensitive to abscisic acid (ABA) as seen in our germination assay and thus is similar to that of the *5ptase13* mutants (Figure 38) (Ananieva et al., 2008). Recently, SnRK1.1 overexpression was shown to result in ABA and glucose hypersensitivity as well as delayed senescence (Baena-Gonzalez et al., 2007; Jossier et al., 2009). While SnRK1.1 overexpression was shown to cause delayed senescence (Baena-Gonzalez et al., 2007), the

atp80 mutation results in premature senescence of rosette leaves (Figure 29D-F). Together, these data suggest that Atp80 and SnRK1.1 function in a similar pathway to control root nutrient sensing and leaf senescence.

While the body of evidence supports a role of Atp80 in nutrient signaling through interaction with 5PTase13 and SnRK1.1, this does not explain the developmental and morphological defects in the rosette leaves of *atp80* mutants. Classical physiological studies have suggested that gradients of the plant growth regulator auxin play a role in controlling tissue differentiation in leaves and shoots (Poethig, 1997). Genes that control auxin polar transport are important for the formation of the auxin gradients (Swarup et al., 2002; Friml, 2003; Robert and Friml, 2009). Some of the genes that play a role in auxin transport are the four members of the AUX/LAX family which encode auxin influx carriers and the eight members of the PIN family (PIN1-8) which encode auxin efflux carriers (Swarup et al., 2002; Friml, 2003). The PIN1 gene and its regulation are of particular importance for my studies since changes in PIN1 expression were observed in *5ptase13-1* mutants along with a decrease in auxin (Lin et al., 2005). PIN1 is regulated by PINOID kinase through a PINOID-dependent binary switch that controls PIN1 polarity and mediates changes in auxin flow to create local gradients for patterning processes (Friml et al., 2004).

Interestingly, I found that one of the PINOID kinase protein interactors, the PINOID-binding protein1 (PBP1), binds to Atp80 as seen in a yeast two hybrid screen and *in vitro* co-immunoprecipitation assays (Figure 26 A,B). I then tested the stability of a recombinant GST-PBP1 in *atp80* and *5ptase13* mutants and compared this to GST-PBP1 stability in wild-type (Figure 37). My results show that Atp80 stabilizes GST-PBP1 while 5PTase13 acts in an opposing manner to destabilize GST-PBP1. PBP1 has been described as a calcium binding

protein that interacts with the PINOID kinase in a calcium dependent manner and acts as a cofactor to positively regulate PINOID kinase activity in specific tissues (Benjamins et al., 2003). Using a GUS staining procedure, I found that PBP1 expression is high in roots while in the cotyledons and rosette leaves it is restricted to veins, a tissue in which auxin plays a major role in differentiation (Figure 27 C,I). This fact further supports a role of PBP1 in auxin transport. I then compared the PBP1 expression pattern with that of Atp80 and 5PTase13 and found that they have similar spatial distribution with Atp80 being abundantly expressed and 5PTase13 showing the lowest expression (Figure 27). Based on these results, I propose that Atp80 interacts with PBP1 to increase its stability likely by preventing PBP1 from proteasomal degradation. Likely, Apt80 acts as a positive regulator of PBP1 to ultimately control auxin polar transport. The role of Atp80 in auxin transport through an interaction with PBP1 could explain why a loss of *atp80* function results in disruption of normal leaf establishment and differentiation.

Taken together these results indicate that there are two important and likely distinct functional roles that Atp80 plays in Arabidopsis. One is that Atp80 functions in nutrient and inositol signaling via interaction with 5PTase13 and SnRK1.1. The other is Atp80-mediated control of auxin transport via formation of a second protein complex with PBP1. Our results also imply that 5PTase13 negatively regulates the Atp80:PBP1 complex. The latter is consistent with a previously established connection between 5PTase13, blue light signaling and auxin homeostasis (Lin et al., 2005; Chen et al., 2008).

APPENDIX TO CHAPTER III

SUPPLEMENTAL DATA

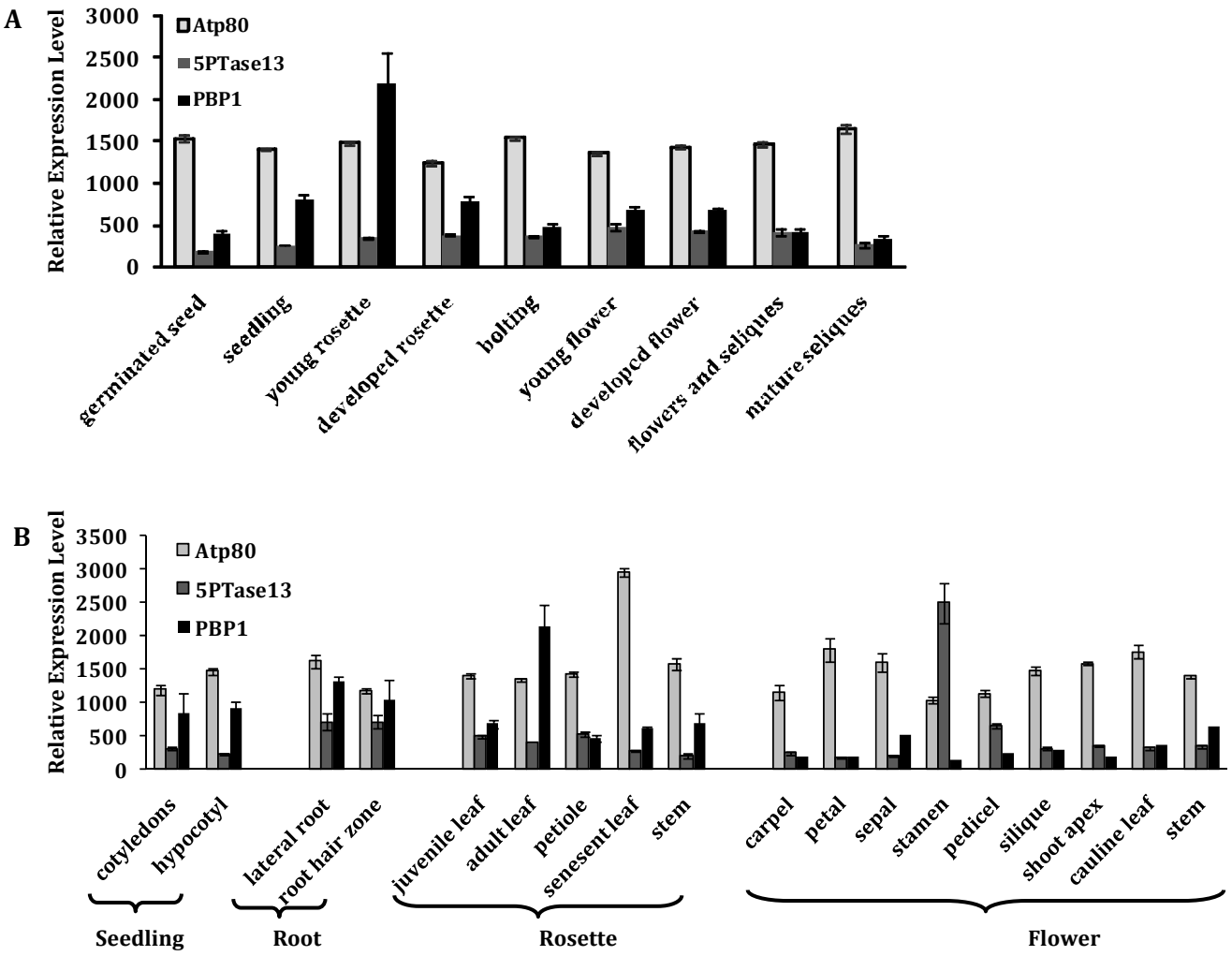

Supplemental Figure S5. GENEVESTIGATOR expression analysis. A. Atp80 expression pattern during different developmental stages as compared to 5PTase13 and PBP1. B. Atp80 expression pattern in different organs as compared to 5PTase13 and PBP1. Data from the Genvestigator web site was analyzed and plotted. Error bars are standard deviation.

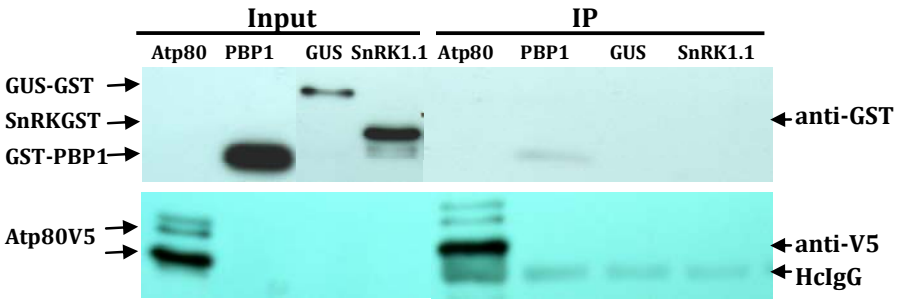

Supplemental Figure S6. GST-PBP1, GUS-GST and SnRKGST can not be pulled down by the anti-V5 sepharose when Atp80V5 is not present. Immunoprecipitation (IP) was carried out using an anti-V5 antibody bound to a protein A sepharose (PAS). Purified and dialyzed recombinant proteins, Atp80V5 (Atp80) SnRKGST (SnRK1.1), GST-PBP1 (PBP1) and GUS-GST (GUS) were incubated for 2 hrs at room temperature in IP buffer before transferring to the antiV5:PAS complex. The resulting IPs were analyzed using a protein gel blotting. Lanes 1-4: Input fractions of Atp80V5 alone (lane 1), GST-PBP1 alone (lane 2), GUS-GST alone (lane 3) or SnRKGST alone (lane 4); Lanes 5-8: Bound (IP) fractions of Atp80V5 alone (lane 5), GST-PBP1 alone (lane 6), GUS-GST alone (lane 7) or SnRKGST alone (lane 8). HcIgG- the heavy chain of the anti-V5 antibody from the antiV5:PAS complex ; GUS-GST was used a negative control. The blot images are representative of three independent experiments.

Table S5. Names of the WD40-containing proteins used to built a phylogenetic tree of sequences related to the WD40 domain of Atp80 in Arabidopsis

Name	At (ID) Number	Function
α-subunit of coatomer protein	At1g62020	modulates Golgi membrane transport*
PRL1 (PLEIOTROPIC REGULATORY LOCUS 1)	At4g15900	nuclear, interacts with SnRK1
Nucleotide binding protein	At1g11160	unknown
unknown	At4g02730	unknown
unknown	At3g21540	unknown
PP1/PP2A phosphatases (PRL2)	At3g16650	nucleotide binding, interacts with CUL4-RING
unknown	At5g52820	unknown
TOZ (TORMOZEMBRYO Defective)	At5g16750	regulates embryo development
unknown	At2g43770	unknown
unknown	At5g23430	unknown
unknown	At5g08390	unknown
unknown	At3g49660	unknown
katanin p80	At1g61210	controls mitotic spindle
EMB2776/LIS (Lachesis)	At2g41500	controls gametic cell fate*
unknown	At1g24530	unknown
unknown	At5g56130	unknown
unknown	At5g13480	unknown
β subunit of coatomer protein	At3g15980	modulates Golgi membrane transport*
TAF5 (TBP-associated factor 5)	At5g25150	putative, uncharacterized
unknown	At2g32700	unknown
unknown	At1g71840	unknown
ATARCA (Tobacco ArcA, RACK1A)	At1g18080	regulates plant development
activated protein kinase C receptor (RACK1B)	At1g48630	isoform of ATARCA
activated protein kinase C receptor (RACK1C)	At3g18130	isoform of ATARCA
unknown	At2g33340	unknown
unknown	At2g26490	unknown
SCD1 (stomatal cytokinesis defective1)	At1g49040	regulates guard cells cytokinesis
LUG (LEUNIG)	At4g32551	regulates embryo and floral development
unknown	At5g15550	unknown
unknown	At1g15440	unknown
unknown	At5g67320	unknown
nucleotide binding protein	At2g47410	unknown
unknown	At5g64730	unknown
unknown	At3g15470	unknown
unknown	At1g04510	unknown
unknown	At5g49430	unknown
unknown	At5g50120	unknown
unknown	At5g54200	unknown
eIF-3 (eukaryotic translation initiation factor3)	At2g46290	putative, uncharacterized
nucleotide binding protein	At5g50230	unknown
unknown	At3g09080	unknown
unknown	At3g49180	unknown
unknown	At3g18860	unknown
unknown	At1g64610	unknown
unknown	At1g24130	unknown
unknown	At3g50390	unknown

unknown	At5g42010	unknown
unknown	At1g73720	unknown

*Functional role as in animals, the putative Arabidopsis homolog is with unknown function.

Table S6. Primers used for PCR/RT-PCR.
Primer Sequence (5' to 3')
Gabi-Kat LB -ATATTGACCATCATACTCATTGC
Atp80For - CACCATGCACCGGGTTGGAAGTG
Atp80Rev- TCTAGCTATAGCCACTCTGTAGTTGAGAATC
Atp80For1- ATGCACCGGGTTGGAAGTGCCG
Atp80Rev1- TCTAGCTATAGCCACTCTG
Atp80For2- CCGAATTCATGCACCGGGTTGGAAAGT
Atp80Rev2- CCGGATCCTTATCTAGCTATAGCCAC
Atp80PromFor- CACCTGAATTTCACATACATATATCTTCAATTCC
Atp80PromRev- TTCAAATTATTCTGAAAGCCTGAAAGG
SnRK1.1For1- CACCATGTTCAAACGAGTAGATGAG
SnRK1.1Rev1- GAGGACTCGGAGCTGAGCAAG
5PTase13For1 -CACCATGGATTCGCTAATTATCGAAG
5PTase13Rev1 –CCGGCTTTTACCTCGTCTAACCG
5PTase13PromFor-CACCCATGACTCTTCTACTACATTC
5PTase13PromRev-CGACAATCAGAGGAATTCAAGAACG
PBP1PromFor- CACCACTCTATGATTGCGTCAATC
PBP1PromRev- TCAATGCCGGTAAAACTCTTCC
PEX4For- CTTAACTGCGACTCAGGGAATCTTCTAAG
PEX4Rev- TCATCCTTTCTTAGGCATAGCGGC

CHAPTER IV

MATERIALS AND METHODS

Phylogenetic Tree Construction

BLASTp was used to identify sequences related to the WD40 regions of either 5PTase13 or Atp80 or potential homologs of Atp80. ClustalW was used to generate an amino acid alignment which was submitted to the Mobyle server (http://mobyle.pasteur.fr) for analysis by either the PAUP4.0 (for the 5PTase13 analysis) or the PhyML (for the Atp80 analysis) program (a likelihood method) to generate a phylogenetic tree with 1000 bootstraps. TreeDyn 198.3 was used to produce a cladogram for the Atp80 homologs analysis.

Plant Growth Conditions

Arabidopsis ecotype Columbia was used for all experiments. Soil-grown plants were maintained in Sunshine Mix in growth chambers at 22°-24°C under 16 hrs of day/light (long day) or 8 hrs of day/light (short day). Visible radiation was provided by mixture of fluorescent/metal halide/high pressure sodium lamps or fluorescent lamps only. Regular-light conditions were 100-130 μE, while low-light conditions were 30-40 μE. All soil grown plants were watered with either sink water only or distilled water ± Miracle-Gro Liquid Houseplant Food (8-7-6: 8 % total nitrogen, N, 7 % available phosphate, P_2O_5, 6 % soluble potash, K_2O, 0.1 % Iron, Fe; Scotts Miracle-Gro Products, Inc.,).

Seedling (Root) Growth and Seed Germination Assays

Age-matched seeds used for assays were harvested from plants grown in parallel on the same shelf in a growth chamber, and seeds were harvested on the same day and ripened for 3-6 weeks at room temperature. Seeds were surface sterilized and plated on no salts or 0.5x MS salts solution (pH 5.7) containing 0.8 % agar. Each agar plate was divided into sections, and between 10- 50 seeds per variant were plated per section. Seeds were stratified on plates at 4^{o}C for 3 d and germinated at 23^{o}C in regular/low light or dark. For all dark experiments, plates the wrapped in foil and placed at room temperature. For sugar treatments, seeds were plated on medium containing 0 %, 1 %, 3 %, or 6 % Glc or Man (Sigma- Aldrich) or 0 %, 1 %, 2 %, 3 %, 6 %, or 11 % Suc (Sigma-Aldrich). Germination was scored as positive when the radicle protruded through the seed coat. Root length was measured in plates that were vertically oriented. For ABA sensitivity experiments, 1 mM ABA (Sigma-Aldrich) was dissolved in 100 % ethanol and added to cooled, sterile medium at a final concentration of 1, 2, or 3 µM ABA. The germination assay was performed under continuous regular light at room temperature in horizontal plates. Hormone/sugar treatment experiments were independently repeated two or three times.

Mutant Isolation

Potential *5ptase13-1* (At1g05630, SAIL_350_F1) and *5ptase13-2* (SALK_081991) as well as *atp80* (At3g05090, Gabi-Kat 007H09) mutants were identified from the SIGnAL database (http://www.signal.salk.edu/cgi-bin/tbnaexpress) (Alonso et al., 2003) and obtained from the Ohio State University Arabidopsis Biological Resource Center (ABRC). Genomic DNA was isolated from soil grown leaves using a DNeasy kit (QIAGEN Inc., Valencia,

CA). DNA from segregating plants was screened with PCR utilizing the SALK, SAIL and Gabi-Kat left border (LB) primers and either 5PTase13 or Atp80 gene specific primers (Supplemental Tables S4 and S6). To amplify 5PTase13, annealing at either 60 or 66 ^{o}C was performed with SALK or SAIL LB primers and 5PTase13 gene-specific primers (13-1for, 13-1rev, 13-2for, and 13-2rev; Supplemental Table S4). The resulting PCR fragments were sequenced and compared to the genomic sequence for each gene to map the T-DNA insertion. For *5ptase13-1*, a second LB-forward primer PCR product was also apparent. The DNA from this fragment was sequenced to confirm that a second, truncated T-DNA was present in tandem in the 5PTase13 gene.

To amplify Atp80, annealing at 59 ^{o}C was performed with a Gabi-Kat LB primer and Atp80 gene-specific primers (Atp80for, Atp80rev; Supplemental Table S6). Each PCR experiment was independently repeated two or three times.

Reverse Transcription-PCR

Total RNA was extracted from 100-150 mg frozen tissue using the RNeasy Plant Mini kit (Qiagen,Valencia,CA). A DNA free kit (Ambion or Qiagen,Valencia, CA) was used to remove contaminating genomic DNA. RNA was measured using a NanoDrop ND-1000 Spectrophotometer (Thermo Scientific NanoDrop Technologies, LLC, Wilmington, DE). Up to two micrograms of total RNA was reverse transcribed using the iScript cDNA Synthesis Kit according to the manufacturer's instructions (Bio-Rad Laboratories, Hercules, CA). One-fourth of the resulting cDNA eluate was used as a template in each PCR reaction, which was prepared in a 25 µl mixture. Amplification of 5PTase13 was achieved using PCR conditions and primers as described before. Amplification of the WD40 region of 5PTase13 was performed using

primers *13WD40for* and *13WD40rev* (Supplemental Table S4). Conditions for actin (Berdy et al., 2001), KIN1 (Knight et al., 1996; Knight et al., 1998) and RD29A (Sanchez and Chua, 2001) amplification have been described and generate a 428-, 342-, 715-bp product, respectively. For CAB1, *CAB1for* and *CAB1rev* primers, for SnRK1.1, *SnRK1.1for* and *SnRK1.1rev*, for SnRK1.2, *SnRK1.2for* and *SnRK1.2rev*, for FRA3, *FRA3for* and *FRA3rev*, for 5PTase12, *5PTase12for* and *5PTase12rev*, for 5PTase13, *5PTase13for* and *5PTase13rev*, for 5PTase14, *5PTase14for* and *5PTase14rev* were utilized at 30-35 cycles and annealing temperatures between 55- 68 °C, resulting in a 621-, 549-, 438-, 493-, 800-, 169-, 447-bp products respectively (Supplemental Table S4). Each RT-PCR experiment was independently repeated at least two times to verify the observed changes in expression.

Quantitative PCR (qPCR)

RNA was extracted and measured as above and the resulting cDNA was used in the quantitative PCR reactions. Quantitative PCR was performed using SYBR GREEN reagents (Applied Biosystems, Foster City, CA). Reactions in triplicate were monitored with the Applied Biosystems 7300 Real-Time PCR instrumentation (Applied Biosystems, Foster City, CA) outfitted with SDS software version 1.3.1. Primer pairs were optimized for detection of one specific gene in this system. Calculations involved comparison of the Atp80 Ct values with the PEX4 Ct values. PEX4 (peroxisomal ubiquitin4) was used as a endogenous control. The normalized values in log form were compared to the WT values, and the inverse log was applied to determine relative changes in Ap80 expression compared to WT.

Extraction and Measurement of Mass Ins(1,4,5)P_3

Filters containing whole 4d-old dark grown WT or *5ptase13* mutant seedlings were floated on a 6 % Glc solution (0.5x MS salts, pH 5.7) or on a control solution (0.5x MS salts, pH 5.7, only) in the dark for 3 d and then frozen in liquid nitrogen at the end of the treatment. Tissues were harvested and mass Ins(1,4,5)P_3 measurements were made as described previously (Burnette et al., 2003). The assays were performed in triplicate, and the experiment was repeated two times. Raw values for Ins(1,4,5)P_3 in Glc-treated samples are as follows: WT1, 1,313 ± 203 pmol g^{-1}; WT2, 1,313 ± 372 pmol g^{-1}.

Yeast Two-Hybrid Screen

The Matchmaker Two-Hybrid System 3 was used (BD Biosciences Clontech). The cDNA corresponding to amino acids 1 to 533 of 5PTase13 or 492 to 753 of Atp80 were amplified by PCR and ligated into pGBKT7 bait vector (BD Biosciences Clontech), verified by DNA sequencing, and transformed into yeast strain AH109. The yeast strain AH109 containing the 5PTase13 WD40 repeat domain (N-terminus) or the Atp80 coiled-coil domain (C-terminus) was transformed with an Arabidopsis 3 d-old etiolated seedling cDNA library (Thelogis). Screening for interactors was performed with SD/-Ade-His-Leu-Trp, 10 mM 3-amino-1,2,4-triazole, and 20 μg mL^{-1} 5-bromo-4-chloro-3-indolyl-b-D-galactopyranoside plates. Candidate clones that grew were rescued from yeast and retested in the original bait and control strains. Prey plasmids that passed all tests were sequenced to identify the Arabidopsis gene insert.

Expression and Purification of V5- and Xpress-tagged SnRK1.1, Atp80 and the WD40 repeat region of 5PTase13 in E. coli

The entire open reading frames of SnRK1.1 and Atp80 were amplified with gene-specific primers SnRK1.1pFor, SnRK1.1pRev and Atp80For1, Atp80Rev1 respectively (Supplemental Tables S4 and S6) and ligated to pCRT7/CT-TOPO vector. This resulted in pSnRKV5 and pAtp80V5, which directed expression of 61.7-kD (SnRK1.1) and 75-kD (Atp80) proteins with C-terminal 6xHis tags and V5 epitope tags (Invitrogen). The WD40 repeat region of 5PTase13 was amplified with gene-specific primers WD40For and WD40Rev (Supplemental Table S4) and ligated to pCRT7/NT-TOPO vector. This resulted in p13WDX, which directed expression of a 65.9-kD protein that corresponds to the WD40 region of 5PTase13 and an N-terminal 6xHis tag and Xpress epitope (Invitrogen, CA).

For expression, pSnRKV5, pAtp80V5 and p13WDX were transformed in *E. coli* BL21(DE3) pLysS cells (Invitrogen) following the manufacturer's instructions. Between 200-500 mL culture cell pellets expressing SnRK1.1V5, Atp80V5 and 13WDX were thawed and resuspended in 10 mL lysis buffer (50 mM KH_2PO_4 pH 7.8, 400 mM NaCl, 100 mM KCL, 10 mM imidazole, 10 % glycerol, 0.5 % TritonX-100), lysed with 1 mg mL^{-1} lysozyme for 30 min and sonicated 5 times x 30 sec each. The lysates were centrifuged at 12,000 x g for 30 min at 4 ^{o}C to pellet cell debris. Soluble cell lysates were incubated with around 200 µl (bed volume) of Ni^{+}-NTA beads (Qiagen, Valencia,CA) for 2 hours at 4 ^{o}C, washed 2 times with 10 mL lysis buffer and eluted with different concentrations of imidazole (70-250 mM) through a column (Bio-Rad Laboratories, Hercules, CA) in 400 µL elution fractions. Eluted SnRK1.1V5, Atp80V5 and 13WDX were dialyzed against dialysis buffer (50 mM Tris pH 7.8, 150 mM NaCl, 5 mM

$MgCL_2$, 0.05 % TritonX-100) overnight and for 3 additional hours the next morning. Protein purity was evaluated via SDS-PAGE and Western blotting.

Expression and Purification of GST-tagged SnRK1.1, Atp80, PBP1 and 5PTase13 in E. coli by using Gateway Technology

The coding regions of SnRK1.1, Atp80 and 5PTase13 minus the stop codons were amplified by high-fidelity PCR (Velocity enzyme, BioRad Laboratories, Hercules, CA) and gene-specific primers (SnRK1.1For1, SnRK1.1Rev1, Atp80For, Atp80Rev, 5PTase13For1, 5PTase13Rev1; Supplemental Table S6) and cloned into the pENTR/D-TOPO vector (Invitrogen). Additionally, a pENTR clone of PBP1 in pENTR22-1-Sfi was ordered from ABRC. The resulting clones were sequenced and recombined via the Gateway system (Invitrogen, CA) using the manufacturer's instructions into pDEST24 or pDEST15 vectors (for PBP1 only). The gateway clones were sequenced again to confirm that the inserts were in frame with the GST epitope tag. These resulted in pSnRK1.1GST, pAtp80GST, pPBP1GST and p5PTase13GST, which directed expression of an estimated 88 kD SnRK1.1 protein, 95 kD Atp80 protein, 41 kD PBP1 protein and an 154 kD 5PTase13 protein with C-terminal (SnRK1.1, p80, 5PTase13) or N-terminal (PBP1) GST epitope tags (Invitrogen, CA).

For expression, pSnRK1.1GST, pAtp80GST, pPBP1GST and p5PTase13GST were transformed in *E. coli* BL21(DE3) cells (Invitrogen, CA) following the manufacturer's instructions. Between 200-500 mL culture cell pellets expressing SnRK1.1GST, Atp80GST, PBP1GST and 5PTase13GST proteins were thawed and resuspended in 10 mL lysis buffer (140 mM NaCl, 2.7 mM KCL, 10 mM Na_2HPO_4, 1.8 mM KH_2PO_4, pH 7.3, 10 % glycerol, 1 % Triton-X-100), lysed with 1 mg mL^{-1} lysozyme for 30 min and sonicated 5 times x 30sec each.

The lysates were centrifuged at 12,000 x g for 30 min at 4°C to pellet cell debris. Soluble cell lysates were incubated with around 200 µl (bed volume) of GST-Sepharose beads (Amersham-Pharmacia Biotech) for 1 hour at room temperature, washed 3 times with 10 mL lysis buffer and eluted with 10 mM glutathione (Sigma-Aldrich) through a column (Bio-Rad Laboratories, Hercules, CA) in 300 µL elution fractions. Eluted SnRK1.1GST, Atp80GST, PBP1GST and 5PTase13GST proteins were dialyzed against buffer (50 mM Tris pH 7.8, 150 mM NaCl, 5 mM $MgCL_2$, 0.05 % TritonX-100) overnight and for 3 additional hours the next morning. Protein purity was evaluated via SDS-PAGE and Western blotting. As a positive control, a GUS-GST protein with a size of approximately 95 kD was expressed and purified following the same procedure as above.

Western Blot

Proteins were electrophoresed on either 8 % or 10 % SDS-PAGE gels and transferred to nitrocellulose using a semi-dry transfer apparatus (Bio-Rad Laboratories, Hercules, CA). The nitrocellulose membranes were incubated in blocking solution: 2.5 %-5 % milk in 1X TBST (50 mM Tris pH 7.5, 0.9 % [w/v] NaCl, and 0.01 % [v/v] Tween-20) buffer for 1 hr at room temperature. For detection of either the V5 or the Xpress epitope tag, a 1:5,000 dilution of the mouse anti-V5 or anti-Xpress monoclonal antibody (Invitrogen, CA), followed by a 1:20,000 dilution of goat anti-mouse horseradish peroxidase-conjugated antibody (Amersham-Pharmacia Biotech) was used. For detection of the GST epitope tag, a 1:4,000 dilution of the rabbit anti-GST monoclonal antibody (Invitrogen, Molecular Probes), followed by a 1:2,000 dilution of goat anti-rabbit horseradish peroxidase-conjugated antibody (BioRad Laboratories, Hercules, CA) was used. For detection of the GFP epitope tag, a 1:1,000 dilution

of the rabbit anti-GFP monoclonal antibody (Invitrogen, Molecular Probes), followed by a 1:2,000 dilution of goat anti-rabbit horseradish peroxidase-conjugated antibody (BioRad Laboratories, Hercules, CA) was used. All antibody solutions were in 2.5 %-5 % milk in 1X TBST buffer and were incubated with the nitrocellulose blots overnight at 4 ^{o}C with rocking. The nitrocellulose blots were washed three times for 10-20 min in 1X TBST buffer. After washing, the membranes were activated with the ECL Plus detection kit (Amersham-Pharmacia Biotech) according to the manufacturer's instructions. The nitrocellulose blots were exposed to an X-ray film for different time points.

Immunoprecipitation

For immunoprecipitations, between 500-1000 ng μL^{-1} of the purified and dialyzed proteins were used. The immunoprecipitation reactions were carried out in immunoprecipitation (IP) buffer consisting of 50 mM Tris-HCl, pH 7.8, 150 mM NaCl, 5 mM $MgCl_2$, 0.05 % Triton-X 100. Proteins were mixed with IP buffer and incubated at room temperature for 2 hrs on a rocking platform. The resulting mixture of two interacting proteins was further incubated with anti-V5:protein A-sepharose (PAS) beads (6 µg mouse anti-V5 monoclonal antibody, Invitrogen,CA, and a 50 % slurry of PAS, Sigma-Aldrich) at room temperature for 2 hrs on a rocking platform. The resulting immunoprecipitates on the beads were washed 3-4 times with 1-1.5 mL IP buffer. Protein A beads carrying the immune complexes were collected after each wash by centrifugation for 1 min. The washed immunoprecipitates were resuspended in 25-50 µL 2X SDS-PAGE loading buffer, separated on 8-10 % SDS-PAGE gels and transferred to a nitrocellulose membrane. Western blot conditions were as described above.

SnRK1 Activity Assay

Whole 7 d-old seedlings were ground in liquid nitrogen and resuspended in extraction buffer (50 mM Tris-HCl, pH 7.8, 1 mM EGTA, 1 mM EDTA, 2 mM dithiothreitol [DTT], 0.05 % Nonidet P-40, 0.5 mM phenylmethylsulfonyl fluoride, 1 mM benzamide, 3 mM glycerophosphate, and plant protease cocktail; Sigma). After centrifugation at 13.2 rpm for 15 min at 4^{o}C, ammonium sulfate was slowly added to the supernatant to 40 % saturation while stirring for 10 min at 4^{o}C and centrifuged for 15 min at 13.2 rpm and 4^{o}C. Precipitated protein was resuspended in 50 mL of fractionation buffer (50 mM Tris-HCl, pH 7.8, 1 mM EGTA, 1 mM EDTA, 2 mM DTT, 0.05 % Nonidet P-40, 0.5 mM phenylmethylsulfonyl fluoride, 1 mM benzamide, 3 mM glycerophosphate, 10 % glycerol, and plant protease cocktail; Sigma-Aldrich). Protein concentration was determined according to the Bradford method (Bradford, 1976), and equal amounts of protein were added to each assay. SnRK1 activity assay was performed as described by Radchuk et al. (2006) with slight modifications. Protein extract (5 mg in 5 mL) was mixed with 5 µL of kinase buffer (50 mM Tris-HCl and 1 mM DTT, pH 7.0), 5 mL of sterile water, 5 mL of SPS peptide stock solution (peptide sequence RDHMPRIRSEMQIWSED; 200 mM), and 5 mL of labeled ATP stock solution (5 mM [γ-^{32}P]ATP, 5mM unlabeled ATP, and 125 mM magnesium chloride). The samples were incubated for 30 min at 30^{o}C, and 10 mL aliquots were spotted twice onto P81 paper. The pieces were washed three times in 125 mM phosphoric acid for 20 min each and transferred to scintillation vials for counting. Two different control reactions were examined along with each reaction assay. The first reaction control contained no SPS peptide, and the second control contained no protein extract. Activity was expressed as nanomoles of phosphate incorporated into peptide

per minute per milligram of protein. The assay was performed using two independently prepared extracts and three replicates of each extract.

β-Galactosidase Enzyme Assay

Culture of yeast transformants was grown overnight on selective media (SCD –leu –trp) at 30°C with ~250 rpm shaking. Overnight culture (1.5 mL) was centrifuged for 30 sec at full-speed and the resulting yeast pellet was resuspended in 665 µL Z-buffer (pH7, $Na_2HPO_4.7H_2O$, $NaH_2PO_4.H_2O$, KCL, $MgSO_4.7H_2O$), 1.8 µL β-ME, 55 µL chloroform and 55 µL 0.1 % SDS. The reaction was started by the addition of 160 µL ONPG (o-nitrophenyl-β-D-galactoside) at 30°C until either a yellow color was developed or the reaction had run for 90-120 min. The reaction was stopped by adding 400 µL 1M Na_2CO_3. The solution was clarified by centrifugation (5 min, 13.2 K). The upper aqueous phase was transferred to a cuvette and read at A_{420}. The A_{420} was converted into Miller units.

Cell-Free Degradation Assay

Conditions described by Lee et al. (2008) were followed. Briefly, 7 d-old light-grown seedlings were ground in liquid nitrogen, resuspended in a buffer (25 mM Tris, pH 7.5, 10 mM $MgCL_2$, 5 mM DTT, and 10 mM NaCl), and centrifuged at 13.2 K for 10 min at 4°C. Purified recombinant SnRK1.1-V5 (SnRKV5; 200-500 ng), Atp80V5 (500 ng), PBP1-GST (500 ng) and total cell extracts (20-30 µg) were mixed in a reaction buffer (25 mM Tris, pH 7.5, 10 mM $MgCL_2$, 5 mM DTT, 10 mM NaCl, and 10 mM ATP) and incubated at 30°C for the indicated times. Reactions were analyzed by SDS-PAGE, followed by western blotting with a 1:5,000 dilution of a mouse anti-V5 antibody (Invitogen, CA) or a 1:4,000 dilution of a rabbit anti-GST

monoclonal antibody (Invitrogen, CA). Ponceau S staining was performed to ensure that equivalent amounts of extracts were analyzed.

Mutant Complementation and GFP Imaging

The 3,408-bp coding region of 5PTase13 minus the stop codon was amplified by high-fidelity PCR (Velocity enzyme, Bio Rad Laboratories, Hercules, CA) by using gene specific primers (5PTase13For1, 5PTase13Rev1, Supplemental Table S4), confirmed by sequencing, cloned into the pENTR/D-TOPO vector (Invitrogen, CA), and recombined via the Gateway system (Invitrogen, CA) using the manufacturer's instructions into pK7FWG2. The 2,259 bp coding region of Atp80 was cloned into pJET vector by using primers Atp80For2 and Atp80Rev2 (Supplemental Table S6) and then subcloned in pEGAD vector to make 35S:Atp80:GFP fusion. The resulting 35S cauliflower mosaic virus promoter:5PTase13:GFP and Atp80:GFP constructs were transformed into *Agrobacterium tumefaciens* by cold shock and were used in stable transformation of wild-type plants and either *5ptase13-1* or *atp80* mutants as described (Bechtold and Pelletier, 1998).

For the 35S:5PTase13:GFPconstruct, 5PTase13/5PTase13:GFP seedlings from at least two independent homozygous lines were identified on kanamycin plates and by screening for GFP production using a Zeiss Axioimager microscope equipped with fluorescence optics. Additionally, two independent homozygous complemented lines with detectable GFP expression in the mutant background (*13-1*/13:GFP-1 and *13-1*/13:GFP-2) were identified and used in growth assays and for subcellular localization. For the 35S:Atp80:GFP construct, independent homozygous lines of Atp80/Atp80:GFP as well as

complemented *atp80*/Atp80:GFP plants were also identified and analyzed the same way as described above.

Seven to fifteen day-old seedlings were used for imaging utilizing Axiovision software (Zeiss). Z-stack series of 15 to 20, 1 mm sections, were collected, and deconvolution with an iterative algorithm was applied. The resulting deconvolved images were reconstituted into a single image using the maximal intensity projection function of Axiovision. To visualize nuclei, seedlings were stained with 1 mg mL^{-1} DAPI (Molecular Probes) solution for 5 min, excess liquid was removed, and the seedlings were mounted in water. Photographs were taken with a Zeiss MC100 camera. GFP was imaged with a filter set consisting of an excitation filter of 540 to 580 nm, a dichroic mirror of 595 nm, and a barrier filter of 600 to 660 nm. DAPI staining was visualized with a standard UV fluorescence filter set.

Promoter GUS Analysis

An 0.8 kb, 2 kb and 1.2 kb promoter fragment of 5PTase13, Atp80 and PBP1 genes, respectively, were amplified from genomic DNA by high-fidelity PCR (Velocity enzyme, Bio-Rad Laboratories, Hercules, CA.) with gene-specific primers (5PTase13PromFor, 5PTase13PromRev, Atp80PromFor, Atp80PromRev, PBP1PromFor, PBP1PromRev; Supplemental Table S6) and cloned into the pENTR/D-TOPO vector (Invitrogen, CA). The resulting promoter clones were recombined into the binary vector pBGWFS7 (Invitrogen, CA) by a LR clonase recombination reaction according to the manufacturer's instructions (Invitrogen, CA). Transgenic plants were generated as described above.

For the GUS staining procedure, either whole seedlings or plant material from different developmental stages was placed in a GUS staining buffer (0.1 % Trion X-100, 50

mM phosphate buffer, 0.5 mM $K_4Fe(CN)_6$ x 3 H_2O, 0.5 mM $K_3Fe(CN)_6$, 2 mM 5-bromo-4-chloro-3-indolyl β-D-glucuronide cyclohexamine salt) vacuum-infiltrated for 20 min, incubated in the stain for overnight at 37°C, and then cleared of chlorophyll with subsequent 70 % and 95 % ethanol extractions at 4°C, according to the published protocol (Jefferson et al., 1987). Stained seedlings and tissues were photographed using an Olympus SZX16 stereoscope with an attached Olympus DP71 camera with DP Controller software (Olympus Corp., Japan).

Histological Characterization

The histological analysis was performed as described (Carland et al., 1999) with slight modifications. Seven day-old wild-type and *5ptase13* mutant cotyledons of soil-grown seedlings in a growth room were fixed in ethanol:chloroform:acetic acid solution (6:3:1) overnight at 4^{o}C and cleared sequentially in 80 % ethanol, 95 % ethanol overnight at 4^{o}C, and 10 % NaOH for 1hr at 42^{o}C. Cotyledons then were stained briefly (30 s to 2 min) in 0.002 % safranin-O (Sigma-Aldrich). Specimens were mounted on slides in 50 % glycerol and visualized with differential interference contrast on a Zeiss Axioimager microscope and Spot digital camera (Zeiss). A total of 50 cotyledons per variant were used.

CHAPTER V

SUMMARY

A canonical pathway of inositol signaling involves signaling-mediated conversion of PtdIns(4,5)P_2 into diacylglycerol and Ins(1,4,5)P_3 and is important for the regulation of various biological events, including growth and development, stress response and disease (Berridge, 2007, 2008). A protein family containing 15 members of the *myo*-inositol polyphosphate 5-phosphatases (5PTases) terminate inositol signaling by hydrolyzing the 5-phosphates from a variety of PtdInsP and InsP substrates, including Ins(1,4,5)P_3 (Berdy et al., 2001). Four of the Arabidopsis 5PTases contain a large, N-terminal extension with five to six WD40 repeat regions that are capable of mediating protein-protein interactions (Zhong and Ye, 2004; Smith, 2008).

The main goal of my research was to identify 5PTase interacting proteins and to understand the functional role of these protein complexes by focusing on one member of the Arabidopsis 5PTase family called 5PTase13. The identification of 5PTase13 protein complexes was done in collaboration with Dr. Erickson from Salisbury University who performed yeast two hybrid screens to obtain candidate interactors. The first protein complex identified and functionally characterized was between the WD40 repeat region of 5PTase13 and a sucrose (Suc) nonfermenting-1-related kinase (SnRK1.1, AKIN10; At3g01090), a central regulator of the transcriptome in response to darkness, energy deprivation and multiple types of stress signals (Baena-Gonzalez et al., 2007; Ananieva et al., 2008). To explore the link between *myo*-inositol signaling and the energy sensor, SnRK1, I isolated two T-DNA insertion

mutants in the 5PTase13 gene and measured the activity of SnRK1 after growing *5ptase13* mutants under various nutrient conditions. I found that loss of 5PTase13 function affects SnRK1 activity, and the impact differs depending on nutrient availability. I showed that *5ptase13* mutants contain significantly elevated SnRK1 activity in the absence of nutrients. In contrast, SnRK1 activity deceases in *5ptase13* mutants when either low nutrients or 6 % Glc is present. To delineate the mechanism of 5PTase13 regulation of SnRK1, I used a cell-free degradation assay and showed that 5PTase13 stabilizes SnRK1.1 under low nutrient conditions as seen by increased proteasomal degradation of SnRK1.1 in *5ptase13* mutants. I also found that a loss of 5PTase13 results in ABA- and sugar-insensitivity, impaired ability to induce expression of ABA- and Glc-regulated genes and lack of Ins(1,4,5)P_3 accumulation in response to Glc.

Probably due to its major role as a central regulator of thousand of genes in response to energy deprivation, SnRK1.1 is highly regulated (Polge and Thomas, 2007; Baena-Gonzalez and Sheen, 2008). PRL1 (Pleiotropic Regulatory Locus 1), for example, is a SnRK1-binding protein that shows glucose-dependent interaction with the SnRK1 regulatory domain and negatively regulates SnRK1 activity (Bhalerao et al., 1999). Interestingly, my data on 5PTase13 reveals an opposing function for the 5PTase13:SnRK1.1 complex as compared to the PRL1:SnRK1.1complex. I present a model that speculates on the relationship between the interacting proteins (Figure 39). As summarized in this model, under low-nutrients or 6 % glucose, 5PTase13 acts as a positive regulator of SnRK1 activity by reducing the amount of SnRK1.1 targeted for proteasomal destruction. In contrast, PRL1 acts as a negative regulator of SnRK1 and facilitates its proteasomal destruction. Therefore, a loss of 5PTase13 function results in low SnRK1 levels and lack of response to sugar and stress as opposed to the

increased levels of SnRK1 noted in *prl1* mutants (Bhalerao et al., 1999; Lee et al., 2008). These findings likely indicate that 5PTase13 and PRL1, both of which contain WD40 repeats, act in opposition to one another with respect to SnRK1.1, perhaps by virtue of protecting from or attracting proteasomal components, respectively.

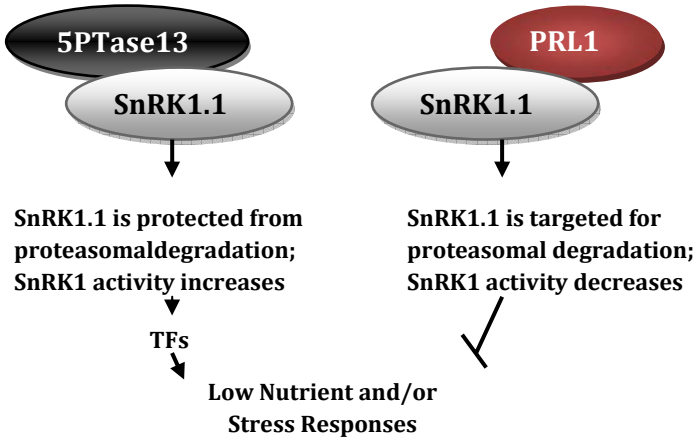

Figure 39. Model of antagonistic SnRK1.1 regulation by 5PTase13 and PRL1. Under low nutrient or 6 % glucose, 5PTase13 acts to protect SnRK1.1 from proteasomal degradation and PRL1 acts to facilitate SnRK1.1 turnover by the proteasome. When SnRK1 is stable/active, transcription factors (TFs) are stimulated to carry out metabolic reprogramming events.

A second area of importance I have considered is why a 5PTase regulates a metabolic modulator and energy sensor? A close analysis of microarray data indicates that SnRK1.1 overexpression and 3 % glucose regulate transcription of genes that encode key enzymes of the inositol signaling and metabolism pathway in opposing ways (Figure 40) (Price et al., 2004). In particular, glucose activates transcription of two genes required for

myo-inositol synthesis (At4g39800; MIPS1 and At3g02870; VTC4), while repressing expression of the *myo*-inositol oxygenase 2 gene (At2g19800; MIOX2) that encodes an enzyme required for *myo*-inositol oxidation to Dglucuronic acid (DGlcA)(Lorence et al., 2004; Price et al., 2004). Together, this could result in an increase in *myo*-inositol available for PtdIns synthesis. At the same time, glucose also represses transcription of three 5PTase genes, which could result in less $InsP_3$ hydrolysis and potentiation of inositol signaling (Price et al., 2004). Indeed, I found that glucose treatment of wild-type seedlings resulted in an increase in $InsP_3$ over a period of 3 days (Ananieva et al., 2008). Recent data also suggest that sugar acts to inhibit SnRK1 activity (Baena-Gonzalez et al., 2007), and under these conditions I have shown that 5PTase13 protects SnRK1.1 from proteasomal destruction. I propose that the protective function of 5PTase13 is to act as a rheostat under high energy or glucose conditions to provide feedback and dampen $InsP_3$ signaling. Together, this may indicate that SnRK1.1 overexpression decreases the energy-demanding synthesis of *myo*-inositol, increases *myo*-inositol oxidation and increases $InsP_3$ hydrolysis. Under extremely limiting nutrient conditions I found that 5PTase13 acts a negative regulator of SnRK1.1, which is consistent with a role for 5PTase13 as a rheostat for SnRK1.1 regulation under different nutrient conditions.

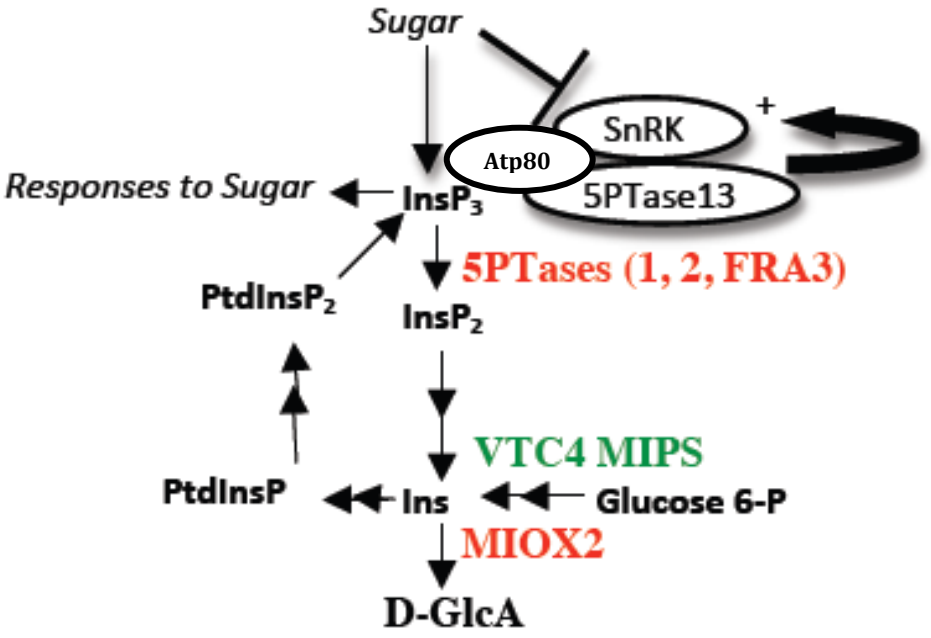

Figure 40. The role of 5PTase13:SnRK1.1 complex in balancing inositol signaling and metabolism. Genes that are upregulated by 3 % glucose are indicated in green, and those downregulated are indicated in red. The net result may increase *myo*-inositol synthesis, decrease *myo*-inositol oxidation, and increase $InsP_3$ accumulation. 5PTase13 and SnRK1.1 can form a complex and under these conditions 5PTase13 protects SnRK1.1 from proteasomal destruction. Thus we propose that 5PTase13 likely regulates SnRK1 in a nutrient dependent manner to contribute to the fine-tuning of inositol signaling and metabolism. Abbreviations are in the text. Atp80 is likely another subunit of the5PTase13:SnRK1.1 complex but its role remains to be further elucidated.

The second protein complex I identified and functionally characterized was between the WD40 repeat region of 5PTase13 and the Arabidopsis homolog (Atp80) of the human WDR48 (HsWDR48; Hsp80) protein. Again this research was done in collaboration with Dr. Erickson who performed the yeast two hybrid screen, identified a homozygous mutation in the Atp80 gene and supplied the T1 generation of Atp80 transgenic plants expressing the Atp80:GFP construct in a wild-type or mutant background. I performed a phylogenetic analysis and found that Atp80 is encoded by a single gene in Arabidopsis with one or two homologues in several plant and animal species as well as three homologues in moss. The Atp80 gene is abundantly expressed in most plant tissues and especially in senescent leaves. Disruption in the Atp80 gene resulted in dramatic defects in rosette leaf development including abnormal leaf differentiation, delayed leaf emergence and premature leaf senescence. The *atp80* mutant seedlings were small in size and displayed arrested root growth under no nutrient and low nutrient conditions but root growth was rescued when 3 % sucrose was added to the growth media. Like its human counterpart, Atp80 contains 7 WD40 domains in its N-terminal half and thus is implicated in protein-protein interactions (Cote-Martin et al., 2008). In this regard, I found that Atp80 physically associates with SnRK1.1 and PINOID binding protein1 (PBP1). While SnRK1.1 is well known for its interaction with 5PTase13, PBP1, a co-factor of PINOID kinase that regulates auxin transport (Benjamins et al., 2003), is a newly discovered protein partner of Atp80 that introduces a role for Atp80 in auxin transport regulation. My results indicate that Atp80 plays roles in nutrient and inostiol signaling as well it may be involved in regulating auxin efflux. My results also suggest that 5PTase13 negatively regulates the Atp80:PBP1 complex. The latter is consistent with

previously made connection between 5PTase13, blue light signaling and auxin homeostasis (Lin et al., 2005; Chen et al., 2008).

In summary, my research established a basis for characterizing the role of the WD40–containing 5PTases and their protein partners in essential plant processes such as nutrient and stress signaling as well as auxin transport. My work is an example of how the Arabidopsis 5PTases can make critical contribution to plant growth, development and stress responses, and thus introduces the Arabidopsis 5PTases as a model for our understanding of the impact signal termination makes in plants.

REFERENCES

Ananieva EA, Gillaspy GE (2009) Switches in nutrient and inositol signaling. Plant Signaling and Behavior **4:** 304-306

Ananieva EA, Gillaspy GE, Ely A, Burnette RN, Erickson FL (2008) Interaction of the WD40 domain of a myoinositol polyphosphate 5-phosphatase with SnRK1 links inositol, sugar, and stress signaling. Plant Physiol **148:** 1868-1882

Andersson MX, Kourtchenko O, Dangl JL, Mackey D, Ellerstrom M (2006) Phospholipase-dependent signalling during the AvrRpm1- and AvrRpt2-induced disease resistance responses in Arabidopsis thaliana. Plant J **47:** 947-959

Andersson U, Filipsson K, Abbott CR, Woods A, Smith K, Bloom SR, Carling D, Small CJ (2004) AMP-activated protein kinase plays a role in the control of food intake. J Biol Chem **279:** 12005-12008

Arai Y, Ijuin T, Takenawa T, Becker LE, Takashima S (2002) Excessive expression of synaptojanin in brains with Down syndrome. Brain Dev **24:** 67-72

Arenas-Huertero F, Arroyo A, Zhou L, Sheen J, Leon P (2000) Analysis of Arabidopsis glucose insensitive mutants, gin5 and gin6, reveals a central role of the plant hormone ABA in the regulation of plant vegetative development by sugar. Genes Dev **14:** 2085-2096

Astle MV, Horan KA, Ooms LM, Mitchell CA (2007) The inositol polyphosphate 5-phosphatases: traffic controllers, waistline watchers and tumour suppressors? Biochem Soc Symp**:** 161-181

Astle MV, Seaton G, Davies EM, Fedele CG, Rahman P, Arsala L, Mitchell CA (2006) Regulation of phosphoinositide signaling by the inositol polyphosphate 5-phosphatases. IUBMB Life **58:** 451-456

Attree O, Olivos IM, Okabe I, Bailey LC, Nelson DL, Lewis RA, McInnes RR, Nussbaum RL (1992) The Lowe's oculocerebrorenal syndrome gene encodes a protein highly homologous to inositol polyphosphate-5-phosphatase. Nature **358:** 239-242

Baena-Gonzalez E, Rolland F, Thevelein JM, Sheen J (2007) A central integrator of transcription networks in plant stress and energy signalling. Nature **448:** 938-942

Baena-Gonzalez E, Sheen J (2008) Convergent energy and stress signaling. Trends Plant Sci **13:** 474-482

Balla T (2001) Pharmacology of phosphoinositides, regulators of multiple cellular functions. Curr Pharm Des **7:** 475-507

Bechtold N, Pelletier G (1998) In planta Agrobacterium-mediated transformation of adult Arabidopsis thaliana plants by vacuum infiltration. Methods Mol Biol **82:** 259-266

Benjamins R, Ampudia CS, Hooykaas PJ, Offringa R (2003) PINOID-mediated signaling involves calcium-binding proteins. Plant Physiol **132:** 1623-1630

Berdy SE, Kudla J, Gruissem W, Gillaspy GE (2001) Molecular characterization of At5PTase1, an inositol phosphatase capable of terminating inositol trisphosphate signaling. Plant Physiol **126:** 801-810

Berridge MJ (1993) Inositol trisphosphate and calcium signalling. Nature **361:** 315-325

Berridge MJ (2007) Inositol trisphosphate and calcium oscillations. Biochem Soc Symp**:** 1-7

Berridge MJ (2008) Inositol trisphosphate and calcium signalling mechanisms. Biochim Biophys Acta

Bhalerao RP, Salchert K, Bako L, Okresz L, Szabados L, Muranaka T, Machida Y, Schell J, Koncz C (1999) Regulatory interaction of PRL1 WD protein with Arabidopsis SNF1-like protein kinases. Proc Natl Acad Sci U S A **96:** 5322-5327

Bradford MM (1976) A rapid and sensitive method for the quantitation of microgram quantities of protein utilizing the principle of protein-dye binding. Anal Biochem **72:** 248-254

Braun M, Baluska F, von Witsch M, Menzel D (1999) Redistribution of actin, profilin and phosphatidylinositol-4, 5-bisphosphate in growing and maturing root hairs. Planta **209:** 435-443

Bunce MW, Bergendahl K, Anderson RA (2006) Nuclear PI(4,5)P(2): a new place for an old signal. Biochim Biophys Acta **1761:** 560-569

Burnette RN, Gunesekera BM, Gillaspy GE (2003) An Arabidopsis inositol 5-phosphatase gain-of-function alters abscisic acid signaling. Plant Physiol **132:** 1011-1019

Calderwood DA (2004) Talin controls integrin activation. Biochem Soc Trans **32:** 434-437

Carland FM, Berg BL, FitzGerald JN, Jinamornphongs S, Nelson T, Keith B (1999) Genetic regulation of vascular tissue patterning in Arabidopsis. Plant Cell **11:** 2123-2137

Carland FM, Nelson T (2004) Cotyledon vascular pattern2-mediated inositol (1,4,5) triphosphate signal transduction is essential for closed venation patterns of Arabidopsis foliar organs. Plant Cell **16:** 1263-1275

Carlson M (1998) Regulation of glucose utilization in yeast. Curr Opin Genet Dev **8:** 560-564

Chen H, Shen Y, Tang X, Yu L, Wang J, Guo L, Zhang Y, Zhang H, Feng S, Strickland E, Zheng N, Deng XW (2006) Arabidopsis CULLIN4 Forms an E3 Ubiquitin Ligase with RBX1 and the CDD Complex in Mediating Light Control of Development. Plant Cell **18:** 1991-2004

Chen X, Lin WH, Wang Y, Luan S, Xue HW (2008) An inositol polyphosphate 5-phosphatase functions in PHOTOTROPIN1 signaling in Arabidopis by altering cytosolic Ca2+. Plant Cell **20:** 353-366

Chen Y, Ji F, Xie H, Liang J, Zhang J (2006) The regulator of G-protein signaling proteins involved in sugar and abscisic acid signaling in Arabidopsis seed germination. Plant Physiol **140:** 302-310

Christie JM (2007) Phototropin blue-light receptors. Annu Rev Plant Biol **58:** 21-45

Ciraolo E, Iezzi M, Marone R, Marengo S, Curcio C, Costa C, Azzolino O, Gonella C, Rubinetto C, Wu H, Dastru W, Martin EL, Silengo L, Altruda F, Turco E, Lanzetti L, Musiani P, Ruckle T, Rommel C, Backer JM, Forni G, Wymann MP, Hirsch E (2008) Phosphoinositide 3-kinase p110beta activity: key role in metabolism and mammary gland cancer but not development. Sci Signal **1:** ra3

Clement S, Krause U, Desmedt F, Tanti JF, Behrends J, Pesesse X, Sasaki T, Penninger J, Doherty M, Malaisse W, Dumont JE, Le Marchand-Brustel Y, Erneux C, Hue L, Schurmans S (2001) The lipid phosphatase SHIP2 controls insulin sensitivity. Nature **409:** 92-97

Cohn MA, Kee Y, Haas W, Gygi SP, D'Andrea AD (2009) UAF1 is a subunit of multiple deubiquitinating enzyme complexes. J Biol Chem **284:** 5343-5351

Communi D, Lecocq R, Erneux C (1996) Arginine 343 and 350 are two active residues involved in substrate binding by human Type I D-myo-inositol 1,4,5,-trisphosphate 5-phosphatase. J Biol Chem **271:** 11676-11683

Cote-Martin A, Moody C, Fradet-Turcotte A, D'Abramo CM, Lehoux M, Joubert S, Poirier GG, Coulombe B, Laimins LA, Archambault J (2008) Human papillomavirus E1 helicase interacts with the WD repeat protein p80 to promote maintenance of the viral genome in keratinocytes. J Virol **82:** 1271-1283

Critchley DR (2004) Cytoskeletal proteins talin and vinculin in integrin-mediated adhesion. Biochem Soc Trans **32:** 831-836

da Silva Xavier G, Leclerc I, Salt IP, Doiron B, Hardie DG, Kahn A, Rutter GA (2000) Role of AMP-activated protein kinase in the regulation by glucose of islet beta cell gene expression. Proc Natl Acad Sci U S A **97:** 4023-4028

da Silva Xavier G, Leclerc I, Varadi A, Tsuboi T, Moule SK, Rutter GA (2003) Role for AMP-activated protein kinase in glucose-stimulated insulin secretion and preproinsulin gene expression. Biochem J **371:** 761-774

Dale S, Arro M, Becerra B, Morrice NG, Boronat A, Hardie DG, Ferrer A (1995) Bacterial expression of the catalytic domain of 3-hydroxy-3-methylglutaryl-CoA reductase (isoform HMGR1) from Arabidopsis thaliana, and its inactivation by phosphorylation at Ser577 by Brassica oleracea 3-hydroxy-3-methylglutaryl-CoA reductase kinase. Eur J Biochem **233:** 506-513

Dale S, Wilson WA, Edelman AM, Hardie DG (1995) Similar substrate recognition motifs for mammalian AMP-activated protein kinase, higher plant HMG-CoA reductase kinase-A, yeast SNF1, and mammalian calmodulin-dependent protein kinase I. FEBS Lett **361:** 191-195

DePass AL, Crain RC, Hepler PK (2001) Inositol 1,4,5 trisphosphate is inactivated by a 5-phosphatase in stamen hair cells of Tradescantia. Planta **213:** 518-524

DeWald DB, Torabinejad J, Jones CA, Shope JC, Cangelosi AR, Thompson JE, Prestwich GD, Hama H (2001) Rapid accumulation of phosphatidylinositol 4,5-bisphosphate and inositol 1,4,5-trisphosphate correlates with calcium mobilization in salt-stressed arabidopsis. Plant Physiol **126:** 759-769

Ercetin ME, Ananieva EA, Safaee NM, Torabinejad J, Robinson JY, Gillaspy GE (2008) A phosphatidylinositol phosphate-specific myo-inositol polyphosphate 5-phosphatase required for seedling growth. Plant Mol Biol **67:** 375-388

Ercetin ME, Gillaspy GE (2004) Molecular characterization of an Arabidopsis gene encoding a phospholipid-specific inositol polyphosphate 5-phosphatase. Plant Physiol **135:** 938-946

Erneux C, Govaerts C, Communi D, Pesesse X (1998) The diversity and possible functions of the inositol polyphosphate 5-phosphatases. Biochim Biophys Acta **1436:** 185-199

Farras R, Ferrando A, Jasik J, Kleinow T, Okresz L, Tiburcio A, Salchert K, del Pozo C, Schell J, Koncz C (2001) SKP1-SnRK protein kinase interactions mediate proteasomal binding of a plant SCF ubiquitin ligase. Embo J **20:** 2742-2756

Franklin-Tong VE, Drobak BK, Allan AC, Watkins P, Trewavas AJ (1996) Growth of Pollen Tubes of Papaver rhoeas Is Regulated by a Slow-Moving Calcium Wave Propagated by Inositol 1,4,5-Trisphosphate. Plant Cell **8:** 1305-1321

Friml J (2003) Auxin transport - shaping the plant. Curr Opin Plant Biol **6:** 7-12

Friml J, Yang X, Michniewicz M, Weijers D, Quint A, Tietz O, Benjamins R, Ouwerkerk PB, Ljung K, Sandberg G, Hooykaas PJ, Palme K, Offringa R (2004) A PINOID-dependent binary switch in apical-basal PIN polar targeting directs auxin efflux. Science **306:** 862-865

Gibson SI, Laby RJ, Kim D (2001) The sugar-insensitive1 (sis1) mutant of Arabidopsis is allelic to ctr1. Biochem Biophys Res Commun **280:** 196-203

Gubler F, Millar AA, Jacobsen JV (2005) Dormancy release, ABA and pre-harvest sprouting. Curr Opin Plant Biol **8:** 183-187

Gunesekera B, Torabinejad J, Robinson J, Gillaspy GE (2007) Inositol polyphosphate 5-phosphatases 1 and 2 are required for regulating seedling growth. Plant Physiol **143:** 1408-1417

Gurung R, Tan A, Ooms LM, McGrath MJ, Huysmans RD, Munday AD, Prescott M, Whisstock JC, Mitchell CA (2003) Identification of a novel domain in two mammalian inositol-polyphosphate 5-phosphatases that mediates membrane ruffle localization. The inositol 5-phosphatase skip localizes to the endoplasmic reticulum and translocates to membrane ruffles following epidermal growth factor stimulation. J Biol Chem **278:** 11376-11385

Halford NG, Hey S, Jhurreea D, Laurie S, McKibbin RS, Paul M, Zhang Y (2003) Metabolic signalling and carbon partitioning: role of Snf1-related (SnRK1) protein kinase. J Exp Bot **54:** 467-475
Hardie DG (2004) The AMP-activated protein kinase pathway--new players upstream and downstream. J Cell Sci **117:** 5479-5487
Hardie DG (2007) AMPK and SNF1: Snuffing Out Stress. Cell Metab **6:** 339-340
Hardie DG (2008) AMPK: a key regulator of energy balance in the single cell and the whole organism. Int J Obes (Lond) **32 Suppl 4:** S7-12
Hardie DG, Carling D (1997) The AMP-activated protein kinase--fuel gauge of the mammalian cell? Eur J Biochem **246:** 259-273
Harthill JE, Meek SE, Morrice N, Peggie MW, Borch J, Wong BH, Mackintosh C (2006) Phosphorylation and 14-3-3 binding of Arabidopsis trehalose-phosphate synthase 5 in response to 2-deoxyglucose. Plant J **47:** 211-223
Heilmann I (2009) Using genetic tools to understand plant phosphoinositide signalling. Trends Plant Sci **14:** 171-179
Huang JZ, Huber SC (2001) Phosphorylation of synthetic peptides by a CDPK and plant SNF1-related protein kinase. Influence of proline and basic amino acid residues at selected positions. Plant Cell Physiol **42:** 1079-1087
Hue L, Rider MH (2007) The AMP-activated protein kinase: more than an energy sensor. Essays Biochem **43:** 121-137
Ijuin T, Takenawa T (2003) SKIP negatively regulates insulin-induced GLUT4 translocation and membrane ruffle formation. Mol Cell Biol **23:** 1209-1220
Ijuin T, Yu YE, Mizutani K, Pao A, Tateya S, Tamori Y, Bradley A, Takenawa T (2008) Increased insulin action in SKIP heterozygous knockout mice. Mol Cell Biol **28:** 5184-5195
Im YJ, Perera IY, Brglez I, Davis AJ, Stevenson-Paulik J, Phillippy BQ, Johannes E, Allen NS, Boss WF (2007) Increasing plasma membrane phosphatidylinositol(4,5)bisphosphate biosynthesis increases phosphoinositide metabolism in Nicotiana tabacum. Plant Cell **19:** 1603-1616
Jefferson AB, Majerus PW (1996) Mutation of the conserved domains of two inositol polyphosphate 5-phosphatases. Biochemistry **35:** 7890-7894
Jefferson RA, Kavanagh TA, Bevan MW (1987) GUS fusions: beta-glucuronidase as a sensitive and versatile gene fusion marker in higher plants. Embo J **6:** 3901-3907
Jones MA, Raymond MJ, Smirnoff N (2006) Analysis of the root-hair morphogenesis transcriptome reveals the molecular identity of six genes with roles in root-hair development in Arabidopsis. Plant J **45:** 83-100
Jossier M, Bouly JP, Meimoun P, Arjmand A, Lessard P, Hawley S, Grahame Hardie D, Thomas M (2009) SnRK1 (SNF1-related kinase 1) has a central role in sugar and ABA signalling in Arabidopsis thaliana. Plant J
Kagawa S, Soeda Y, Ishihara H, Oya T, Sasahara M, Yaguchi S, Oshita R, Wada T, Tsuneki H, Sasaoka T (2008) Impact of transgenic overexpression of SH2-containing inositol 5'-phosphatase 2 on glucose metabolism and insulin signaling in mice. Endocrinology **149:** 642-650
Knight H, Brandt S, Knight MR (1998) A history of stress alters drought calcium signalling pathways in Arabidopsis. Plant J **16:** 681-687
Knight H, Trewavas AJ, Knight MR (1996) Cold calcium signaling in Arabidopsis involves two cellular pools and a change in calcium signature after acclimation. Plant Cell **8:** 489-503
Kost B, Lemichez E, Spielhofer P, Hong Y, Tolias K, Carpenter C, Chua NH (1999) Rac homologues and compartmentalized phosphatidylinositol 4, 5-bisphosphate act in a common pathway to regulate polar pollen tube growth. J Cell Biol **145:** 317-330

Krinke O, Novotna Z, Valentova O, Martinec J (2007) Inositol trisphosphate receptor in higher plants: is it real? J Exp Bot **58:** 361-376
Kuchin S, Vyas VK, Kanter E, Hong SP, Carlson M (2003) Std1p (Msn3p) positively regulates the Snf1 kinase in Saccharomyces cerevisiae. Genetics **163:** 507-514
Laby RJ, Kincaid MS, Kim D, Gibson SI (2000) The Arabidopsis sugar-insensitive mutants sis4 and sis5 are defective in abscisic acid synthesis and response. Plant J **23:** 587-596
Lage R, Dieguez C, Vidal-Puig A, Lopez M (2008) AMPK: a metabolic gauge regulating whole-body energy homeostasis. Trends Mol Med **14:** 539-549
Lau CK, Bachorik JL, Dreyfuss G (2009) Gemin5-snRNA interaction reveals an RNA binding function for WD repeat domains. Nat Struct Mol Biol **16:** 486-491
Leclerc I, Kahn A, Doiron B (1998) The 5'-AMP-activated protein kinase inhibits the transcriptional stimulation by glucose in liver cells, acting through the glucose response complex. FEBS Lett **431:** 180-184
Lee JH, Terzaghi W, Gusmaroli G, Charron JB, Yoon HJ, Chen H, He YJ, Xiong Y, Deng XW (2008) Characterization of Arabidopsis and rice DWD proteins and their roles as substrate receptors for CUL4-RING E3 ubiquitin ligases. Plant Cell **20:** 152-167
Lee Y, Choi YB, Suh S, Lee J, Assmann SM, Joe CO, Kelleher JF, Crain RC (1996) Abscisic Acid-Induced Phosphoinositide Turnover in Guard Cell Protoplasts of Vicia faba. Plant Physiol **110:** 987-996
Lee Y, Kim YW, Jeon BW, Park KY, Suh SJ, Seo J, Kwak JM, Martinoia E, Hwang I, Lee Y (2007) Phosphatidylinositol 4,5-bisphosphate is important for stomatal opening. Plant J **52:** 803-816
Lemtiri-Chlieh F, MacRobbie EA, Webb AA, Manison NF, Brownlee C, Skepper JN, Chen J, Prestwich GD, Brearley CA (2003) Inositol hexakisphosphate mobilizes an endomembrane store of calcium in guard cells. Proc Natl Acad Sci U S A **100:** 10091-10095
Li D, Roberts R (2001) WD-repeat proteins: structure characteristics, biological function, and their involvement in human diseases. Cell Mol Life Sci **58:** 2085-2097
Li H, He Z, Lu G, Lee SC, Alonso J, Ecker JR, Luan S (2007) A WD40 domain cyclophilin interacts with histone H3 and functions in gene repression and organogenesis in Arabidopsis. Plant Cell **19:** 2403-2416
Lin PC, Hwang SG, Endo A, Okamoto M, Koshiba T, Cheng WH (2007) Ectopic expression of ABSCISIC ACID 2/GLUCOSE INSENSITIVE 1 in Arabidopsis promotes seed dormancy and stress tolerance. Plant Physiol **143:** 745-758
Lin WH, Wang Y, Mueller-Roeber B, Brearley CA, Xu ZH, Xue HW (2005) At5PTase13 modulates cotyledon vein development through regulating auxin homeostasis. Plant Physiol **139:** 1677-1691
Ling K, Doughman RL, Firestone AJ, Bunce MW, Anderson RA (2002) Type I gamma phosphatidylinositol phosphate kinase targets and regulates focal adhesions. Nature **420:** 89-93
Ling K, Schill NJ, Wagoner MP, Sun Y, Anderson RA (2006) Movin' on up: the role of PtdIns(4,5)P(2) in cell migration. Trends Cell Biol **16:** 276-284
Loewus F (1969) Metabolism of inositol in higher plants. Ann N Y Acad Sci **165:** 577-598
Loewus FA (2006) Inositol and plant cell wall polysaccharide biogenesis. Subcell Biochem **39:** 21-45
Lorence A, Chevone BI, Mendes P, Nessler CL (2004) myo-inositol oxygenase offers a possible entry point into plant ascorbate biosynthesis. Plant Physiol **134:** 1200-1205
Lou Y, Gou JY, Xue HW (2007) PIP5K9, an Arabidopsis phosphatidylinositol monophosphate kinase, interacts with a cytosolic invertase to negatively regulate sugar-mediated root growth. Plant Cell **19:** 163-181

Lowe M (2005) Structure and function of the Lowe syndrome protein OCRL1. Traffic **6:** 711-719
Lu CA, Lin CC, Lee KW, Chen JL, Huang LF, Ho SL, Liu HJ, Hsing YI, Yu SM (2007) The SnRK1A protein kinase plays a key role in sugar signaling during germination and seedling growth of rice. Plant Cell **19:** 2484-2499
Marion E, Kaisaki PJ, Pouillon V, Gueydan C, Levy JC, Bodson A, Krzentowski G, Daubresse JC, Mockel J, Behrends J, Servais G, Szpirer C, Kruys V, Gauguier D, Schurmans S (2002) The gene INPPL1, encoding the lipid phosphatase SHIP2, is a candidate for type 2 diabetes in rat and man. Diabetes **51:** 2012-2017
McCartney RR, Schmidt MC (2001) Regulation of Snf1 kinase. Activation requires phosphorylation of threonine 210 by an upstream kinase as well as a distinct step mediated by the Snf4 subunit. J Biol Chem **276:** 36460-36466
Michell RH (2008) Inositol derivatives: evolution and functions. Nat Rev Mol Cell Biol **9:** 151-161
Minokoshi Y, Alquier T, Furukawa N, Kim YB, Lee A, Xue B, Mu J, Foufelle F, Ferre P, Birnbaum MJ, Stuck BJ, Kahn BB (2004) AMP-kinase regulates food intake by responding to hormonal and nutrient signals in the hypothalamus. Nature **428:** 569-574
Moore B, Zhou L, Rolland F, Hall Q, Cheng WH, Liu YX, Hwang I, Jones T, Sheen J (2003) Role of the Arabidopsis glucose sensor HXK1 in nutrient, light, and hormonal signaling. Science **300:** 332-336
Munnik T, Testerink C (2008) Plant phospholipid signaling - 'in a nutshell'. J Lipid Res
Murthy PP (1996) Inositol phosphates and their metabolism in plants. Subcell Biochem **26:** 227-255
Ooms LM, Horan KA, Rahman P, Seaton G, Gurung R, Kethesparan DS, Mitchell CA (2009) The role of the inositol polyphosphate 5-phosphatases in cellular function and human disease. Biochem J **419:** 29-49
Ortega X, Perez LM (2001) Participation of the phosphoinositide metabolism in the hypersensitive response of Citrus limon against Alternaria alternata. Biol Res **34:** 43-50
Park J, Cho NH, Choi JK, Feng P, Choe J, Jung JU (2003) Distinct roles of cellular Lck and p80 proteins in herpesvirus saimiri Tip function on lipid rafts. J Virol **77:** 9041-9051
Park J, Lee BS, Choi JK, Means RE, Choe J, Jung JU (2002) Herpesviral protein targets a cellular WD repeat endosomal protein to downregulate T lymphocyte receptor expression. Immunity **17:** 221-233
Perera IY, Heilmann I, Boss WF (1999) Transient and sustained increases in inositol 1,4,5-trisphosphate precede the differential growth response in gravistimulated maize pulvini. Proc Natl Acad Sci U S A **96:** 5838-5843
Perera IY, Heilmann I, Chang SC, Boss WF, Kaufman PB (2001) A role for inositol 1,4,5-trisphosphate in gravitropic signaling and the retention of cold-perceived gravistimulation of oat shoot pulvini. Plant Physiol **125:** 1499-1507
Perera IY, Hung CY, Brady S, Muday GK, Boss WF (2006) A universal role for inositol 1,4,5-trisphosphate-mediated signaling in plant gravitropism. Plant Physiol **140:** 746-760
Pierre M, Traverso JA, Boisson B, Domenichini S, Bouchez D, Giglione C, Meinnel T (2007) N-myristoylation regulates the SnRK1 pathway in Arabidopsis. Plant Cell **19:** 2804-2821
Poethig RS (1997) Leaf morphogenesis in flowering plants. Plant Cell **9:** 1077-1087
Polge C, Thomas M (2007) SNF1/AMPK/SnRK1 kinases, global regulators at the heart of energy control? Trends Plant Sci **12:** 20-28
Prestwich GD (2004) Phosphoinositide signaling; from affinity probes to pharmaceutical targets. Chem Biol **11:** 619-637
Price J, Laxmi A, St Martin SK, Jang JC (2004) Global transcription profiling reveals multiple sugar signal transduction mechanisms in Arabidopsis. Plant Cell **16:** 2128-2150

Price J, Li TC, Kang SG, Na JK, Jang JC (2003) Mechanisms of glucose signaling during germination of Arabidopsis. Plant Physiol **132:** 1424-1438
Raboy V (2003) myo-Inositol-1,2,3,4,5,6-hexakisphosphate. Phytochemistry **64:** 1033-1043
Radchuk R, Radchuk V, Weschke W, Borisjuk L, Weber H (2006) Repressing the expression of the SUCROSE NONFERMENTING-1-RELATED PROTEIN KINASE gene in pea embryo causes pleiotropic defects of maturation similar to an abscisic acid-insensitive phenotype. Plant Physiol **140:** 263-278
Reeves RH, Irving NG, Moran TH, Wohn A, Kitt C, Sisodia SS, Schmidt C, Bronson RT, Davisson MT (1995) A mouse model for Down syndrome exhibits learning and behaviour deficits. Nat Genet **11:** 177-184
Robert HS, Friml J (2009) Auxin and other signals on the move in plants. Nat Chem Biol **5:** 325-332
Rolland F, Baena-Gonzalez E, Sheen J (2006) Sugar sensing and signaling in plants: conserved and novel mechanisms. Annu Rev Plant Biol **57:** 675-709
Sanchez JP, Chua NH (2001) Arabidopsis PLC1 is required for secondary responses to abscisic acid signals. Plant Cell **13:** 1143-1154
Sasaoka T, Hori H, Wada T, Ishiki M, Haruta T, Ishihara H, Kobayashi M (2001) SH2-containing inositol phosphatase 2 negatively regulates insulin-induced glycogen synthesis in L6 myotubes. Diabetologia **44:** 1258-1267
Schill NJ, Anderson RA (2009) Out, in and back again: PtdIns(4,5)P(2) regulates cadherin trafficking in epithelial morphogenesis. Biochem J **418:** 247-260
Schmid AC, Wise HM, Mitchell CA, Nussbaum R, Woscholski R (2004) Type II phosphoinositide 5-phosphatases have unique sensitivities towards fatty acid composition and head group phosphorylation. FEBS Lett **576:** 9-13
Schneider JF, Boltshauser E, Neuhaus TJ, Rauscher C, Martin E (2001) MRI and proton spectroscopy in Lowe syndrome. Neuropediatrics **32:** 45-48
Schneider S, Schneidereit A, Konrad KR, Hajirezaei MR, Gramann M, Hedrich R, Sauer N (2006) Arabidopsis INOSITOL TRANSPORTER4 mediates high-affinity H+ symport of myoinositol across the plasma membrane. Plant Physiol **141:** 565-577
Schuller HJ (2003) Transcriptional control of nonfermentative metabolism in the yeast Saccharomyces cerevisiae. Curr Genet **43:** 139-160
Shisheva A (2003) Regulating Glut4 vesicle dynamics by phosphoinositide kinases and phosphoinositide phosphatases. Front Biosci **8:** s945-946
Sleeman MW, Wortley KE, Lai KM, Gowen LC, Kintner J, Kline WO, Garcia K, Stitt TN, Yancopoulos GD, Wiegand SJ, Glass DJ (2005) Absence of the lipid phosphatase SHIP2 confers resistance to dietary obesity. Nat Med **11:** 199-205
Smith TF (2008) Diversity of WD-repeat proteins. Subcell Biochem **48:** 20-30
Smith TF, Gaitatzes C, Saxena K, Neer EJ (1999) The WD repeat: a common architecture for diverse functions. Trends Biochem Sci **24:** 181-185
Sondek J, Bohm A, Lambright DG, Hamm HE, Sigler PB (1996) Crystal structure of a G-protein beta gamma dimer at 2.1A resolution. Nature **379:** 369-374
Suganuma T, Pattenden SG, Workman JL (2008) Diverse functions of WD40 repeat proteins in histone recognition. Genes Dev **22:** 1265-1268
Sugden C, Crawford RM, Halford NG, Hardie DG (1999) Regulation of spinach SNF1-related (SnRK1) kinases by protein kinases and phosphatases is associated with phosphorylation of the T loop and is regulated by 5'-AMP. Plant J **19:** 433-439
Swarup R, Parry G, Graham N, Allen T, Bennett M (2002) Auxin cross-talk: integration of signalling pathways to control plant development. Plant Mol Biol **49:** 411-426

Takahashi S, Katagiri T, Hirayama T, Yamaguchi-Shinozaki K, Shinozaki K (2001) Hyperosmotic stress induces a rapid and transient increase in inositol 1,4,5-trisphosphate independent of abscisic acid in Arabidopsis cell culture. Plant Cell Physiol **42:** 214-222

Tan X, Calderon-Villalobos LI, Sharon M, Zheng C, Robinson CV, Estelle M, Zheng N (2007) Mechanism of auxin perception by the TIR1 ubiquitin ligase. Nature **446:** 640-645

Tang RH, Han S, Zheng H, Cook CW, Choi CS, Woerner TE, Jackson RB, Pei ZM (2007) Coupling diurnal cytosolic Ca2+ oscillations to the CAS-IP3 pathway in Arabidopsis. Science **315:** 1423-1426

Thelander M, Olsson T, Ronne H (2004) Snf1-related protein kinase 1 is needed for growth in a normal day-night light cycle. Embo J **23:** 1900-1910

Torii KU, McNellis TW, Deng XW (1998) Functional dissection of Arabidopsis COP1 reveals specific roles of its three structural modules in light control of seedling development. Embo J **17:** 5577-5587

Tsujishita Y, Guo S, Stolz LE, York JD, Hurley JH (2001) Specificity determinants in phosphoinositide dephosphorylation: crystal structure of an archetypal inositol polyphosphate 5-phosphatase. Cell **105:** 379-389

van Nocker S, Ludwig P (2003) The WD-repeat protein superfamily in Arabidopsis: conservation and divergence in structure and function. BMC Genomics **4:** 50

Voronov SV, Frere SG, Giovedi S, Pollina EA, Borel C, Zhang H, Schmidt C, Akeson EC, Wenk MR, Cimasoni L, Arancio O, Davisson MT, Antonarakis SE, Gardiner K, De Camilli P, Di Paolo G (2008) Synaptojanin 1-linked phosphoinositide dyshomeostasis and cognitive deficits in mouse models of Down's syndrome. Proc Natl Acad Sci U S A **105:** 9415-9420

Wada T, Sasaoka T, Funaki M, Hori H, Murakami S, Ishiki M, Haruta T, Asano T, Ogawa W, Ishihara H, Kobayashi M (2001) Overexpression of SH2-containing inositol phosphatase 2 results in negative regulation of insulin-induced metabolic actions in 3T3-L1 adipocytes via its 5'-phosphatase catalytic activity. Mol Cell Biol **21:** 1633-1646

Wall MA, Coleman DE, Lee E, Iniguez-Lluhi JA, Posner BA, Gilman AG, Sprang SR (1995) The structure of the G protein heterotrimer Gi alpha 1 beta 1 gamma 2. Cell **83:** 1047-1058

Wang X, Li W, Piqueras R, Cao K, Deng XW, Wei N (2009) Regulation of COP1 nuclear localization by the COP9 Signalosome via direct interaction with CSN1. Plant J

Wilson WA, Hawley SA, Hardie DG (1996) Glucose repression/derepression in budding yeast: SNF1 protein kinase is activated by phosphorylation under derepressing conditions, and this correlates with a high AMP:ATP ratio. Curr Biol **6:** 1426-1434

Woscholski R, Finan PM, Radley E, Totty NF, Sterling AE, Hsuan JJ, Waterfield MD, Parker PJ (1997) Synaptojanin is the major constitutively active phosphatidylinositol-3,4,5-trisphosphate 5-phosphatase in rodent brain. J Biol Chem **272:** 9625-9628

Wymann MP, Schneiter R (2008) Lipid signalling in disease. Nat Rev Mol Cell Biol **9:** 162-176

Wymann MP, Zvelebil M, Laffargue M (2003) Phosphoinositide 3-kinase signalling--which way to target? Trends Pharmacol Sci **24:** 366-376

Xiong L, Lee B, Ishitani M, Lee H, Zhang C, Zhu JK (2001) FIERY1 encoding an inositol polyphosphate 1-phosphatase is a negative regulator of abscisic acid and stress signaling in Arabidopsis. Genes Dev **15:** 1971-1984

Yu JW, Rubio V, Lee NY, Bai S, Lee SY, Kim SS, Liu L, Zhang Y, Irigoyen ML, Sullivan JA, Zhang Y, Lee I, Xie Q, Paek NC, Deng XW (2008) COP1 and ELF3 control circadian function and photoperiodic flowering by regulating GI stability. Mol Cell **32:** 617-630

Zhang X, Hartz PA, Philip E, Racusen LC, Majerus PW (1998) Cell lines from kidney proximal tubules of a patient with Lowe syndrome lack OCRL inositol polyphosphate 5-phosphatase and accumulate phosphatidylinositol 4,5-bisphosphate. J Biol Chem **273:** 1574-1582

Zhang X, Jefferson AB, Auethavekiat V, Majerus PW (1995) The protein deficient in Lowe syndrome is a phosphatidylinositol-4,5-bisphosphate 5-phosphatase. Proc Natl Acad Sci U S A **92:** 4853-4856

Zhang Y, Primavesi LF, Jhurreea D, Andralojc PJ, Mitchell RA, Powers SJ, Schluepmann H, Delatte T, Wingler A, Paul MJ (2009) Inhibition of SNF1-Related Protein Kinase1 Activity and Regulation of Metabolic Pathways by Trehalose-6-Phosphate. Plant Physiol **149:** 1860-1871

Zhong R, Burk DH, Morrison WH, 3rd, Ye ZH (2004) FRAGILE FIBER3, an Arabidopsis gene encoding a type II inositol polyphosphate 5-phosphatase, is required for secondary wall synthesis and actin organization in fiber cells. Plant Cell **16:** 3242-3259

Zhong R, Burk DH, Ye ZH (2001) Fibers. A model for studying cell differentiation, cell elongation, and cell wall biosynthesis. Plant Physiol **126:** 477-479

Zhong R, Ye ZH (2004) Molecular and biochemical characterization of three WD-repeat-domain-containing inositol polyphosphate 5-phosphatases in Arabidopsis thaliana. Plant Cell Physiol **45:** 1720-1728

Zhou L, Jang JC, Jones TL, Sheen J (1998) Glucose and ethylene signal transduction crosstalk revealed by an Arabidopsis glucose-insensitive mutant. Proc Natl Acad Sci U S A **95:** 10294-10299

Zimmermann P, Hirsch-Hoffmann M, Hennig L, Gruissem W (2004) GENEVESTIGATOR. Arabidopsis microarray database and analysis toolbox. Plant Physiol **136:** 2621-2632